



“New mechanisms and concepts for exploiting electroactive
Polymers for Wave Energy Conversion”

FP7-ENERGY-2012-1-2STAGE
FUTURE EMERGING TECHNOLOGIES

Grant Agreement N. 309139

**Architectures and material-property specifications for first-
and second- generation PolyWECS**

| | | | |
|---|-------------|--|---|
| Deliverable No. | | 1.1 | |
| WP No. | 1 | WP Title | Concepts and modeling |
| Task | T1.1 | Task Title | Definition of conceptual devices |
| Nature (R: Report, P: Prototype, O: Other) | | R | |
| Dissemination level (PU, PP, RE, CO) | | PU | |
| Lead beneficiary: | | 2-SSSA | |
| Authors List: | | Marco Fontana (SSSA) Rocco Vertechy (SSSA) Giacomo Moretti (SSSA) David Forehand (UEDIN) David Ingram (UEDIN) | |
| Status (F: final; D: draft; RD: revised draft): | | F | |
| File Name: | | D1.1 Architectures and mat props.pdf | |
| Due Delivery Date: | | M12, M16 | |
| Actual Delivery Date: | | 13 November 2013, 26 February 2014 | |

Version History table

| Version no. | Dates and comments |
|--------------------|---|
| 1 | 29 Sept 2013, first draft structure |
| 2 | 20 Oct 2013, draft to be circulated for Partners' data inputs |
| 3 | 31 Oct 2013, partners' data collection and finalization |
| 4 | 13 Nov 2013, final document |
| 5 | 26 Feb 2014, second submission following PO's comments |

INDEX

| | |
|--|----|
| INDEX..... | 3 |
| Executive summary | 6 |
| 1. INTRODUCTION | 9 |
| 1.1 Wave Energy Converters..... | 9 |
| 1.1.1 Working Principle | 9 |
| 1.1.2 Example of Existing Systems..... | 10 |
| 1.1.3 Traditional Power Take Off Systems..... | 17 |
| 1.2 Dielectric Elastomer Generators..... | 20 |
| 1.2.1 Working Principle | 22 |
| 1.3 Dielectric Elastomer Wave Energy Converters..... | 23 |
| 1.3.1 First-Generation Devices..... | 24 |
| 1.3.2 Second-Generation Devices | 24 |
| 1.3.3 SoA and Patent | 24 |
| 1.3.4 Environmental impact | 33 |
| 1.4 Conclusions..... | 33 |
| 2. GENERAL MODELS AND MATERIAL-PROPERTY SPECIFICATIONS | 35 |
| 2.1 Introduction..... | 35 |
| 2.2 Electro-Elastic Models..... | 35 |
| 2.2.1 Problem Definition..... | 35 |
| 2.2.2 Conservation of Energy..... | 36 |
| 2.2.3 Balance Equations and Constitutive Relations | 37 |
| 2.2.4 Constitutive Relations for Dielectric Elastomers | 37 |
| 2.3 Analysis of Conversion Cycles..... | 38 |
| 2.2.1 Maximal Convertible Energy..... | 39 |
| 2.4 Relevant Material Properties | 42 |
| 2.4.1 Dielectric Constant..... | 42 |
| 2.4.2 Electrical Break-down field | 43 |
| 2.4.3 Rupture stretch | 44 |

| | |
|--|-----------|
| 2.4.4 Hyperelastic parameters | 44 |
| 2.4.5 Effect of Material Properties on DE-WEC Response..... | 45 |
| 2.4.6 Other relevant properties | 45 |
| 2.5 Conclusions..... | 46 |
| 3. ARCHITECTURE OF FIRST-GENERATION POLYWECS | 48 |
| 3.1 Introduction..... | 48 |
| 3.2 WEC Architectures | 48 |
| 3.2.1 Oscillating Flap | 48 |
| 3.2.2 Oscillating Buoy..... | 49 |
| 3.2.3 Multi-body Systems | 49 |
| 3.3DEG Architectures..... | 50 |
| 3.3.1 Equi-biaxial DEG..... | 50 |
| 3.3.2 Planar Uniaxial DEG..... | 52 |
| 3.3.3 Lozenge-Shaped DEG..... | 53 |
| 3.3.4 Conical DEG | 53 |
| 3.3.5 Cylindrical DEG..... | 54 |
| 3.4 Preliminary hydrodynamic models..... | 55 |
| 3.4.1 Preliminary Wave to Wire Model of a First Generation PolyWEC | 57 |
| 3.5 Conclusions..... | 68 |
| 4. ARCHITECTURE OF SECOND-GENERATION POLYWECS | 69 |
| 4.1 Introduction..... | 69 |
| 4.2 Architecture of Poly-OWC | 69 |
| 4.3 Architecture of Poly-SubMe..... | 71 |
| 4.4 Preliminary wave to wire models of second-generation PolyWECS | 73 |
| 4.3.1 Rectangular Diaphragm Oscillating Water Column..... | 73 |
| 4.3.2 Circular Diaphragm Oscillating Water Column | 81 |
| 4.4 Conclusions..... | 90 |
| 5. CONCLUSIONS AND FUTURE WORKS | 91 |
| 5.1 Conclusions..... | 91 |

| | |
|------------------------|----|
| 5.2 Future works | 91 |
| References | 93 |

EXECUTIVE SUMMARY

Wave energy has a great potential as renewable source of electricity. Studies have demonstrated that significant percentage of world electricity could be produced by Wave Energy Converters (WECs). However electricity generation from waves still lacks of spreading because the combination of harsh environment and form of energy makes the technical development of cost effective WECs particularly difficult. PolyWEC project introduces a new class of Polymeric WECs (PolyWECS), characterised by the employment of Dielectric Elastomer (DE) transducers. The goal is to introduce a radical change in the traditional architecture of WECs that usually includes three basic components: mechanical wave absorbers, a mechanical transmission and a power take-off system. Due to their nature, PolyWECS can be conceived in a way that such three components are integrated into a single deformable lightweight and low-cost polymeric element. DEs have been largely investigated in the form of actuators for robotics and ICT applications. Preliminary studies on energy generation through DEs demonstrated their great potential in terms of cost effectiveness, efficiency and reduced complexity. Due to their intrinsic low mass, flexibility and resilience, as well as their capacitive nature and high voltage operation, DE technology perfectly matches the requirements of WECs.

This document reports a part of the work carried out during the first 12 months within the work-package 1 (WP1) "Concepts and modeling". The main objective of the activities carried out in this work package, are the following: Task 1.1 identifies and defines possible architectures of Wave Energy Converters based on Dielectric Elastomers; Task 1.2 develops numerical models that are able to predict the energetic performance of PolyWECS. The knowledge of PolyWECS energy productivity provides the fundamental information for future techno-economic assessment and feasibility studies of the proposed concepts.

Beyond the aspects examined in WP1, there are other critical points influencing the feasibility of PolyWEC concepts. These are, i.e., the adaptability of the polymeric materials to the sea environment (in terms of resistance to corrosion, fouling, UV and solar radiation, temperature) and their fatigue lifetime. These aspects will be considered in a future stage of the project and will be treated (together with the energetic performance estimative examined in this work) as input variables for economic life-cycle analyses.

According to the PolyWEC general approach, the activities of WP1 have been organized in two successive levels of development: first-generation and second-generation devices. First-generation PolyWECS are characterized by indirect interaction between dielectric elastomer generator unit (DEGU) and fluid. That is, the deformations of DE membranes are not directly generated by fluid pressures but by a mechanical interface. On the contrary, second-generation PolyWECS are characterized by direct interaction between DEGU and fluid, which occurs over wide contact surfaces. That is, fluid-DEGU interaction is not mediated by any mechanical means, and DE membrane deformation is directly generated by wave-induced fluid pressures.

Dielectric Elastomer Generators can assume various structures and layouts. Correspondingly, they can feature very different characteristics in terms of: mechanical response, electrical response, reliability, easy of manufacturing, dynamic response, etc. Within the research community of Electroactive Polymers several type of transducers have been studied as actuators but many of them have not yet been investigated as generators.

After a brief description of the relevant working principle of DEG, in the first part of this document, we report a description of possible relevant solutions for their implementation and modelling.

In the second section of this deliverable, we report models and methods that have been employed for identifying relevant properties that are required for the materials to be employed for the deployment of DEGs and the effect of such properties on their overall performances.

In the third and fourth section, first-generation and second-generation PolyWEC architectures are respectively defined. In the last part of these sections, preliminary wave to wire models have been deployed

(for first- and second-generation devices) in order to evaluate the performances of a set of relevant architectural solutions.

Several types of systems have been identified for either off-shore, shoreline and on-shore installation. Preliminary simplified hydrodynamic/electro-elastic analyses have been conducted on WECs equipped with DEG, such as the Surging Flap WEC and the Oscillating Water Column. The energetic performances of these architectures have been compared with those obtained with optimal Power Take-Off systems (i.e. ideal electric motors).

The main conclusions and outcomes that have been reached can be summarized as follows:

- The use of simplified analyses (i.e. linear hydrodynamics) provides a smart tool to assess the performances of the examined concepts. In relative terms, to compare the performances of the new concepts with traditional solutions, the approach proposed in this work results satisfactory.
- Preliminary results show that the obtained fraction of power extracted from ocean waves by WECs that employ proposed architectures, is comparable with that of WECs employing traditional generators. This is particularly promising since the proposed concepts are very simple and require the use of reduced number of components.
- Materials that are available on the market could already provide satisfactory performances.
- It is expected that novel solutions can be found during the prosecution of the project in order to slightly improve the already promising performances.

List of acronyms:

WEC: Wave Energy Converter;

DE: Dielectric Elastomers;

DEG: Dielectric Elastomer Generator (to refer to the whole generator);

DEGU: Dielectric Elastomer Generation Unit (to refer to the transduction unit);

OWC: Oscillating Water Column;

Poly-OWC: Polymeric Oscillating Water column (based on dielectric elastomer transducers);

CCDEM: Cylindrical Curved Dielectric Elastomer Membrane;

ICDEM: Inflated Circular Dielectric Elastomer Membrane;

PTO: Power Take Off

MWL: Mean Water Level

SWL: Surface Water Level

1. INTRODUCTION

Wave Energy is one of the most promising renewable resources, being highly concentrated (up to 100 kW per meter of wave front width) [1], clean, and presenting a large potential (global estimated gross available power of about 4 TW) [2]. Moreover, wave energy realizes a good matching between energy availability and energy consumption, both because the major part of the population is concentrated in the coastal regions and because the source presents a seasonal variability that follows electricity demand.

Many recent studies estimate that, in the next few years, Wave Energy will experiment a growth comparable to the one of Wind Energy and Photovoltaic in the past years [3] [4].

Up to date, it is possible to assert that wave energy conversion is in its pre-commercial phase: several technical solutions have been proposed [5] [6], but a technological standard has not been found yet.

Effectively, some nodal criticalities still make the installation of Wave Energy Converters (WECs) an unresolved issue, in particular:

- Since the resource presents good intensities far from the shores, complex mooring systems and underwater cables are required.
- Ocean and sea waves are very variable in terms of height, period and wavelength: devices operating in a large range off the nominal operative conditions are required, moreover, survivability in extreme sea conditions has to be guaranteed.
- Sea water represents a chemically and physically aggressive environment.
- A traditional WEC comprises several rigid components, which are made of stiff, heavy, shock-sensitive, corrosion-sensitive and costly metallic materials, and include wave-interacting bodies, mechanical/hydraulic transmissions, electromagnetic generators, step-up transformers and eventually frequency changers or rectifiers.

Basing on the mentioned presuppositions, the PolyWEC project aims at investigating new concepts of WEC based on Electroactive polymers, in particular Dielectric Elastomers (DEs), that may simplify and improve the efficiency of the existing technical solutions so as to reduce the overall conversion costs associated to the exploitation of ocean wave energy.

1.1 Wave Energy Converters

1.1.1 Working Principle

Many possible classifications have been proposed for the existing WEC concepts. The most common classification is based on the relative dimensions of the WEC with respect to the incident wavelength and on the orientation of the WEC with respect to the wave propagation direction [1]. We consider two significant dimensions for the bodies, identified by sectioning the devices with a plane parallel to the Surface Water Level (SWL).

The following categories of devices can be identified (Figure 1).

- Point Absorbers: they have both the significant dimensions much smaller than the wavelength. These devices are often axi-symmetric about a vertical axis. Such devices can capture energy from a wave front that is larger than their dimensions, exploiting three-dimensional effects.
- Attenuators: they have one dimension much larger than the other one (and comparable with the wavelength λ), with the first being parallel to the wave propagation direction. It is usual for attenuators to be compliant or articulated structures.
- Terminators: these devices have the dominant dimension (comparable with λ) perpendicular to the wave propagation direction. They can be either compliant or rigid. An efficient terminator will create waves that are exactly in anti-phase with the incident wave.

Both terminator and attenuator devices have directionally dependent efficiency.

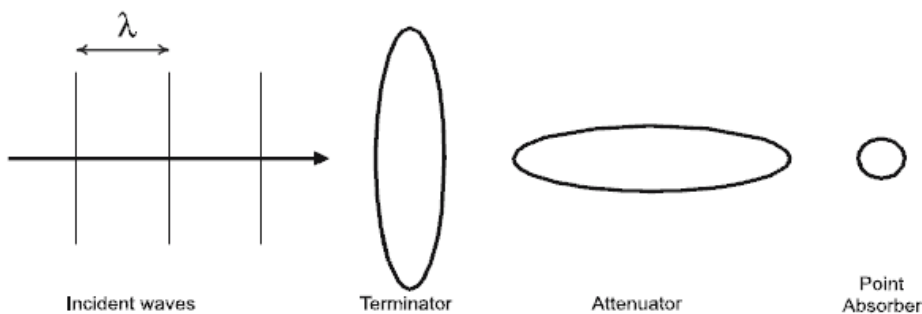


Figure 1 - WECs classification

A further classification may be given basing on the operating principle of the converter. Three main categories can be identified: Wave Activated Bodies, Oscillating Water Columns, Overtopping Devices.

- **Wave Activated Bodies:** these converters include a main body that oscillates due to the wave-induced forces. Such converters may be further subdivided, referring to the motion type of the main body, into linear oscillating bodies (provided with alternating linear motion) and rotating oscillating bodies (provided with alternating rotary motion).
- **Oscillating Water Columns:** these devices exploit the action of the waves to cause the reciprocating motion of a column of water enclosed in a duct that is open to the sea on one side and to an air chamber on the other. The motion of the column alternately compresses/expands the air enclosed in the chamber, which then activates an air turbine.
- **Overtopping Devices:** In these devices, a ramp is usually present that allows the wave (when a crest approaches the device) to overtop the converter and to spill over into a basin where the water is stored. The resulting hydraulic head is used to generate electricity with a turbine.

Referring to this last classification, the following sections present an overview on the existing solutions for the conversion of Wave Energy and a state of the art of the existing technologies.

1.1.2 Example of Existing Systems

Wave Activated Bodies

Wave activated bodies represent the most common solution for wave energy conversion, and are implemented in a number of different solutions.

Linear oscillators: heaving buoys

Heaving buoys are one of the most well-known solutions for wave energy conversion. Heaving buoys can be either submerged or semi-submerged and can exploit hydraulic PTOs (a fluid is compressed and delivered to a hydraulic circuit for the conversion) or linear electric generators.

Falcão [5] presents a review of heaving buoy technology by also describing specific installations.

One of the first attempt was a device named G-1T, consisting of a wedge-shaped buoy with rectangular section (1.8 m x 1.2 m at sea surface); the PTO was a hydraulic ram in a circuit including a gas accumulator [6].

The concept of a single heaving body moored to the seabed brings some difficulty due to the relatively high distance between the sea surface and seabed plane and to the variations in water depth induced by tidal effect.

Two-body systems may be an alternative. In this second kind of devices, energy is converted from the relative motion between two bodies that oscillate differently.

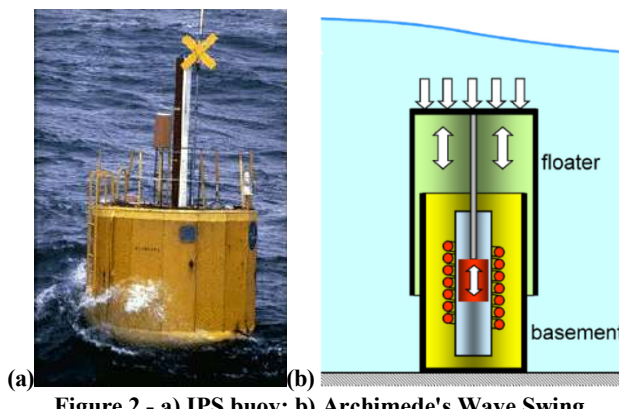


Figure 2 - a) IPS buoy; b) Archimede's Wave Swing

IPS buoy

One of the most interesting two-body point absorber for wave energy conversion is the IPS buoy (Figure 2.a) [5], developed in Sweden by the company InterProject Service (IPS). It consists of a buoy rigidly connected to a fully submerged vertical tube open at both sides. The tube houses a piston whose motion drives a PTO.

Archimede's Wave Swing

Another interesting example of a two-body heaving device is represented by the Archimede's Wave Swing (Figure 2.b), a fully submerged heaving device developed in Holland, consisting on an oscillating upper part and a bottom-fixed basement. The wave-induced motion of the moving part drives a linear electric generator, with the interior air pressure acting like a spring. A prototype was built and tested off Portugal coasts in 2004 [1][5]. The maximum peak power of the prototype was 2 MW, whereas rated stroke and velocity were 7 m and 2.2 m/s respectively. The overall mass of the device was 7000 tons (primarily due to the sand ballast tanks), of which 400 tons was the mass of the moving part.

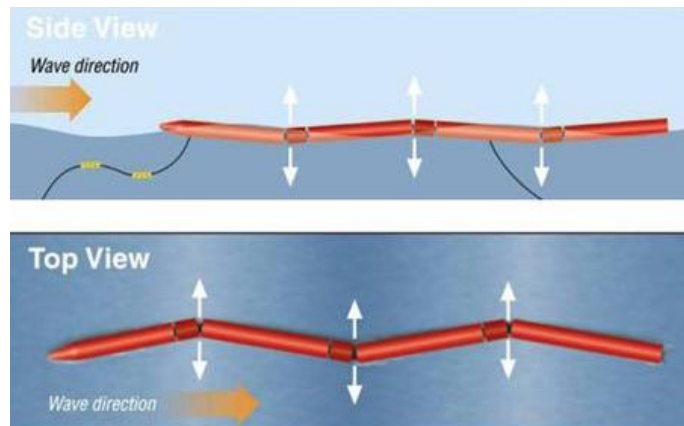


Figure 3 - Pelamis schematic views

Rotary oscillators

Oscillating WECs provided with rotary motion can be either articulated or hinged to a fixed pivot.

As an example of the first category, we describe the Pelamis WEC; for the second one, we show the Salter's Duck prototype and the Surging devices.

Pelamis

The Pelamis WEC (see Figure 3), developed by the Scottish company “Pelamis Wave Power” is a semi-submerged articulated structure composed by 4 floating cylindrical sections linked by hinged joints and held in place by a slack mooring system that allows the machine to auto-align with the propagation direction of the incoming wave [1].

The energy conversion depends on the relative angular motion of the cylindrical sections pairs: the wave-induced motion of the joints is resisted by hydraulic rams, which pump high-pressure oil through hydraulic motors driving three electrical generators.

In their first paradigm, the cylinders have a diameter of 3.5 m and a length of 30 m, the power modules have a diameter of 3.5 m and a length of nearly 5 m, for a total length of the machine of about 140 m. The device is placed offshore, in deep-water and semi-submerged by 2/3. The nominal power output of the machine is 750 kW; a 10 kV three-phase power transformer is situated in the front floating cylinder and sends the electrical energy to a substation in land via underwater power cables [7].

The Pelamis has been the first commercial-scale wave energy converter to generate electricity to a national grid from offshore waves: in 2004, a full-scale prototype machine was installed at EMEC (European Marine Energy Center) in the Orkney Islands (UK).

In 2008, the first wave farm was built at Aguçadoura, off the northwest coast of Portugal, under commission of the Portuguese electricity company Enersis (Figure 4). The wave farm was composed by three first generation Pelamis machines (P1), for a nominal power of 2.25 MW. The farm started generating in July 2008, but was put off in November 2008 due to the financial difficulties of Enersis's parent company Babcock & Brown (www.pelamiswave.com).



Figure 4 - Aguçadoura Pelamis wave farm

Salter's Duck

One of the first methods to extract energy from the waves was invented in 1974 by Professor Stephen Salter of the University of Edinburgh, Scotland, in response to the Oil Crisis [7][8].

The device is essentially a cam that is free to rotate about a pivot.

The 'paunch' of the duck is shaped in such a way that the dynamic pressure induced to particle motions forces the duck to rotate through an axis (indicated with O in Figure 5), capturing part of the kinetic energy within the wave. Moreover, the changing hydrostatic pressure contributes to the rotation by causing the buoyant forebody near the 'beak' to rise up and fall down.

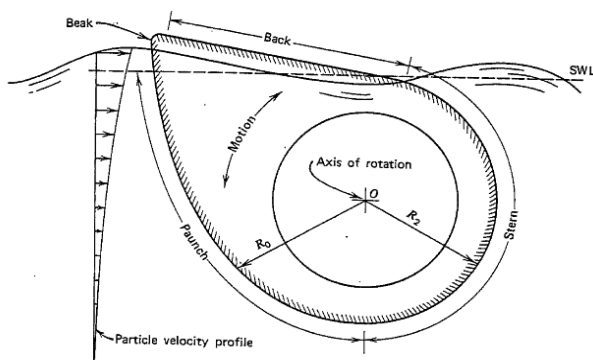


Figure 5 - Salter's duck schematic [4]

Salter's duck prototypes were first built and tested at Edinburgh University. Then, a prototype was constructed in 1976 off Dores Beach in Scotland.

Even if it has been experimentally proved that Salter's Duck is one of the most efficient WECs, no real installation has been attempted, primarily because of its complex hydraulic PTO system, that is not well suited to incremental implementation and because of the high costs and risks of a full-scale prototype [7].

Surging Wave Energy Converters

The Oscillating Wave Surge Energy Converter (OWSEC) is a concept of shoreline or near-shore WEC [9][10]. The OWSEC consists on a hinged flap (or paddle) rotating about a horizontal axis that is placed perpendicular to the direction of propagation of the wave.

Two main conceptual prototypes exist: one having the pivot axis above the SWL and the other with the axis underwater in the vicinity of the seabed (see Figure 6).

Since the fluid particles velocity is larger near the SWL, hinging the flap at the bottom generally represents a better solution, since this produces higher wave-induced torques on the device. However, in shallow water the horizontal water particles motion is still significant at the sea bed, whilst the horizontal motion of the flap would be zero at the hinge.

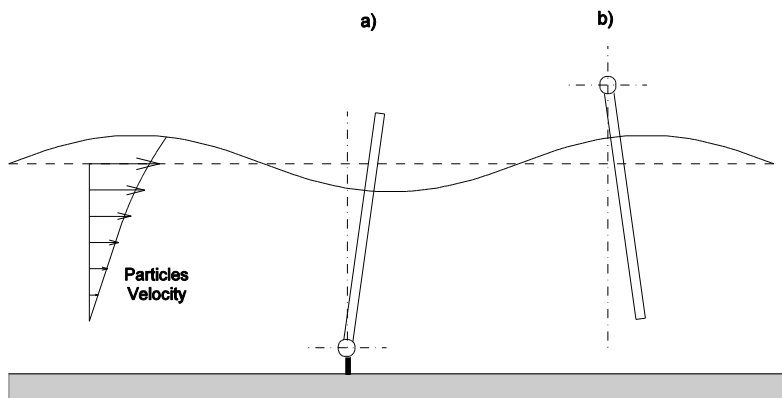


Figure 6 - Wave Surged hinged a) at the bottom b) at the top

Hinging the paddle above the SWL provides two benefits: first, the PTO system is easily accessible; secondly, the top hinged paddle suffers no end-stop problems and could feasibly swing through a full 360° angle [10].

Up to date, some OWSEC prototypes can be identified that are in a pre-commercial stage of development. All of them are hinged from the bottom to a pivot that lies in the vicinity of the sea-bed. A description of these devices can be found in [9].

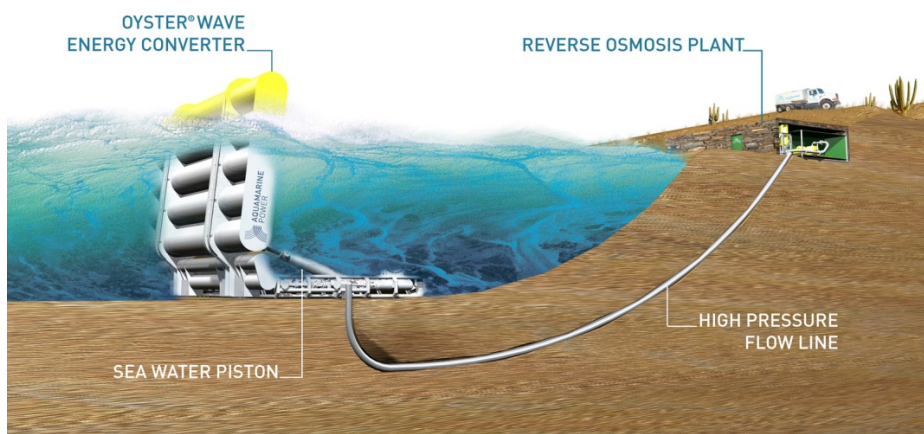


Figure 7 - Oyster device with its power extraction circuit

The most famous example of OWSEC is probably the Oyster device, that has been developed by Queen's University Belfast and by the company Acquamarine Power LTD.

In its present configuration, Oyster is located at a nominal water depth of 12 m (which in many locations is close to the shoreline). The system consists in a buoyant flap, 18 m wide and 10 m high, hinged at its base to a fixed frame anchored to the sea bed. The flap oscillates moving two hydraulic cylinders which pump water at high pressure through a pipeline back to the beach (see Figure 7). On the shore, there is a small hydro-electric plant consisting of a Pelton wheel turbine driving a variable speed electrical generator. The nominal power output of the device is 350 kW [11].

Oscillating Water Column

The Oscillating Water Column (OWC) system consists on a hollow structure built on the shoreline or mounted on a floating structure. The hollow structure is open to the sea and partially submerged, with the immersed part filled with water (namely the water column) and the upper part containing air (namely the air chamber).

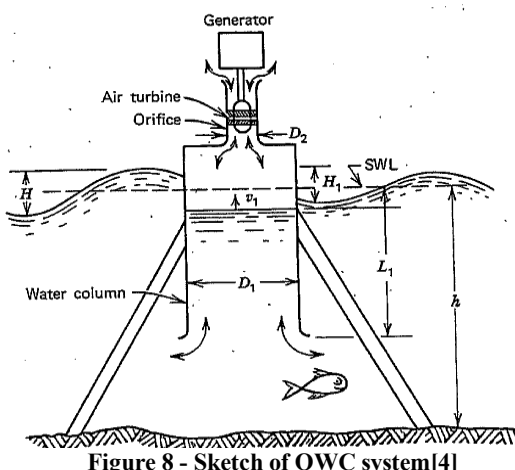


Figure 8 - Sketch of OWC system[4]

When a wave crest approaches the structure, the internal water level rises, generating a compression of the air contained in the chamber. Successively, when the wave returns to the sea, an air depression occurs. The energy contained in the compressed/expanded air is converted into electricity via a turbo-generator.

The turbine (usually of the Well's type) is designed in such a way that it is able to produce power with reciprocating air-flows without the need of reversing its rotating direction [4][7].

Fixed-Structure OWCs

Fixed structure OWCs have a partly submerged concrete or steel structure, open below the water surface, inside which air is trapped above the water free surface.

Among the fixed-structure OWC prototypes, we recall the LIMPET (Figure 9.a) and Pico projects (Figure 9.b) [1].

LIMPET OWC

LIMPET (Land Installed Marine Power Energy Transmitter) prototype was built by Wavegen company in Islay Island, Scotland, in 2000. The PTO of LIMPET consisted in a pair of Well's turbine with a nominal power of 250 kW each and featuring a blades diameter of 2.6 m.

PICO OWC

Another relevant installation is that of the Pico plant, off the Azores coasts [1]: this is a 400 kW rated plant, equipped with a 2.3 m diameter Wells turbine coupled to an asynchronous generator. The turbine includes two fixed guide-vane stators, one at each side of the rotor.

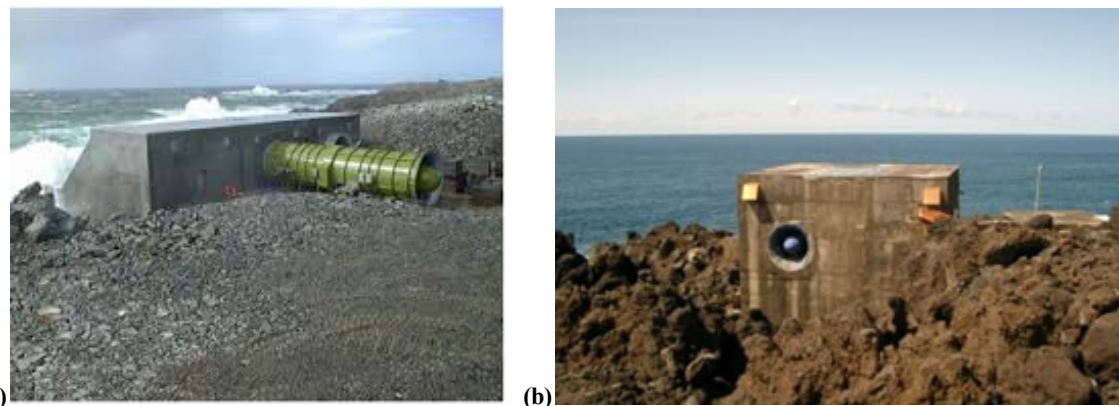


Figure 9 - a) LIMPET OWC b) Pico OWC

Floating-Structure OWCs

Floating-structure OWCs take advantage not only of the cavity resonance but also of the heaving motion of the associated float [4].

Floating-OWC structures were among the first investigated systems, with the most ancient prototype being the Backward Bent Duct Buoy (BBDB) proposed in the seventies [5].

Another, more recent example of a floating-OWC is the Mighty Wale, developed in Japan by the Marine Science and Technology Center. The device consists of a floating structure (with a length of 50 m, a breadth of 30 m and a draught of 12 m) which has three air chambers and buoyancy tanks. Each air chamber is connected to a Wells turbine that drives an electric generator. The total rated power is 110 kW. The device was deployed near the Gokasho Bay, Japan, in 1998 and tested for several years [5].

Overtopping Devices

In their usual form, this kind of devices are provided with a reservoir tank where water, collected through a ramp by exploiting an overtopping mechanism, forms a pressure head with respect to the SWL that can be usefully exploited in a hydraulic turbine.

In the following, two classes of devices are considered: on-shore devices (with the reservoir located on the shoreline) and off-shore devices. For the first category, the TAPCHAN prototype is considered; for the second category, Wave Dragon prototype is described.

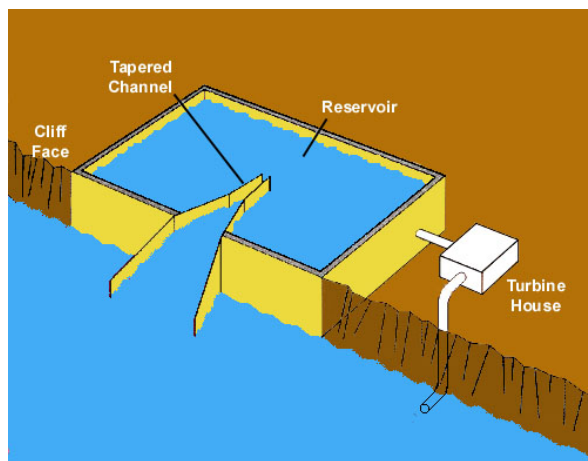


Figure 10 - Schematic of the TAPCHAN WEC

On-Shore Overtopping Devices

TAPCHAN stands for Tapered Channel device (Figure 10). The device was developed in Norway during the eighties.

The TAPCHAN comprises a gradually narrowing channel with wall heights typically of 3 to 5 m above SWL. Waves enter the wide end of the channel; as they propagate through the narrowing channel, the wave height is amplified until the wave crests spill over the walls to the reservoir, which is raised above the SWL.

The water in the reservoir returns to the sea passing through a conventional low-head Kaplan turbine, which works in quite stable conditions due to the storage capacity of the reservoir.

A 40 m wide prototype with 350 kW of rated power was built in 1985 at Toftestallen, Norway, and operated for several years until the early 1990s, when modification works destroyed the tapered channel [12].

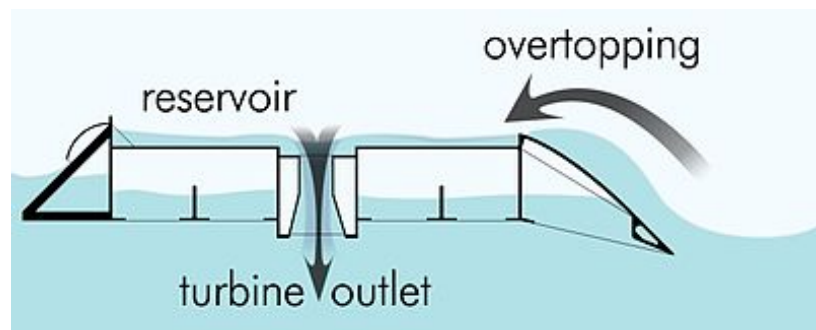


Figure 11 - Wave Dragon conceptual scheme

Off-Shore Overtopping Devices

The Wave Dragon is a floating overtopping WEC, developed in Denmark by the Wave Dragon Aps company. It has been the world's first near-shore WEC producing power to the grid [7].

It consists of two arms, behaving as wave reflectors, focusing the waves towards a ramp (see Figure 11). Behind the ramp there is a reservoir, where the water that runs up the ramp is collected and temporarily stored. The PTO consists of several variable speed low-head hydro-turbines directly coupled to permanent magnet generators [13]. Compared to other types of WEC, one point of interest is that Wave Dragon is a relatively simple and reliable device. In fact, the only moving parts are the hydro-turbines. This is essential for a device operating in near-shore conditions, where the extreme forces seriously affect any moving part [7].

A 57 m-wide and 237 t (including ballast) prototype of the Wave Dragon has been deployed in Nissum Bredning, Denmark (see Figure 12). Such a prototype was constructed to match a wave climate with estimated power per unit crest length of 0.4 kW/m only and had a rated power output of 20 kW. The prototype was grid connected in May 2003 and has been tested for 3 years and a half. The Nissum Bredning prototype is a traditional (ship-like) steel plate construction, primarily made by 8 mm steel plates. The total steel weight of the main body plus the ramp is 150 t. To obtain the desired 237 tonnes total weight, 87 tons of water ballast are added (www.wavedragon.net).



Figure 12 - Wave Dragon prototype at Nissum Bredning (DK)

With respect to a typical North Sea condition, the tested prototype represent a 1/4.5 scale model: indeed, referring to a yearly average power per unit crest width of 24 kW/m, a 22000 tons reinforced concrete structure is required,

occupying an area of about 150 m x 260 m and having rated power of 4 MW [13]. However, according to the site of the company, the dimensions can be scaled differently in order to adapt the device to stronger wave climates too.

1.1.3 Traditional Power Take Off Systems

In this paragraph, a review of existing PTO systems traditionally used in WEC systems is presented. Only the most significant examples are considered here. For a comprehensive description, the reader can refer to the works by Cruz [1] and Falcão [5].

Air turbines for OWCs

Two types of air turbines are generally associated to the idea of OWC prototypes: the Well's turbine and the Impulse turbine.

The key design parameter impacting the turbine performance is the rotational speed, which is operationally determined by the required torque-speed characteristic and the generator power output [1].

Two matching principles have to be followed when designing a turbine for an OWC system:

- The turbine must provide a damping effect (that, among other, limits the air flow exiting the system) that maximizes the conversion from wave energy to air flow kinetic energy.
- The turbine must also maximize the conversion from air kinetic energy to mechanical energy (namely the energy transferred to the generator) over the range of effective flow rates. Notice that, in any case, this conversion is upper bounded by the Betz limit (no more than 16/27 of the kinetic energy of air can be converted to mechanical energy for the generator).

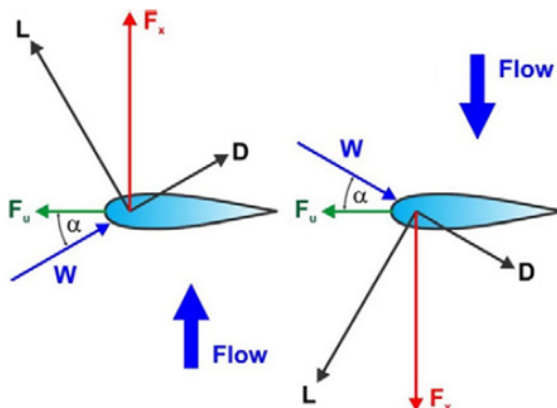


Figure 13 - Wells turbine operating principle

Wells Turbine

The Wells turbine was invented during the seventies by Allan Wells of Queen's University Belfast. It is a self-rectifying air turbine, that means that its torque does not depend on the air flow direction. This is an essential feature since the operating principle of OWC provokes air moving in a certain direction while the water level in the column is raising, and in the opposite direction when the water level drops. Several versions have been studied: single rotor with or without guide vanes (used in the Pico plant), twin rotors in series, two counter-rotating rotors (used in the LIMPET plant). The Wells turbine is the most frequently proposed PTO for OWC systems [5].

The turbine is based on a symmetric airfoil; its operating principle is shown in Figure 13.

Aerodynamic lift (L) and drag (D) forces are generated perpendicular and parallel respectively to the relative flow velocity. Indicating with α the angle of attack of the relative velocity w with respect to the cord of the profile, the resulting total force can be resolved into a tangential and an axial component F_T and F_X respectively.

$$F_T = L \sin \alpha - D \cos \alpha$$

$$F_X = L \cos \alpha + D \sin \alpha$$

Notice that, for any direction of the flow, the direction of F_T remains the same, thus, being F_T the force that generates the torque about the turbine rotation axis, the device is able to work with an air flow moving in each of the two directions. However, at very low flow rates, F_T is negative because the aerodynamic drag tends to overpass the lift. Moreover, for excessive air-flow rates the turbine does not work due to the boundary layer separation condition (stall) [1].

The choice of symmetric airfoils is necessary in order to guarantee the self-rectifying behaviour of the turbine. However, as compared to cambered profiles, this provides worse values for the aerodynamic efficiency.

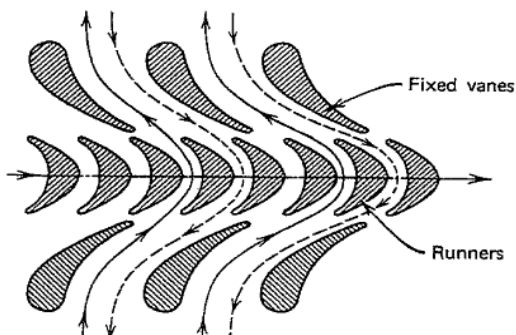


Figure 14 - Impulse turbine blades

Impulse Turbine

The most popular alternative to the Wells turbine is the self-rectifying impulse turbine. It has a rotor that is equal to the one of a conventional single-stage steam turbine (with symmetric blades). Since the turbine is required to be self-rectifying, instead of a single row of guide vanes there are two specular rows, one at each side of the rotor (see Figure 14) [4][5].

To maximize the power capture efficiency, pivoting guide vanes were tested. However, potential problems with maintenance of such a complex mechanism brought to the mechanical simpler but less efficient solution with fixed vanes [1].

Comparisons between impulse turbine and Wells turbine are not easy and in general are valid only in a small operation range, since the efficiency of the Wells turbine strongly depends on the Reynolds number [5]. In general, being Wells turbines characterized by higher rotational speed, this type of turbine enhances the energy storage (due to the flywheel effect), thus providing more constant power output to the grid, and is expected to allow a cheaper electric generator to be used. On the other hand, thanks to its lower blade tip velocity, the impulse turbine is less constrained by Mach number and centrifugal stresses limitations [5].

Hydraulic systems

Hydraulic systems are generally based on an high-pressure oil circuit, that usually includes a gas accumulator system (with time energy storage capacity of few wave periods) with the aim of smoothing the power output of the connected WEC so as to make it as constant as possible [5].

Other components are

- An hydraulic cylinder or ram with the aim of converting the mechanical energy acquired by the WEC to hydraulic potential energy;
- A hydraulic motor used to run an electric generator.

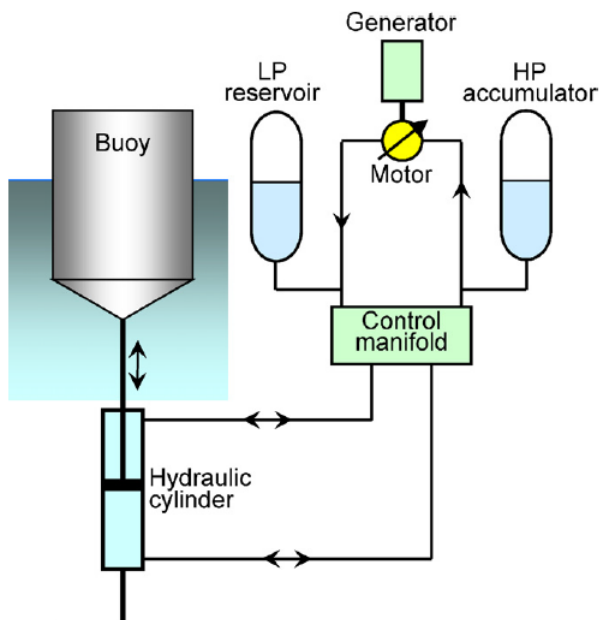


Figure 15 - Hydraulic PTO of a heaving WEC [5]

The schematic of a typical hydraulic circuit for the extraction of energy from a heaving WEC is shown in Figure 15.

Beyond the well-known criticalities brought by hydraulic circuits (high number of components, heaviness, sensitivity to damages), these systems are probably the most suited to handle relevant forces like those acting on WECs. The net force generated by an oil circuit with a typical pressure of 350 bar is at least one order of magnitude higher than those allowed by an electrical machine [1].

For this reason, high-pressure oil circuits have been tested as PTO systems both in translational heaving WECs (buoys) and rotational devices (like Pelamis or Oyster).

Linear Electric Generators

The use of linear electric generators may represent an advantage for applications that involve linear or reciprocating motion since they bring a simplification in the design and in the mechanical interface (gears and shafts).

In Figure 16 a comparison is shown between the operation of a rotary generator (on the left) and a linear generator (on the right) coupled with a heaving WEC.

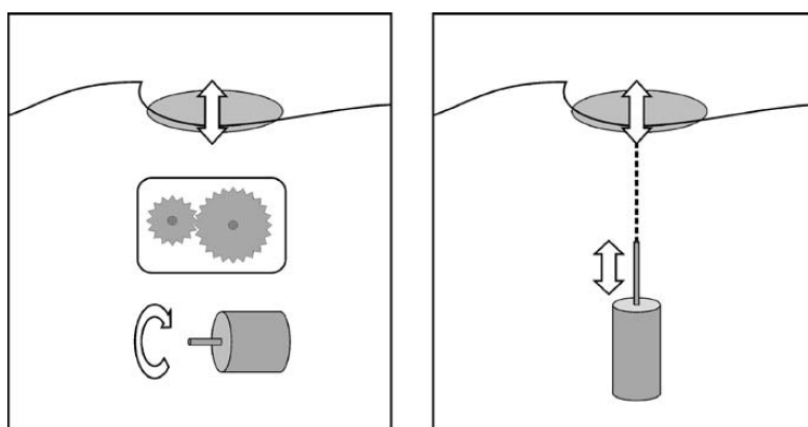


Figure 16 - Comparison between rotary and linear generator [1]

To convert the slow reciprocating motion of the ocean wave into a fast rotating motion, that is required by conventional high-speed rotating electrical machines, some kind of intermediate conversion step is necessary. This is usually obtained via gears or shafts.

A low speed linear generator can be directly connected to the heaving WEC without any intermediate system [1].

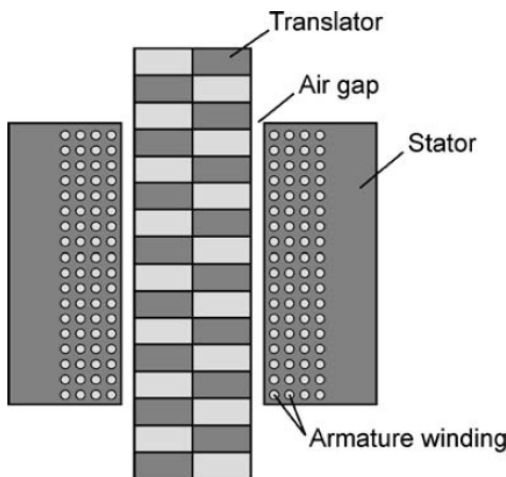


Figure 17 - Operating principle of linear generator [1]

A linear electromagnetic generator consists of a moving part (translator), on which magnets are mounted with alternating polarity. The translator plays the same role of the rotor in rotating generators. It moves linearly next to a stationary stator provided with windings (see Figure 17).

An air gap is present between the translator and the stator. The translation of the moving part generates time dependent variations in the magnetic field that induce a voltage in the windings.

In wave energy applications the translator reciprocating motion matches the motion of the actual device (usually at speeds two orders of magnitude lower than the typical velocities of rotary generators). At such low speeds, the forces are very large. This makes linear generators be rather bulky and heavy.

With respect to their rotary counterparts, the lower transmission requirements of linear generators are usually counter-balanced by increased specifications on the electrical machine itself.

1.2 Dielectric Elastomer Generators

Dielectric Elastomers (DEs) are incompressible solids which exhibit non-linear elastic finite deformations and linear strain-independent dielectric properties. DEs can deform in response to an applied electric field, and can alter the electric field and/or potential in response to an undergone deformation. Thanks to this Electro-Mechanical (EM) coupling, DEs are currently being investigated as transduction materials for solid-state actuators, sensors and generators [14].

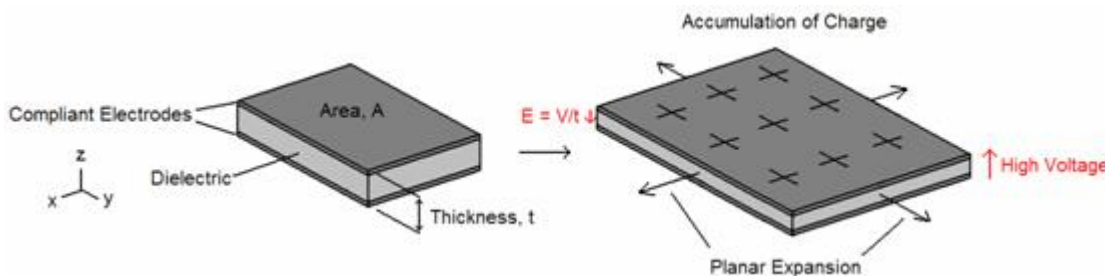


Figure 18 – DE transducer architecture and working principle

As shown in Figure 18, DE transducers comprise one or more sheets of incompressible dielectric rubber (in Figure 18 only one sheet is considered) which are sandwiched between compliant electrodes to form a deformable

capacitor. In actuator mode, electrostatic attraction between oppositely charged electrodes is used to convert electricity into mechanical energy. In sensor mode, measurements of the deformable capacitance are used to infer transducer strains or stresses (that is, displacements or forces). In generator mode, mechanical energy is converted into direct electricity via the variable-capacitance electrostatic generator principle.

Properties of DEs which make them suited for transduction applications are: low mass density; large deformability; high energy density; rather good electro-mechanical conversion efficiency; moderate or low cost; solid-state monolithic embodiment with no sliding parts; easy to manufacture, assemble and recycle; good chemical resistance to corrosive environments; silent operation.

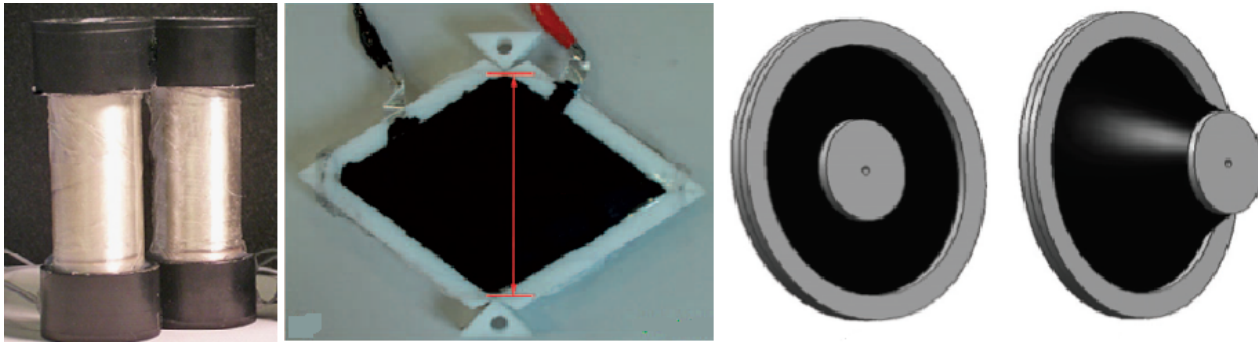


Figure 19 - Some architectures of DE transducer

Examples of commercially available DEs are acrylic elastomers, silicone elastomers and natural rubber, which are usually provided in the form of thin membranes (films) and distributed in rolls.

Neglecting their EM response, these polymers are widespread in a number of different applications; for instance: acrylic elastomers are commonly employed as pressure-sensitive adhesives; silicone elastomers are used for the manufacturing of gaskets and sealants in the automotive, construction and household fields; natural rubber is used for the manufacturing of vehicles tires and medical protection systems (such as gloves).

Practical examples of DE transducers with lozenge [16], cylindrical [18] and conical [19] shape are shown in [20-21].

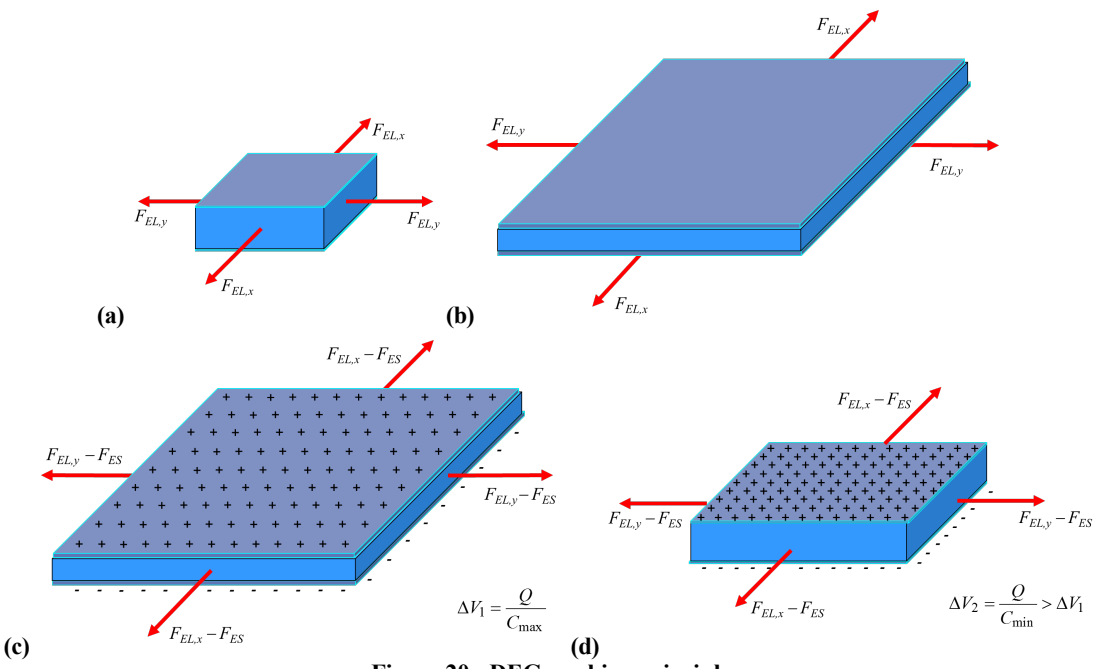


Figure 20 - DEG working principle

1.2.1 Working Principle

As stated before, a DEG can be considered as a deformable capacitor (the capacitance of which varies with the deformation) that is operated cyclically. The working principle of DEGs is briefly schematized in Figure 20. Starting from an undeformed configuration (Figure 20.a), the DEG is first subjected to an external mechanical load so that its area expands to a maximum value (see Figure 20.b). Since the material is nearly incompressible, while the area of the DE membrane (and thus of the electrodes) increases, its thickness decreases, and the capacitance of the resulting condenser is maximum (being the electrodes surface maximum and the membrane thickness minimum). In this configuration, opposite charges ($+Q, -Q$) are deposited on the electrodes (Figure 20.c). Once fully charged, the membrane is brought back to its original configuration (Figure 20.d). This reduces DEG capacitance, thereby producing (in presence of a constant charge Q) an increase in the electric energy stored in the DEG. Clearly, part of the mechanical energy conferred to the membrane during the deformation phase has been converted into electrical energy.

The conversion mechanism can be alternatively explained by noticing that the electrostatic attraction of the charges residing on the opposite electrodes yields a decrease in the force that is required to maintain the DE membrane in the stretched state. For this reason, as represented in Figure 20, the tractive force ($F_{el} - F_{es}$) during membrane contraction is lower than the tractive force (F_{el}) during membrane expansion. As a consequence, the mechanical work returned by the DEG during the contraction phase is lower than the mechanical work absorbed during the expansion phase (the difference between these works representing the amount of energy that is converted into electricity).

The working principle described above is only ideal. In the reality, some energy dissipation occurs due to both mechanical and electrical dissipative phenomena. The most important causes for these energy losses are: internal material visco-elasticity; power dissipation due to the resistivity of the electrodes; leakage currents through the DE membrane thickness.

With regard to energy conversion performances, a significant parameter that is employed to evaluate and compare different DEG architectures is the energy per unit weight of elastomer that the generator is able to convert. This parameter plays a significant role in the determination of the amount of material that is required in a given application and, thus, in the determination of the level of compactness that the resulting DEG can achieve.

A summary of the major achievements in DEG technology is provided below.

A pioneer experimental study on DEGs was carried out by Pehrine et al. [22] who measured energy densities of 0.4 J/g and estimated possible densities up to 1.5 J/g.

Koh et al. [23][24] performed a theoretical study on a square DEG that is subjected to an equi-biaxial state of deformation (namely, as depicted in Figure 21 the membrane is stretched uniformly along the two sides). For this configuration, a maximum energy density of 3.2 J/g was estimated.

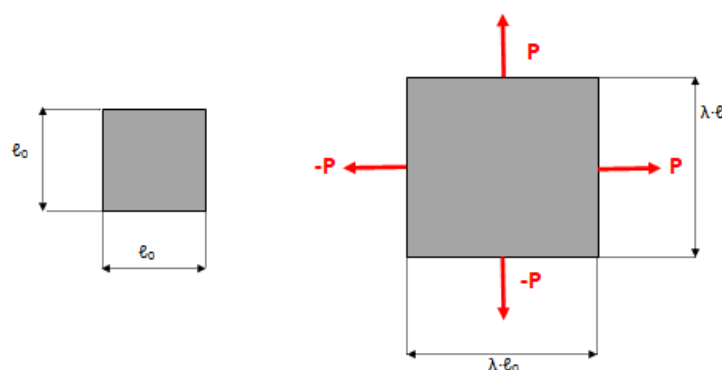


Figure 21 - Equi-biaxial state of deformation

For a similar configuration, Jean-Mistral [25] measured a maximum energy density of 1.7 J/g.

Similar to piezoelectric ceramics, DEGs generally work at high voltages, typically in the range 1-10 kV [22]. This requires proper driving circuits and electrical/electronic components. To date, the availability of transistors that could be used for this specific application is very limited.

1.3 Dielectric Elastomer Wave Energy Converters

The present paragraph introduces the use of DEGs in Wave Energy Converters (WECs).

A traditional WEC comprises several rigid components, which are made of stiff, heavy, shock-sensitive, corrosion-sensitive and costly metallic materials, and include wave-interacting bodies, mechanical/hydraulic transmissions, electromagnetic generators, step-up transformers and eventually frequency changers or rectifiers.

In a first simple approach, the employment of DEGs may be confined only to the replacement of the traditional (electric or hydraulic) PTO system of existing WEC architectures.

In a more ambitious perspective, DEGs could integrate all the components of a WEC (including wave-interacting bodies, mechanical transmissions and power electronics) into a single soft electroactive elastomeric body, which undergoes liquid-like deformations under the action of sea waves.

The interesting aspects concerning the application of DEGs to wave energy conversion can be summarized in the following points:

- DE materials are soft, resilient and lightweight. Thanks to their high deformability, they are suited to be directly coupled with moving oscillating WECs that undergo large displacements without the necessity of any intermediate mechanical transmission.
- Polymeric materials are corrosion-resistant. Thus, they are particularly suited for applications in aggressive environments (like sea water).
- Many common polymeric materials are already widely spread and largely used. Thus, they are available at relatively low price.
- Traditional electrical and mechanical generators are not suited to operate within the sea environment, since they are made by a number of sensitive moving parts that have to be kept isolated from the water. DEGs application would significantly reduce the amount of moving mechanical parts. Moreover, due to the simplicity of their mechanical layout (that essentially includes an articulated frame and a deformable membrane), they allow a drastic reduction in the number of parts that can potentially meet mechanical failure.
- As already mentioned, a large variety of DEGs can be designed, each exploiting a particular motion condition (angular pitch oscillation, linear reciprocating motion, movements with multiple degrees of freedom). Therefore, for a particular design of a WEC device, a proper architecture for the corresponding polymeric PTO can be investigated and identified.
- DEGs convert the energy from the waves into high-voltage direct-current electricity, that is immediately ready to be delivered to the coast via long underwater transmission lines. Therefore, their application would allow to solve the troublesome problem of using frequency changers to interface a natural low frequency system (the WEC moving within the waves) and a system that requires high frequency (the traditional electric apparatus, since traditional electric machines usually have a high nominal frequency of operation).

As a counterpart, some possible criticalities are listed below:

- DE materials may be subjected to aging and performance losses during their lifecycle.
- DE materials present both mechanical (hysteretic) and electrical losses. A proper analysis of the limitations to the amount of convertible energy has to be carried out, and a targeted choice of the materials has to be done.
- In order to avoid the rupture of the polymeric material, DEGs must be subjected to limited displacements (in order to keep the strain on the elastomeric membranes below the rupture value). WECs operating in real sea are subjected to storms and gales that provoke very large oscillation amplitudes of the moving part of the converter. DEGs for WECs should be designed in a way that the material is kept below the stretch safety value in a certain range of conditions; when the sea conditions exceed the safety limit, the oscillating body must be halted or, anyway, the DEG must be disconnected from the moving body. In order to achieve this result, proper safety devices (like controlled clutches, brakes etc.) must be designed.
- DEGs are a relatively new concept. In fact, their study and application is limited to experimental laboratory-scale applications. Many of the weak points of this technology have not been identified yet, mainly because of the lack of sufficient trials in a real operating environment.

Based on the different mode of interaction between the DEG Unit (DEGU) and the fluid, two types of Polymeric WECs can be identified: first-generation devices and second-generation devices. The characteristics and peculiarities of each kind of Polymeric WEC are described in the following sections.

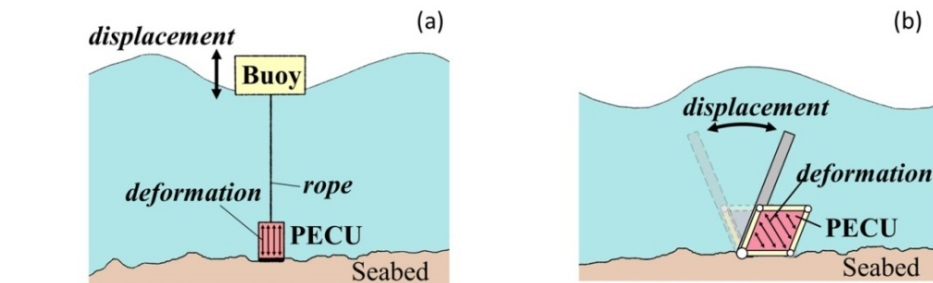


Figure 22 - Examples of first-generations DE-WECs

1.3.1 First-Generation Devices

These devices are characterized by the indirect interaction between DEGU and fluid. In this case, DE deformations are not directly generated by fluid pressures, but by a mechanical interface (see Figure 22.a and Figure 22.b). Thus, in this case, two distinct bodies are identified: a WEC, that is the body mechanically excited by the waves; a DEG PTO that converts kinetic and potential energy of the WEC to electrical energy.

Examples of first generation DE-WECs are heaving or pitching bodies (buoys, flaps etc) that activate a deformable DEG provided with a rigid frame that is partially built within the WEC.

Due to the absence of direct fluid-DEGU interaction, the modeling, design and control of first-generation DE-WECs is simplified.

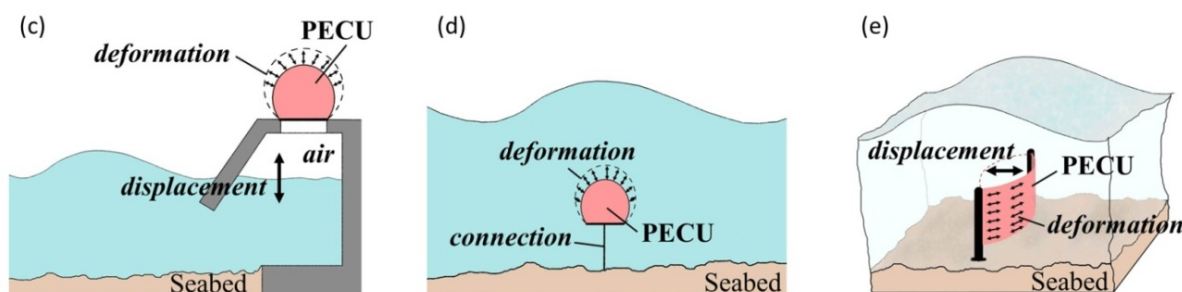


Figure 23 - Examples of second-generation DE-WECs

1.3.2 Second-Generation Devices

These devices are characterized by direct interaction between DEGU and fluid, which occurs over wide contact surfaces.

In this case, fluid-DEGU interaction is not mediated by any mechanical means, and DE membrane deformation is directly generated by wave-induced fluid pressures (see Figure 23).

As a result, second-generation devices are highly-integrated WECs that feature the minimal number of mechanical and electrical components beside the DEGU. Moreover, thanks to their intrinsic and tunable compliance, such devices make it possible to optimize and control their radiation impedance in order to achieve maximal wave-energy extraction.

Examples of second generation converters are close-chamber oscillating water-columns exploiting a deformable membrane instead of an air turbine and inflatable bodies.

With respect to first-generation devices, this second type of DE-WECs is much more difficult to model, design and control.

1.3.3 SoA and Patent

1.3.3.1 First-generation DE-based WEC prototypes

In August 2007, SRI International and HYPER DRIVE Corp. tested a generator prototype designed to provide on-board power to a navigation buoy. The generator (Figure 25) was a cylindrical tube with a diameter of 40 cm and a height of 1.2 m. Two hollow roll-type DEG modules, each of about 30 cm in diameter and 20 cm in height (in the stretched state), were placed inside the tube. A 62 kg inertial mass attached at the bottom of the DEGs guaranteed both the pre-stretch of the polymeric membranes of the DEGas well as the transmission of the oscillating forces generated by the wave-induced buoy oscillations.

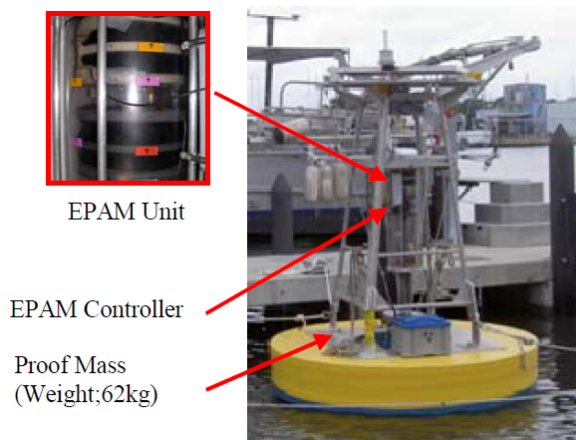


Figure 25: First prototype based on mass inertia.

The considered WEC was able to produce a peak power of 1.2 W, with an average power of 0.25 W, in a sea state featuring a wave height of about 10 cm. The estimated energy conversion efficiency was 70-75% (not including hydrodynamic losses) [30].

A second experiment [31] was based on an articulated multi-buoy system exploiting the same type of DEG. In this case (Figure 26) the oscillating forces came from the differential oscillation of the different buoys. In presence of an incident wave, the relative movement between two buoys stretched a DEG roll using a lever arm. In this case the average produced power was 1W.

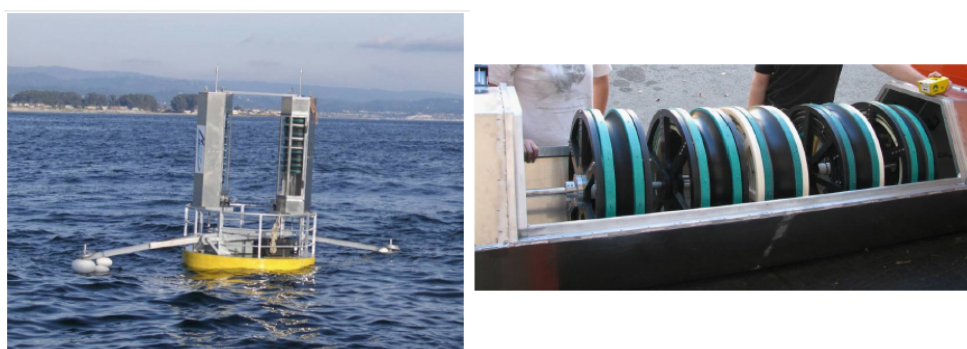


Figure 26: First prototype based on differential floating bodies forces.

One last experiment, based on a small-scale prototype (see Figure 27), had the goal of demonstrating that the energy output of DE-based WECs is almost independent of wave period [32]. The considered prototype was based on a floating body having a DEG attached on the mooring line. As reported in Figure 28, the electricity generated per cycle as a function of the wave period shows that the energy output is largely independent of wave period, except for a short interval of wave periods. In fact, for wave periods of approximately 1.2 s, a peak on the energy output occurs. This phenomenon is probably related to the system resonance frequency.

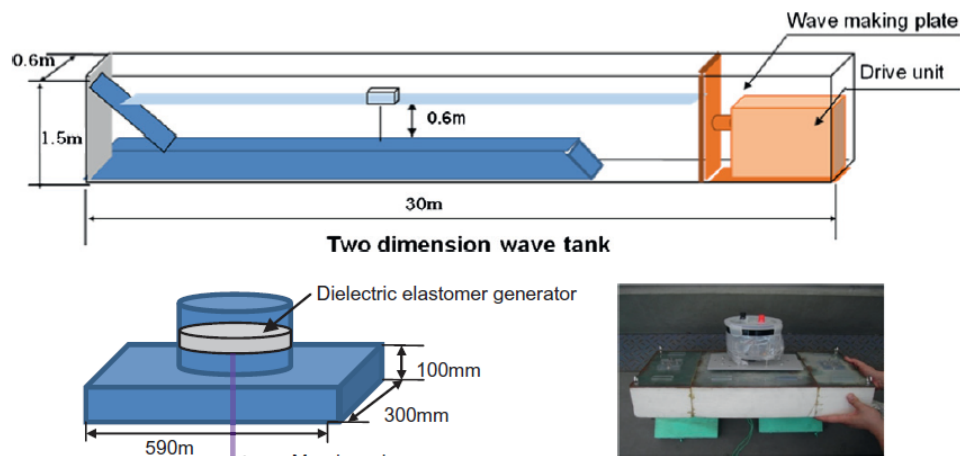


Figure 27: The two dimension wave tank and the mooring method for the floating body.

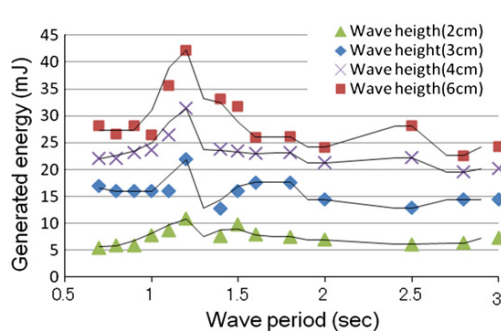


Figure 28: Electrical energy output as function of wave period and height.

The researchers foresee the possibility to develop a DE-based buoy with 6 MW of rated power and capable of producing energy at approximately 19 US cents/kWh [32].

1.3.3.2 Second-generation DE-based WEC prototypes

The “Standing Wave Tube Electro Active Polymer Wave Energy Converter” (S3) is a project developed by Single Buoy Mooring (SBM) and covered by the patent WO2010146457 [33].

The S3 is a floating submerged Wave Energy Converter (WEC) that is made by a cylindrical DEG. The system is a multiple degrees of freedom resonant flexible WEC. It is made by a long elastomeric tube, several wave lengths long, having DE rings on its walls. The tube is closed at both ends and filled with pressurized sea water at a pressure higher than the external sea water pressure, in order to create a static pre-strain on the EAP (Figure 29).

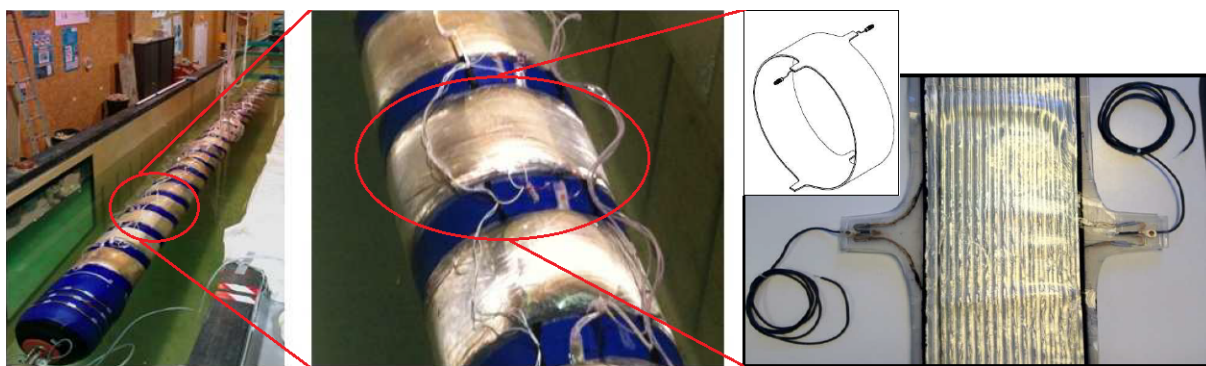


Figure 29: S3 prototype with cylindrical DEGs

The tube can expand or contract in diameter while its length is kept constant using axial fiber reinforcements. When ocean waves travel above the S3, a time-varying pressure is applied on the tube walls; this induces local changes in diameter and time-varying stretching of the DEGs which are used to perform energy harvesting cycles (Figure 30). The output is high voltage multiphase Direct Current with low ripple.

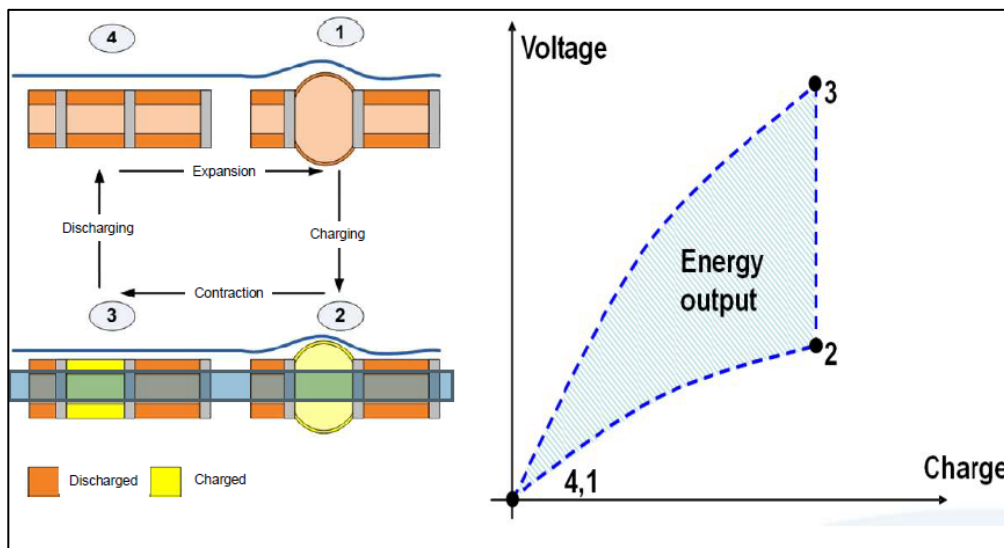


Figure 30: One type of energy harvesting cycle on the S3 WEC

In 2010, SBM proved the concept of the S3 WEC using a small-scale model: a 11m long and 40 cm diameter silicone tube with 25 cylindrical DEGs. The peak power produced in the tests was 2 W, while the mean power was 0.45 W. SBM claims that this small scale S3 WEC is capable to produce an average power of 100W in waves with a height of $H_s=20$ cm and a period of $T_p=3$ s. SBM is currently developing a new prototype at the SEMREV test center in France.



Figure 31: S3 small-scale model, inflation test up to 40% strain and installation with horizontal mooring.

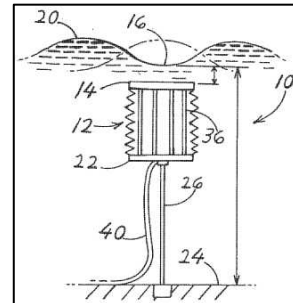
1.3.3.3 Patents

This section provides a list of patented WEC concepts that feature DEGs as PTO for energy conversion. For each patented concept, system description and main bibliographic data are provided.

Wave Power Generator Systems (WO2008133774A1)

Applicant: SINGLE BUOY MOORINGS

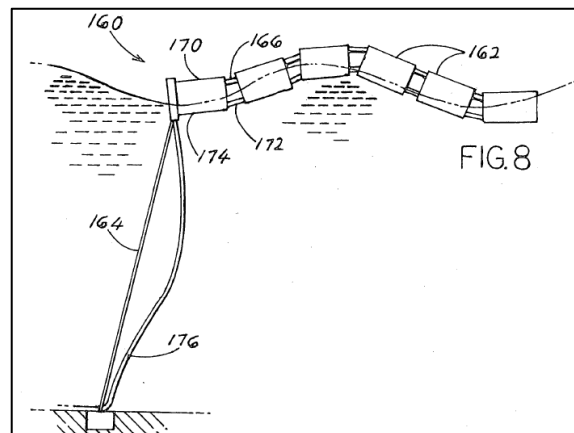
In the system (10), a buoyant element (12) has upper and lower parts (14, 22) connected by a quantity (36) of Synthetic Stretchable Materials (SSMs), with the lower part anchored at a fixed height above the sea floor (24) and with the upper part movable vertically to stretch and relax the SSM as waves pass over.



Wave Power Generator Systems (WO2008133774A1)

Applicant: SINGLE BUOY MOORINGS

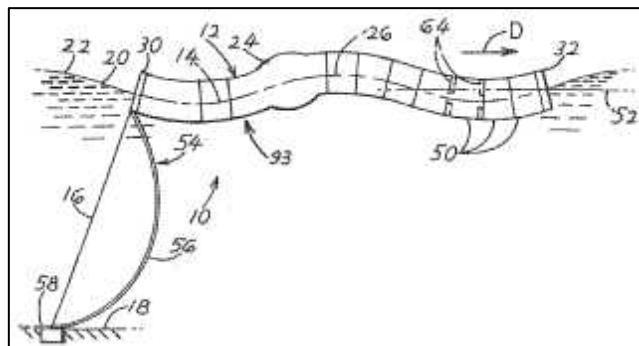
System (160) includes a series of rigid buoys (162) that float on the sea surface and that are connected in tandem by SSMs. One end of the series is linked to the sea floor by an anchor line (164). SSM material (166) connects the upper ends (170) of adjacent buoys, and SSM material (172) connects the lower ends (174) of adjacent buoys. The buoys rotate with respect to one another as they float in a wave. The pivoting results in the SSM material (166,172) stretching and relaxing and creating electricity that is carried out through an electrical cable (176).



Wave Energy Converter (US8120195)

Applicant: SINGLE BUOY MOORINGS

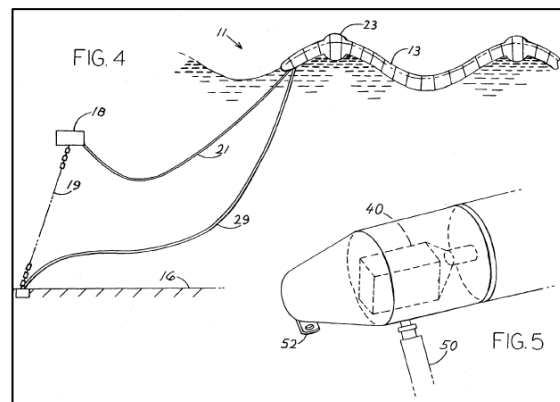
An elongated elastic tube (12) floats at the sea surface (20) (or at a shallow depth below it) and extends, at least partially parallel, to the direction of wave propagation (D). The tube bends as a wave passes by, stretching and relaxing a SSM (44, 60, 62) which generates electricity.



Environmental Electrical Generator (WO2010146457)

Applicant: SINGLE BUOY MOORINGS

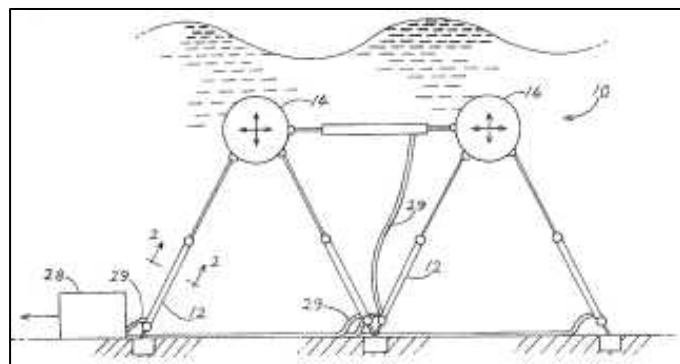
System (11) includes a floating flexible tube (13) with one bow end that is moored by mooring lines (21,19) to the sea floor (16). The tube consists of multiple segments or capacitors which have the shape of tubular ring segments. Both ends of the tube are closed and pressurized by a fluid (like water or pressured air) that is contained within the tube. Due to sea waves action, the fluid contained in the tube creates a travelling bulge (23) which forces the capacitors to strain in radial direction.



Environmental Electrical Generator (WO2010146457)

Applicant: SINGLE BUOY MOORINGS

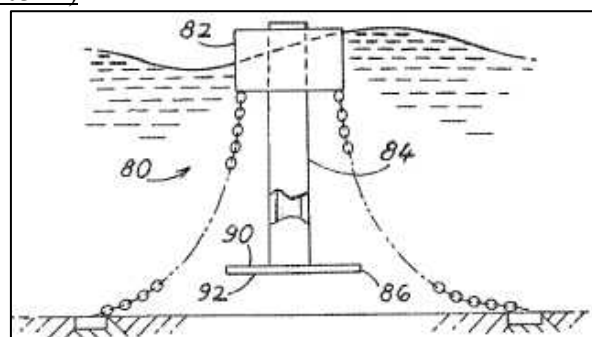
DEG rolls in a waterproof cover (12) are used as deformable capacitors. The capacitors are connected to buoyant elements (14) and are integrated in the mooring lines that are connected to the seafloor. Even in a quiescent sea (with no waves) the main layers (or rolls) of the capacitor devices are pre-tensioned. When the crest of a wave passes over the apparatus, the buoyant member rises and stretches the SSM layers of the capacitors.



Enhanced wave power generators (US2009202303A1)

Applicant: SINGLE BUOY MOORINGS

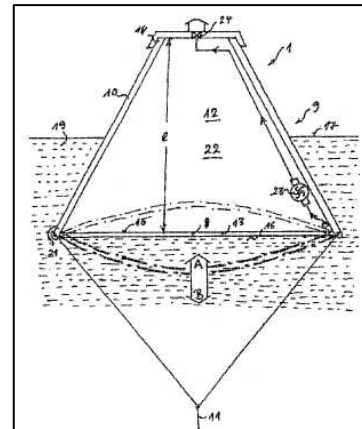
The System includes a float (82) that lies at the sea surface and moves up and down with the waves. A motion-resistant element (90) moves horizontally with the float but resists vertical movement. Electricity-generating apparatus is coupled to the float and to the resistant element for generating electricity as the float moves vertically relative to the resistant element.



Wave Energy Transformer for the Conversion of Mechanical Wave Energy into Electrical Energy, with Electro Active Polymer Foil and Arranged as Wave Follower in Floating Body (DE102009053393)

Applicant: BOSCH

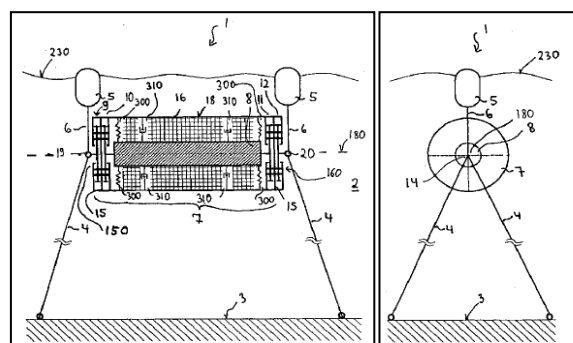
The wave energy transformer (1) has a DEG foil (8) and is arranged as a wave follower (9) in a floating body (10). The floating body has a flask-shaped upward and downward open hollow body (12), which has a diaphragm (13). The diaphragm prevents the passage of the hollow body. The diaphragm houses the DEG foil.



Wave Energy Converter for Converting Kinetic Energy into Electrical Energy (WO2012000618)

Applicant: BOSCH

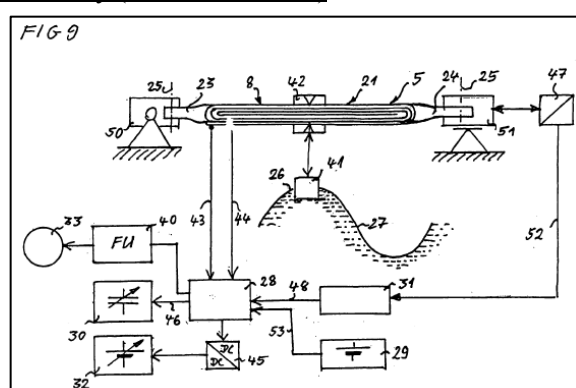
The invention relates to a wave energy converter for converting kinetic energy of wave motion into electrical energy. The wave energy converter has a cylinder (7), which is guided in the fluid (2) in a way that it can follow the motion of the fluid (2) itself. A second body (8) is coupled to the cylinder (7) and can experience a relative motion with respect to the cylinder itself. An energy conversion unit (16) is used to convert the kinetic energy of the relative motion between the second body (8) and the cylinder (7) into electrical energy. The energy conversion unit (16) contains a capacitor, which contains an electroactive polymer. The capacitance of the capacitor changes when the electroactive polymer is deformed. The relative motion between the second body and the cylinder causes a capacitance change.



Energy Transformer with Electroactive Polymer Film Body (WO2011060856)

Applicant: BOSCH

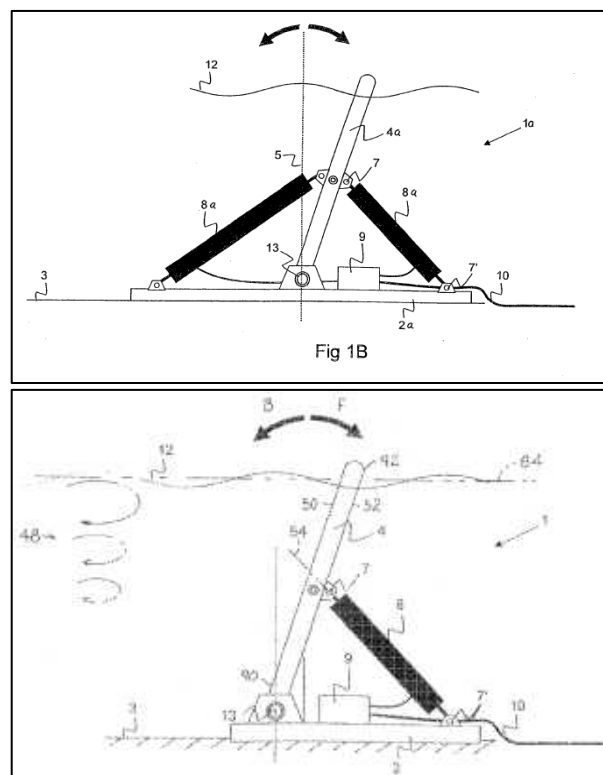
A wave energy transformer (5), made by electroactive polymers, is clamped at both ends (23) and (24) to holders (50) and (51) or fixed by screws (25). The movement of the shaft (26) is transmitted to the electroactive polymers through a coupling element (42) linked to a floating body (41).



Near Shore WEC System (WO2011151693A2)

Applicant SINGLE BUOY MOORINGS

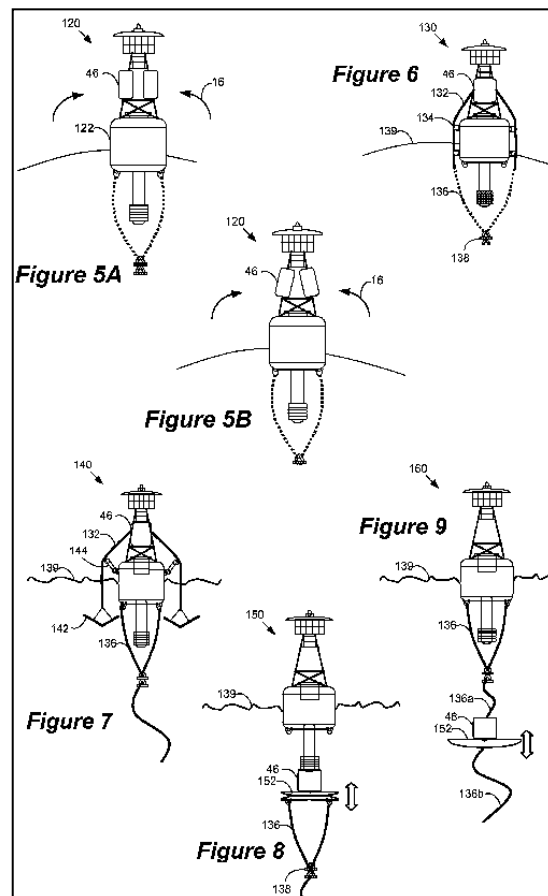
The system is designed with the aim of obtaining energy from water movements in shallow waters, using panels (4) that are pivotally mounted (13) near the sea floor in shallow water and that extend up to the sea surface, or that are pivotally mounted above the sea surface and extend down into the water. As water near the sea surface moves in ellipses (48), or largely back and forth, the panel pivots back and forth. A cylinder (8), with one end (7') mounted on a stationary base and the opposite end (7) connected to the panel, carries at least one sheet of elastomeric material that has electrodes on opposite faces. As the panel pivots back and forth, the sheet is repeatedly stretched and relaxed to vary the voltage between the electrodes so as to generate electricity. A cylinder (8) can be used whose ends move toward and away from each other, or a cylinder can be used whose ends pivot about the cylinder axis relative to each other.



Wave Powered Generation Using Electroactive Polymers (US2007257490)

Applicant: Stanford Research Institute International

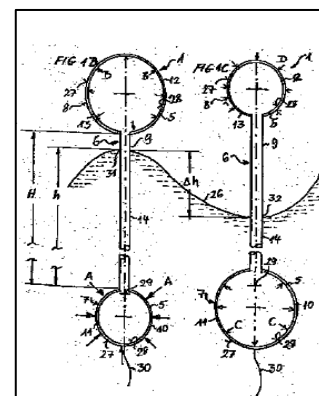
Buoys (120,130,140,150,160) include multiple “Mechanical Energy Conversion Systems” (MECS) enclosed in self-contained units (46). MECS convert mechanical energy into electrical energy using electroactive polymers. In a buoy (120), MECS (46) are located around the upper periphery of the buoy body, away from the its vertical center (120). While in Figure 5A MECS (46) can exploit only the up and down heaving motion of buoy (120), in Figure 5B MECS (46) can exploit also any angular motion(16) of the buoy (120). In Figure 6, upwards and downwards motion of the buoy (130) transmits mechanical energy to MECS (46) through cables (132) linked to anchoring point (138) via mooring cables (136). Figure 7 represents a similar system whose cables (132) are linked to water brakes (142) that resist both upwards and downwards motions of buoy. In Figure 8 water brake (152) includes a rigid plate that resists both upwards and downwards motions of the buoy (150). Mooring cables (136) are attached to the bottom of the water brake (152). Movement of the buoy (150) relative to the base (138) is damped by a brake (152) and causes a net displacement of the MECS (46).In Figure 9, the buoy (160) has a first mooring cable (136a) linked to a MECS (46) that is fixed on a water brake (152)that is anchored to the second mooring cable (136b). Relative motion of the buoy with respect to the water level (139) generates a pulling load on a cable (136a) that transmits mechanical energy to the MECS (46).



Wave Energy Transformer, i.e. Electro-Active Polymer Transformer, for use as Point Absorber Generator in a Wave Energy Plant. (DE102009054059)

Applicant: BOSCH

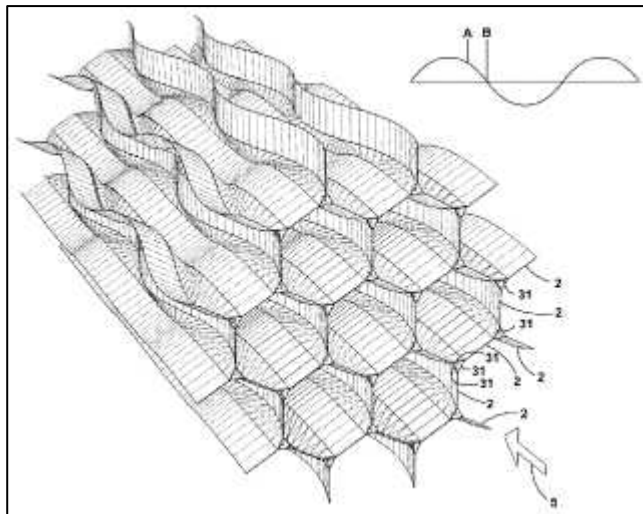
The transformer (1) has a connecting element (9) comprising a connecting tube (14) that connects a sub-wave body (7) and a trans-wave body (8). The sub-wave body and the trans-wave body include two balloons (10) whose skins (11, 13) comprise two electroactive polymer films (5).



Compliant Mechanisms for Extracting Power from Moving Fluid (WO2011011028A1, US2010078941A1, US2010026003A1)

Applicant: Pliant Energy Systems

This flexible and elastic mechanism is made by a sheet-shaped material, that is deformed during fabrication through an applied force in order to create undulations in the mentioned material, whose stresses are maintained through restraining components, that preserve the mentioned. When the material is placed in a moving fluid, the resulting pressure differentials cause the positions of the undulations within the material to travel along the material in the same direction of the moving fluid. Power is produced by using electroactive polymers, which exhibit an electrical response to mechanical strain, whereby the strains caused by the travel of undulations along the material create an electrical current which is extracted via two or more electrodes.



1.3.4 Environmental impact

Environmental impact of WECs was discussed by Muetze and Vining [34]. The employment of DEs does not introduce further substantial criticalities, since DEs are not chemically aggressive nor pollutant. On the contrary, this technology tends to minimize some effects, e.g., underwater noise emission, which is of impact towards sea fauna, and above water noise emission, which is of impact on human population.

The principal criticalities connected to WECs concern sea-life and ship navigation. More specifically

- impact on animals and seabed includes underwater noise emission, animals collisions with devices, electromagnetic fields and vibrations interfering with the fauna, sedimentation and turbidity, seabed changes due to foundations/ hard substrates.
- impact on the coastline includes interference with navigation and visual impact. Since waves are surface phenomena, a great part of the possible WECs partially emerge from water. The employment of fully submerged devices (see Figure 23), in this sense, results more sustainable.

A possible positive effect, particularly for large wave farms, is wave attenuation, which makes the devices useful for two tasks: 1) electric energy generation, 2) waves breaking.

1.4 Conclusions

In this section, a review of the state of the art of WECs has been outlined and the concepts of DE-based WECs (PolyWECs) have been introduced.

To date, different WECs prototypes have been proposed, patented, experimented and, in some sporadic case, full-scale installed. Nonetheless, Wave Energy is still far from the identification of a technical standard.

It seems that the development of the wave energy sector has been obstructed by a series of techno-economic criticalities, in particular:

- the difficulty of operating complex devices in a harsh and aggressive environment, like the salty water;
- the difficulty of guaranteeing good energy conversion performances in a wide range of operative conditions and different sea states.

DEG based WECs show several promising attributes that could bring different simplifications to WEC architectures by reducing the number of moving parts and the amount of components which are sensible to the aggressive environment and present large failure probability (electric generators, hydraulic rams).

The large number of possible DEG architectures demonstrates that a good adaptability to different types of WECs, performing different motion types, is expectable. The flexibility that typically features the design of DEGs allows good margins in terms of layout and operation.

In particular, two main categories of PolyWECS have been defined:

- First generation PolyWECS, exploiting a primary mechanical interface (heaving/ pitching buoys, oscillating paddles etc.) which moves a DEG;
- Second generation PolyWECS, in which the deformation of the DE material is directly driven by the moving fluid.

First generation concepts allow to secure the polymeric transducer from the salty water (since no direct contact is strictly required) and introduce important simplifications to existing WECs architectures thanks to their direct drive, high voltage, solid-state operation. However, they do not completely fulfil the improvement since they still include several mechanical elements that are likely to be bulky, heavy and expensive.

Second generation concepts present an extremely reduced number of parts, but are more difficult to implement, and model since their effectiveness strongly depends on the response of the polymer to direct contact with sea water.

Some concepts of DE-based WECs were already presented in literature or patented. Nonetheless, to date, no systematic studies have been addressed to this subject. For this reason, the PolyWEC project can contribute to provide clear and univocal methodologies to assess the performance of polymeric WECs.

2. GENERAL MODELS AND MATERIAL-PROPERTY SPECIFICATIONS

2.1 Introduction

The general working principle of DEGs has been described in sub-section 1. It has been observed that a crucial parameter for a DEG is the amount of energy per unit volume that the generator can convert in a cycle.

DEGs are operated cyclically, and are controlled to perform an Energy Conversion Cycle (ECC). To accomplish this, a DEG is provided with a proper control electronics, that makes it possible to regulate the charge (or the voltage) present on the DEG electrodes during its motion.

In this section, the following aspects are presented:

- electro-elastic models for the analysis and design of DEGs;
- methods for the analysis of ECCs;
- material properties affecting the maximal energy that can be produced by DEGs.

2.2 Electro-Elastic Models

This sub-section describes a reduced continuum finite-deformation Electro-Mechanical (EM) model that is suited for the analysis and finite element simulation of DE transducers.

Sub-section 2.2.1 provides the statement of the problem; sub-section 2.2.2 defines the total EM energy of a general system comprising elastic dielectrics and conductors; sub-section 2.2.3 derives the balance equations, boundary conditions and constitutive relations for the considered general EM system; sub-section 2.2.4 specifies the constitutive relations holding for typical DE materials. Additional details on the modelling of DE transducers can be found in [35]-[37].

2.2.1 Problem Definition

Referring to Figure 32, consider a closed and electrically isolated EM system \mathcal{V} , which comprises dielectric and conducting bodies (electrodes) that move and deform in free space under the action of externally applied loads of electro-mechanical origin. For every motion and deformation of \mathcal{V} : 1) no mass can enter or leave the boundary of \mathcal{V} ; 2) energy can cross the boundary of \mathcal{V} in the form of electrical and mechanical work; 3) no interaction occurs between the electrical charges that lie within \mathcal{V} and those outside (i.e. the boundary of \mathcal{V} is either electrically shielded from its exterior or has an infinite extent).

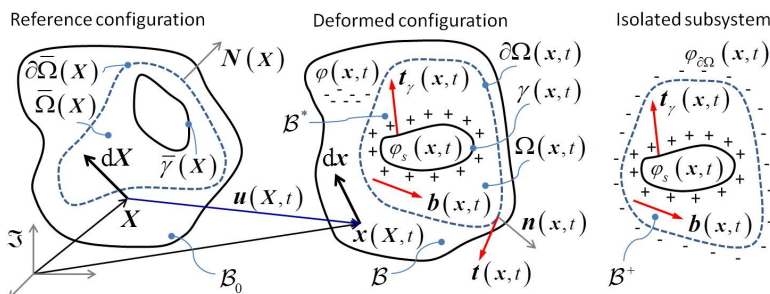


Figure 32 - EM system: reference and actual configuration, and isolated subsystem

Regarding kinematics, define with \mathfrak{I} a fixed frame with respect to which the motions and deformations of \mathcal{V} are measured (with \mathcal{V} specifically indicating the current deformed configuration), and identify with \mathcal{V}_0 the reference (stress-free) configuration. For any arbitrary time instant $t \geq 0$, consider a general material point P of \mathcal{V} and indicate with X and $x(X,t)$ (where $x(X,0) \equiv X$) the position vectors expressing the location occupied by P when the EM system is in \mathcal{V}_0 and \mathcal{V} respectively. Then, with reference to Figure 32, the following definitions hold

$$\mathbf{u}(X,t) = \mathbf{x}(X,t) - \mathbf{X}, \quad \mathbf{F}(X,t) = \partial \mathbf{x} / \partial \mathbf{X} = \text{GRAD}(\mathbf{x}), \quad J(X,t) = \det \mathbf{F}, \quad (1)$$

where: \mathbf{u} is the displacement field; \mathbf{F} is the deformation gradient; J is the Jacobian determinant.

Regarding EM system loadings, the physical space contained within $\bar{\omega}$ features: a distribution of electric charges (namely free and injected electrons or ions), with densities $\varphi(\mathbf{x},t)$ and $\varphi_\gamma(\mathbf{x},t)$, respectively defined per unit of deformed volume dv of $\bar{\omega}$ and per unit of deformed area ds of the physical surface $\gamma(t)$ (for instance a conducting electrode); a distribution of matter with mass density, $\rho(\mathbf{x},t)$, defined per unit volume dv. The same physical space is also subjected to: purely mechanical loads represented by a body force field (for instance the gravity field), $\mathbf{b}(\mathbf{x},t)$, defined per unit volume dv; and a traction vector, $\mathbf{t}_\gamma(\mathbf{x},t)$, defined per unit area ds of $\gamma(t)$ (for instance a body boundary).

Beside the displacement field, the other variables that complete the description of the state of $\bar{\omega}$ are the electric potential $\phi(\mathbf{x},t)$, the electric displacement vector $\mathbf{D}(\mathbf{x},t)$, and the electric field $\mathbf{E}(\mathbf{x},t)$ such that

$$\mathbf{E} = -\partial\phi/\partial\mathbf{x} = -\text{grad}\phi. \quad (2)$$

2.2.2 Conservation of Energy

Consider an arbitrary but closed subsystem of $\bar{\omega}$, hereafter called $\bar{\omega}^*$, which (for every time instant $t > 0$) is identified by the volume $\Omega(t)$ and bounded by the closed surface $\partial\Omega(t)$ with unit normal $\mathbf{n}(\mathbf{x},t)$. In Figure 32, one of these possible subsystems is indicated with a blue dash-dotted line.

Irrespective of the specific response of the substances contained therein, the evolution of $\bar{\omega}^*$ is governed by a balance of EM energy. Differently from $\bar{\omega}$, $\bar{\omega}^*$ is not electrically isolated, and thus interactions may exist between the electrical charges that lie within $\Omega(t)$ and those outside. According to potential theory, and as represented on the right side of Figure 32, $\bar{\omega}^*$ is equivalent to an identical electrically isolated subsystem $\bar{\omega}^+$ which has the boundary $\partial\Omega(t)$ covered by a single layer of charges with surface density

$$\varphi_{\partial\Omega} = -\mathbf{D} \cdot \mathbf{n}. \quad (3)$$

Thus, the conservation of total EM energy for the arbitrary subsystem $\bar{\omega}^*$ reads as

$$d(K \nexists W)/dt = P_{me} + P_{el}, \quad (4)$$

where $\mathcal{U}_{me}(t)$ and $\mathcal{U}_{el}(t)$ are the external mechanical and electrical powers entering in $\bar{\omega}^+$ (that is in $\bar{\omega}^*$) from the outside of its boundary $\partial\Omega(t)$, namely

$$P_{me} = \int_{\Omega(t)-\gamma(t)} \mathbf{b} \cdot \dot{\mathbf{u}} dv + \int_{\gamma(t)} \mathbf{t}_\gamma \cdot \dot{\mathbf{u}} ds + \int_{\partial\Omega(t)-\gamma(t)} \mathbf{t} \cdot \dot{\mathbf{u}} ds, \quad (5.1)$$

$$P_{el} = \int_{\Omega(t)-\gamma(t)} \phi d(\varphi dv)/dt + \int_{\gamma(t)} \phi d(\varphi_\gamma ds)/dt + \int_{\partial\Omega(t)-\gamma(t)} \phi d(\varphi_{\partial\Omega} ds)/dt, \quad (5.2)$$

with $\dot{\mathbf{u}}(\mathbf{x},t)$ being the velocity field ($\dot{\mathbf{u}} = d\mathbf{u}/dt$); whereas $\mathcal{U}(t)$ and $\mathcal{U}(t)$ are the kinetic and potential energies associated to the physical space contained in $\bar{\omega}^+$

$$K(t) = \int_{\Omega(t)-\gamma(t)} 0.5\rho\dot{\mathbf{u}}^2 dv, \quad W = \int_{\Omega(t)-\gamma(t)} (\rho\Psi + \mathbf{E} \cdot \mathbf{D}) dv, \quad (5.3)$$

with $\Psi(\mathbf{F}, \mathbf{E})$ being the energy density (per unit volume dv) of deformation and polarization of a given material. Note that Ψ does not include the energy required to build the electrostatic field in $\bar{\omega}^+$ (this is accounted by the term $\mathbf{E} \cdot \mathbf{D}$).

Equation (4), together with equations (5), represents the conservation of total EM energy of the arbitrary subsystem $\bar{\omega}^*$, expressed in global form and referred to the deformed configuration $\bar{\omega}$ of the overall EM system.

Resorting to the Gauss's divergence theorem along with Equations (1) and (6), the conservation of total EM energy of \mathcal{P}^* in Lagrangian description follows as

$$\begin{aligned} & \int_{\Omega(t)-\gamma(t)} \left[\rho \ddot{\mathbf{u}} - \operatorname{div} \left(\rho \mathbf{F} \frac{\partial \Psi^T}{\partial \mathbf{F}} + \mathbf{D} \otimes \mathbf{E} \right) - \mathbf{b} \right] \cdot \dot{\mathbf{u}} d\mathbf{v} - \int_{\gamma(t)} \left(\mathbb{I} \rho \mathbf{F} \frac{\partial \Psi^T}{\partial \mathbf{F}} + \mathbf{D} \otimes \mathbf{E} \mathbb{I} \cdot \mathbf{n} + \mathbf{t}_\gamma \right) \cdot \dot{\mathbf{u}} ds + \\ & + \int_{\partial\Omega(t)-\gamma(t)} \left[\left(\rho \mathbf{F} \frac{\partial \Psi^T}{\partial \mathbf{F}} + \mathbf{D} \otimes \mathbf{E} \right) \cdot \mathbf{n} - \mathbf{t} \right] \cdot \dot{\mathbf{u}} ds + \\ & - \int_{\Omega(t)-\gamma(t)} \phi \frac{d}{dt} (\varphi - \operatorname{div} \mathbf{D}) d\mathbf{v} - \int_{\gamma(t)} \phi \frac{d}{dt} (\varphi_\gamma - \mathbb{I} \mathbf{D} \mathbb{I} \cdot \mathbf{n}) dS + \int_{\Omega(t)-\gamma(t)} \left(\mathbf{D} + \rho \frac{\partial \Psi}{\partial \mathbf{E}} \right) \cdot \dot{\mathbf{E}} d\mathbf{v} = 0 \end{aligned} . \quad (6)$$

2.2.3 Balance Equations and Constitutive Relations

Equation (6) holds for any arbitrary volume Ω (with boundary $\partial\Omega$) and for any general EM process. Thus, satisfaction of Eq. (6) requires:

$$\rho \ddot{\mathbf{u}} = \operatorname{div} \boldsymbol{\sigma} + \mathbf{b} \text{ on } \Omega - \gamma, \text{ and } \mathbf{t}_\gamma = -\mathbb{I} \boldsymbol{\sigma} \mathbb{I} \cdot \mathbf{n} \text{ on } \gamma, \quad (7)$$

$$\operatorname{div} \mathbf{D} = \varphi \text{ on } \Omega - \gamma, \text{ and } \mathbb{I} \mathbf{D} \mathbb{I} \cdot \mathbf{n} = \varphi_\gamma \text{ on } \gamma, \quad (8)$$

$$\boldsymbol{\sigma}^T(\mathbf{F}, \mathbf{E}, T) = \rho \frac{\partial \Psi}{\partial \mathbf{F}} \mathbf{F}^T + \mathbf{E} \otimes \mathbf{D} \text{ with } \mathbf{t} = \boldsymbol{\sigma} \cdot \mathbf{n}, \quad (9)$$

$$\mathbf{D}(\mathbf{F}, \mathbf{E}, T) = -\rho \frac{\partial \Psi}{\partial \mathbf{E}}. \quad (10)$$

For the considered EM system, Equations(7) and (10) represent the Lagrangian form of the balance of linear momentum (with the second relation of Equation (9) being the stress theorem holding in the deformed configuration), whereas Eqs. (8) and (10) are the electrostatic equations.

2.2.4 Constitutive Relations for Dielectric Elastomers

Equations (7)-(10) hold for any conservative elastic dielectric body that admits an energy density function of deformation and polarization. Particular problem solutions require specific definitions of $\Psi(\mathbf{F}, \mathbf{E})$. A possible form for DEs is

$$\Psi = \Psi_{MR} + \Psi_{es} + \Psi_{vol}, \quad (11.1)$$

$$\Psi_{MR} = \frac{c_1}{\bar{\rho}} \left[\operatorname{trace}(\mathbf{FF}^T) - 3 \right] + \frac{c_2}{\bar{\rho}} \left[\left(\operatorname{trace}(\mathbf{FF}^T) \right)^2 - \operatorname{trace} \left((\mathbf{FF}^T)^2 \right) - 3 \right], \quad (11.2)$$

$$\Psi_{es} = -0.5 \varepsilon \mathbf{E}^2 / \rho, \quad \Psi_{vol} = -p(J-1) / \bar{\rho}, \quad \bar{\rho} = J \rho. \quad (11.3)$$

where Ψ_{MR} is the Mooney-Rivlin strain-energy function for hyperelastic materials (only dependent on the DE shear moduli c_1 and c_2), Ψ_{es} is a purely electrostatic energy function (only dependent on the DE permittivity ε), and Ψ_{vol} is a constraining term introduced to enforce the incompressibility condition ($J = 1$, with p being a Lagrange multiplier identifiable as a hydrostatic pressure).

With this energy density function, the constitutive relations (9) and (10), which complete the EM model for DEs together with Equations (7) and (8), read as

$$\boldsymbol{\sigma}(\mathbf{F}, \mathbf{E}) = \rho \mathbf{F} \left(\frac{\partial \Psi_{MR}}{\partial \mathbf{F}} \right)^T + \boldsymbol{\varepsilon} \left(\mathbf{E} \otimes \mathbf{E} - \frac{1}{2} \mathbf{E}^2 \mathbf{1} \right) - p \mathbf{1}, \quad (12)$$

$$\mathbf{D} = \boldsymbol{\varepsilon} \mathbf{E}. \quad (13)$$

2.3 Analysis of Conversion Cycles

Let us consider a DEG with one kinematic degree of freedom (i.e. a lozenge-shaped generator, or a generator subjected to equi-biaxial deformations). If the DEG is electrically activated (that is, if a charge Q is present on its electrodes), the state of the system is fully described (for any of its configurations) by means of two physical quantities only. In fact, being a deformable capacitor, the state of a DEG is completely determined by:

- the area of the electrodes (or, equivalently, some characteristic length or displacement identifying the geometric configuration of the DEG)
- the charge Q present on the electrodes (or any other variable describing the electric state of the DEG).

Basing on this presupposition, each equilibrium state for the system can be described by two “state variables”. Such variables are not necessarily those mentioned above (electrodes surface, charge). In practice, in technical literature, a DEG can be described by using one of the following couples of variables [24]:

- Force-Displacement (or Stress-Stretch): these mechanical variables are typically used in continuum mechanics to characterize the static and dynamic response of a material to an external load. The term “displacement” indicates here the length difference between the deformed configuration and the relaxed configuration for a significant dimension of the DEG (i.e., the side length for a square membrane, a diagonal length for a lozenge etc.). Since the force required to keep the membrane within the generator in a given configuration depends on the amount of charge present on the electrodes, the considered variables (force and displacement) are fully representative of the physics of the generator.
- Charge-Voltage: in a capacitor, the value of charge present on the electrodes and of voltage applied to the device are linked by the value of the capacitance. Since the capacitance is a function of the dimensions of the capacitor, furnishing both charge and voltage for a DEG is equivalent to provide some information on both the geometric configuration of the system and on its electric activation state. Again, these two variables are sufficient to describe the physical state of a DEG.

That is, the state of the elastomer can be represented by a point either on the Force-Displacement (Stress-Stretch) plane or on the Charge-Voltage (Q - V) plane. In these planes, transformations that imply the passage from an equilibrium state (described by a single point) to one another are represented by curves.

The use of Force-Displacement and of Charge-Voltage planes is a very useful tool to visualize the Energy Conversion Cycle (ECC) of a DEG generator, as well as to evaluate its performances.

Let us consider the example of Figure 33, relative to a DEG undergoing a mono-axial deformation. In first place, the DEG is stretched from its initial geometrical configuration (point A) to a maximally deformed geometrical configuration (point B); in second place, the DEG is activated with a charge Q so that it reaches a different state (point C, the charging phase is assumed to be instantaneous so that the stretch of the membrane during this phase remains constant); in third place, by keeping the same charge Q on the electrodes, the DEG is brought back to its initial configuration (point D); lastly, by keeping the same geometrical configuration, the charge Q is removed from the electrodes so that the DEG comes back to the initial state (point A).



Figure 33 - Energy conversion cycle on Force-Position and Charge-Voltage planes

The following aspects have to be underlined:

- Since the DEG works in a cyclical way, the transformations defining its operation describe a closed cyclic path (in both planes).
- Purely mechanic transformations (that occur when no charge and voltage are present on the membrane) are obviously not visible on the Q - V plane.

In the following, only the description in the Q - V plane will be considered and used.

2.2.1 Maximal Convertible Energy

The formalism introduced above for the study of ECCs can be used to assess the maximal energy that can be converted by a specific DEG[24].

The calculation of this maximum relies on the identification of characteristic failure mechanisms for DEGs; namely: electrical break-down, material loss of tension and mechanical rupture.

The constraints determined by these failure mechanisms can be represented as continuous limiting curves on both Force-Displacement (Stress-Stretch) and Charge-Voltage planes. Since the gathered energy can be expressed as the integral of the mechanical force over the deformation or as the integral of the voltage over the charge, the areas enclosed by these limiting curves represent the maximum amount of energy that the DEG can convert in a cycle. The analytic results for a DEG undergoing equi-biaxial deformations (with geometry shown in Figure 21) are briefly described in the following.

Symbols:

- Q charge
- V voltage
- $\varepsilon = \varepsilon, \varepsilon_0$ dielectric constant
- t thickness
- B volume of DE
- E electric field
- E_{BD} break-down electric field
- λ stretch
- λ_u rupture stretch
- ℓ side length of the square sample
- ℓ_0 side length in the undeformed configuration
- A electrodes surface
- A_0 electrodes surface in the undeformed configuration

The capacitance of the DEG is given by

$$C = \frac{Q}{V} = \frac{\varepsilon A}{t} = \frac{\varepsilon A^2}{B} \quad (14)$$

Given the incompressibility of the material, the volume B remains constant during the deformation. The failure conditions, in term of V and Q , are described as follows:

Electrical break-down: The break-down condition puts an upper limit to the maximum allowed value for the electric field within the polymeric membrane.

The electric field inside a plane capacitor is expressed by

$$E = \frac{V}{t} = \frac{VA}{B} \quad (15)$$

From equation (14), the surface A can be expressed in terms of Q and V and replaced in equation (15). Then, the condition $E \leq E_{BD}$ takes thus the form

$$VQ \leq \varepsilon BE_{BD}^2 \quad (16)$$

On the Q - V plane, the boundary curve for the break-down condition is a hyperbola.

Mechanical rupture: The rupture condition can be easily expressed referring to the stretch level of the material, imposing the condition $\lambda \leq \lambda_u$.

Considering an equi-biaxial deformation, the side length of the deformed square is

$$\ell = \lambda \ell_0 \quad (17)$$

and the electrodes area in the deformed configuration is

$$A = \lambda^2 A_0 \quad (18)$$

Using Equations (14) and (18), the iso- λ curves (representing transformations with constant value of the stretch on the material) result as the straight lines:

$$V = \frac{B}{\varepsilon A_0^2 \lambda^4} Q \quad (19)$$

Therefore, the rupture criterion requires that

$$V \geq \frac{B}{\varepsilon A_0^2 \lambda_u^4} Q \quad (20)$$

Loss of tension: During operation, the polymeric membrane must always be kept in tension to avoid wrinkles (buckling) that may disrupt the functioning of the DEG.

The loss of tension condition has the general form $\sigma \geq 0$, where σ represents the value of the planar principal stress of the membrane (that is the same in both principal directions).

Using Equation (12), the loss of tension condition takes the form

$$\sigma = \lambda \frac{\partial \Psi_{MR}(\lambda)}{\partial \lambda} - \varepsilon E^2 \geq 0 \quad (21)$$

where Ψ_{MR} is the hyperelastic strain-energy function of the DE material (expressed in Mooney Rivlin Form, but other forms are possible). Since

$$E = \frac{V}{t} = \frac{V}{B} \lambda^2 \ell_0^2 \quad (22)$$

$$\lambda = \sqrt[4]{\frac{B}{\varepsilon A_0^2} \frac{Q}{V}} \quad (23)$$

the loss of tension condition becomes an implicit equation in V and Q , that depends on the form of the constitutive relation chosen for Ψ_{MR} .

Figure 34 reports the limiting curves expressed by Equations (16), (20) and (21). The area colored in yellow represents the numerical value of the maximum energy that can be converted in a cycle by the considered equi-biaxial DEG.

In order to convert this maximum amount of energy, the DEG must be supplied with proper driving electronics. In particular: the DEG must be loaded mechanically from the minimum stretch (identified by the loss of tension condition) to the maximum one (identified by the rupture condition); subsequently, it has to be electrically charged (instantaneously, thus, at constant stretch); finally, it has to be progressively discharged following the break-down curve until the loss of tension condition is encountered. The last part of the discharging phase is a complex transformation during which the mechanical stress within the membrane is zero.

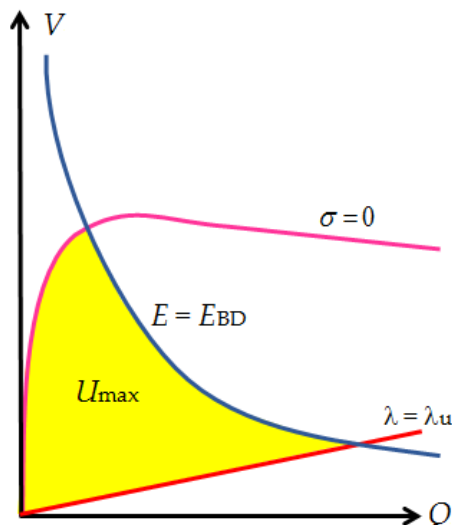


Figure 34 -Available energy and operation limits for an equi-biaxial DEG

Notice that the area enclosed by the failure lines contains all the equilibrium points that guarantee a safe operation for the DEG. Any eventual ECC, different from the just described optimal one, must be contained within the mentioned region.

To better assess the influence of DE material properties and of DEG geometry on the maximal energy that can be converted, it is often convenient to resort to the following dimensionless variables:

$$Q^* = \frac{Q}{\varepsilon E_{BD} A_0} \quad (24)$$

$$V^* = \frac{V}{E_{BD} B / A_0} \quad (25)$$

With such definitions, the limiting curves for break-down and mechanical rupture conditions become respectively

$$V^* Q^* = 1 \quad (26)$$

$$V^* = \frac{Q^*}{\lambda_u^4} \quad (27)$$

Besides, the loss of tension condition can be approximated by the following iso-stretch straight line passing through the origin of the axes

$$V^* = \frac{Q^*}{\lambda_{l,\min}^4} \quad (28)$$

Notice that, using the new dimensionless coordinates, the positions of the limit curves on the Q^* - V^* plane do not depend neither on the specific material properties of the material (ε and E_{BD}) nor on the amount of material volume B , and are only affected by the limit values of the stretch (namely λ_u and $\lambda_{l,\min}$).

The surface enclosed by the optimal ECC, on the Q^* - V^* plane, is a dimensionless energy:

$$En^* = \frac{En}{\varepsilon E_{BD}^2 B} \quad (29)$$

To a first approximation, such a value is independent from the electrical properties of the material. The mechanical properties, instead, intervene directly in the determination of the ECC area by determining the slope of the iso-stretch lines (through λ_u and $\lambda_{l,\min}$). However, it should be noticed that the linearization of the loss of tension condition (accomplished via Equation (28)) relies on the identification of a value of $\lambda_{l,\min}$ that depends both on the mechanical parameters contained in Ψ_{MR} and on the electric constants ε and E_{BD} .

The reported analysis neglect any thermal or electro-strictive effect (that is, the variation of the dielectric constant as function of material deformation). For material exhibiting this kind of behaviour, the study of the ECCs should be addressed via different material models.

2.4 Relevant Material Properties

Basing on the previous considerations, some relevant material properties can be identified. For each of these properties, general considerations can be drawn in regards to effect they have on the maximum energy that can be converted by general DEGs.

The most relevant material properties are here schematically introduced.

2.4.1 Dielectric Constant

The working principle of DEGs (based on the concept of variable capacitance condenser) requires the elastomeric membrane (housed between the compliant electrodes) to be non-conductive (since it constitutes the dielectric mean between the armatures, with the aim of electrically decoupling the opposite faces of the capacitor).

The dielectric constant for a generic medium is expressed by

$$\varepsilon = \varepsilon_r \varepsilon_0 \quad (30)$$

where ε_0 is the permittivity of the vacuum, that amounts to $8.85 \cdot 10^{-12} F \cdot m^{-1}$, and ε_r is the relative dielectric constant of the material.

In general, high values of ε_r are desirable for DEGs. In fact, as shown in Equation (29), for a given value of E_n^* (that, as already mentioned, is almost independent from the electrical properties of the elastomeric material), the effective amount of converted energy is directly proportional to the value of ε_r .

Typical values of the dielectric constant for common DE materials are reported in Table 1 (cfr. [16][27]).

| Elastomer | ε_r |
|----------------|-----------------|
| Natural Rubber | 2.7 |
| Silicone | 3-7 |
| Acrylic | 3-4.5 |

Table 1 - Relative dielectric constant for some classes of DEs

2.4.2 Electrical Break-down field

As already mentioned, the break-down limitation determines an upper admitted value, E_{BD} , for the electric field within the polymeric capacitor.

Generally, E_{BD} is considered as a constant intrinsic parameter of the material. However, some dependence of this parameter on the deformation may exist.

For instance, according to Koh et al. [24], acrylic elastomers undergoing equi-biaxial deformation exhibit a strain-dependent break-down field that varies according to the relationship

$$E_{BD}(\lambda) = \bar{E}_{BD} \lambda^R \quad (31)$$

In general, high values for the break-down field are desirable. In fact, as shown in Equation (29) and in Figure 35, larger values of E_{BD} lead to larger amounts of converted energy.

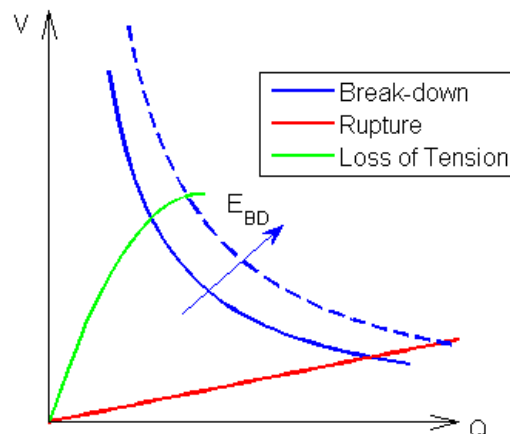


Figure 35 - Effect of an increase in E_{BD} on ECCs

Typical values of break-down field for common DE materials are reported in Table 2.

| Elastomer | E_{BD} [MV/m] |
|----------------|-----------------|
| Natural Rubber | 30-200 |
| Silicone | 30-100 |
| Acrylic | 30-200 |

Table 2 - Break-down field for some classes of DEs

2.4.3 Rupture stretch

The condition of mechanical rupture of the polymeric material can be expressed as a limitation on the maximum allowed value, λ_u , of the stretch within the material.

As already mentioned, DE materials exhibit large values of limiting stretches (over 500%). A large value of λ_u is obviously desired in order to obtain a large amount of convertible energy.

As shown in Equation (27) and in Figure 36, large values of λ_u produce a rupture curve with low slope, and, consequently, an ECC that encloses a larger area.

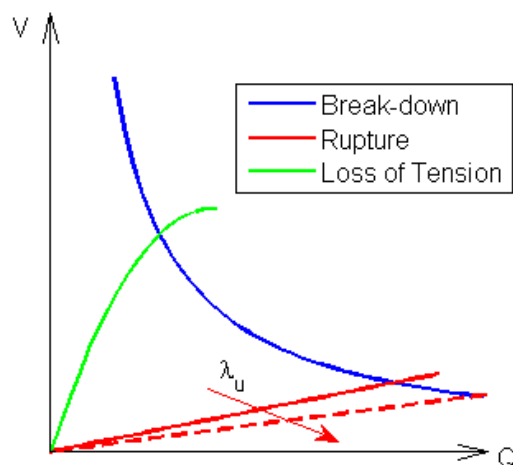


Figure 36 - Effect of an increase in λ_u on the ECC

Typical values of rupture stretch for common DE materials are reported in Table 3.

| Elastomer | λ_u |
|----------------|-------------|
| Natural Rubber | 5-7 |
| Silicone | 3 |
| Acrylic | 4-8 |

Table 3 - Rupture stretch for some classes of DEs

2.4.4 Hyperelastic parameters

DE materials are non-linear elastic solids. As described in Section 2.1, their mechanical behavior is usually described by a proper hyperelastic model (in Equation (11) given in Mooney-Rivlin form).

As a general rule, the hyperelastic energy function can be recast in the form

$$\Psi_{MR} = \mu \cdot \psi(\lambda_1, \lambda_2) \quad (32)$$

where μ represents the shear modulus of the material (roughly expressing its stiffness).

As a general rule, sufficiently large values of μ are desired. In fact, as shown in Equation (32) and in Figure 37, an increase in the value of μ produces an increase in the slope of the limit curve corresponding to the loss of tension condition.

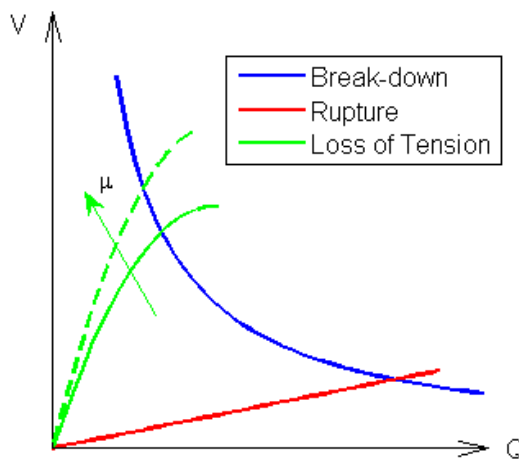


Figure 37 - Effect of an increase in μ on the ECC

In other words, assuming a linearization for the loss of tension condition, like in Equation (28), the resulting value of the parameter $\lambda_{I,min}$ decreases with μ increasing. Consequently, the ECC encloses a larger area. That is, in case the generator is able to operate the optimal ECC (bounded by the limit curves representing the failure conditions), the effect of using a stiffer material is an increase in the energy that can be converted by the DEG.

2.4.5 Effect of Material Properties on DE-WEC Response

Up to this point, it has been assumed that the DEG undergoes a conversion cycle bounded by the transformations identified by the failure conditions discussed above. Beside appropriate power electronics and controller, this hypothesis requires the availability of an external source of mechanical work that is capable of exerting on the generator the required forces and displacements exhibited by the DEG in the Force-Displacement plane.

This is not generally the case when the DEG needs to absorb a significant amount of energy from a mechanical system, such as a wave interacting body, having an intrinsic impedance (namely a specific dynamic response). In this circumstance, maximization of the energy that can be harvested by a DEG may require the appropriate matching of the impedance of the DEG to that of the source of the mechanical energy. From the point of view of material property specifications, this could modify the requirements described in the preceding sections for both mechanical and electrical parameters.

Referring to wave energy harvesting and according to linear waves theory [4], the amount of energy that can be extracted is maximized when the system composed by WEC and PTO has a natural frequency that equals that of the incident wave (in the hypothesis of monochromatic waves). In this context, the major effect of using DEGs as PTO corresponds to a modification of the overall stiffness response of the WEC.

In particular, this stiffness modification depends on the following electro-mechanical properties and design parameters of the DEG:

- The shear modulus (μ) of the DE material;
- The dielectric constant multiplied by the square of the maximum electric field employed during the ECC (namely, $\epsilon \cdot E^2$);
- The level of pre-stretch of the DE membrane.

2.4.6 Other relevant properties

In addition to properties that have a direct effect on the operational performance of DEG based WECs, there are several material properties that have important influence on technical operation, engineering and maintenance of such devices. In particular, the operation of DE-WECs in marine environment brings up a series of technical issues:

- *Effect of sea water on the devices parts lifetime:* the marine environment is harsh and chemically aggressive. This represents a criticality for traditional WECs, which are made by steel parts that are sensitive to corrosion and fouling. DE-based solutions reduce the number of moving parts, thus, they

may be less affected by fouling problems. Nonetheless, the survivability of the DEGs, put in direct contact with the salty water, has to be assessed. The most critical parts within polymeric generators are compliant electrodes, can be sensible to erosion and salt deposition phenomena. In order to guarantee their survivability, electrodes should be insulated from water by adding additional passive polymeric membranes. Such membranes have the only aim of covering the electrodes and do not participate to the electric activation process. The addition of further material to the DE stacks provokes an increase in the PTO stiffness. Nonetheless, this effect is marginal, especially if soft polymers (such as silicones) are used for the protection.

- *Ambient aging of DE materials:* Aging effects may be provoked on elastomeric materials by a series of ambient conditions, i.e., 1) direct contact with water, 2) exposition to UV radiation, 3) temperature. A distinction has to be made between first and second generation PolyWECS.

In first generation devices, direct contact between DEGU and water is not functionally required, and may be avoided, e.g., protecting the DEGs with deformable or moving sleeves. These measures also prevent the material from direct radiation exposition.

In second generation PolyWECS, since direct fluid-membrane interaction is functional to the conversion process, water-polymer contact is unavoidable.

Results of experiments on natural rubber (which is one of the eligible DE materials that could be employed) aging in sea water are present in literature. Malek and Stevenson [38] carried out experiments on a natural rubber sample exposed for 42-year to sea water at a depth of 24 m. They detected that no attack from marine organisms had occurred, moreover, the amount of absorbed water was less than 5 % and this had no adverse effect on properties. Mot and Roland [39] carried out accelerated aging experiments, based on cyclic deformation loads, on natural rubber immersed in hot air and hot sea water. They concluded that sea water aging consequences were less marked. Rubber aging is primarily due to oxidation [39], consequently, aging effect in water are less pronounced than in air. Also, the effect of temperature on aging is ascribable to its influence on oxygen solubility in sea water. However, effects of ambient on dielectric properties are to be investigated.

- *Fatigue lifetime of DE materials.* Cyclic stretch experiments on elastomeric materials are reported in literature [40] [41] and underline that elastomers fatigue lifetime involves a number of variables, i.e., stretch amplitude, stretch rate, temperature, sample dimensions. Simplified fatigue models are going to be assumed and employed for providing forecasts.

The mentioned technical issues have an influence on PolyWECS lifecycle and limit their useful lifetime. In order to determine which is the minimum economically acceptable life for these devices, a broad techno-economic analysis of the concepts is required. This type of analysis requires a number of input data, i.e., expected energetic productivity and costs.

Consequently, prior to deepen these aspects, reliable tools for PolyWECS energy performance prediction have to be developed.

2.5 Conclusions

In this section, mathematical electro-elastic models for DEs have been introduced. With reference to a specific stretch condition (that is, equi-biaxial stretch), such models have been employed to carry out a sensitivity analysis of the relevant material properties affecting the energy performance of DEGs.

The overall effects of DE materials electro-mechanical parameters on wave energy harvesting via DEGs can be summarized as follows:

- *Mechanical material parameters:* Relevant mechanical parameters are: 1) limit stretch value, determined by mechanical rupture (the larger the rupture stretch, the broader the allowed operative range for the DEG); 2) mechanical stiffness (namely, shear modulus). In an ideal context, rigid materials allow larger energy conversion capabilities; in a practical context, they may increase to much the stiffness response of the WEC, which could make it unsuitable for the operation in specific wave climates. Depending on the specific converter, location of installation and reference sea states, a trade off for the material shear modulus needs to be found.

- *Electrical material parameters*: in an ideal context, maximum values for the product $\varepsilon \cdot E^2$ allow larger energy conversion capabilities; in a practical context, they may modify excessively the stiffness response of the WEC (either increasing or decreasing it depending on the specific DEG architecture), which could make it unsuitable for the operation in specific wave climates. Depending on the specific converter, location of installation and reference sea states, a trade off for the product $\varepsilon \cdot E^2$ needs to be found.
- *Material pre-stretch*: since DEs are non-linear materials, irrespective of their electro-mechanical properties, the practical stiffness of a DEG with specific architecture can be tuned by properly pre-tensioning the DE membrane. Thus, in a practical context, appropriate values of DE membrane pre-stretches need to be chosen depending on the specific converter, location of installation and reference sea states.

Specific technical issues interest the application of DEGs to the marine environment (i.e., fouling and corrosion phenomena; aging effects due to salinity and radiation, fatigue lifetime). These aspects require specific analysis and will be considered in a successive stage of the research.

3. ARCHITECTURE OF FIRST-GENERATION POLYWECS

3.1 Introduction

The first generation of DE-based WECs is characterized by indirect interaction between the DEG and the fluid. That is, the deformation of the DE membrane is not produced directly by wave-induced fluid pressures, but by a mechanical interface that is in direct contact with the water. Due to the absence of direct interaction between the deformable DE membrane and the water, the coupling between wave-structure hydrodynamics and DEG electro-elasticity only occurs at a global level, and only affects a limited number of degrees of freedom (usually a very small number). This limits the complexity required for the analysis, optimization and development of these devices and enables the use of models, methodologies and tools already developed in the fields of wave energy harvesting and dielectric elastomer transducers. Nonetheless, these studies are not simple since the available models/methodologies/tools need to be properly interfaced and since the resulting fluido-electro-elastic problems result in being highly non-linear.

In the following: Sub-section 3.2 describes the WEC architectures that seem more promising for integration with a DEG PTO; Sub-section 3.3 describes the DEG architectures that could be used as PTO systems in existing WECs; Sub-section 3.4 presents an example that shows the complexity behind the study of first-generation DE-based WECs.

3.2 WEC Architectures

3.2.1 Oscillating Flap

A first WEC architecture that could be suited for wave energy harvesting via DEGs is the oscillating flap. As described in Section 1, this type of WEC consists of a buoyant flap hinged at the sea bottom and exploits the surging motion of waves. In traditional systems (such as the Oyster device by Aquamarine Power) the wave-induced oscillatory motion of the flap is used to pump water to the coast via hydraulic pistons and high-pressure flow lines. At the coasts, the high-pressure water is then converted into electricity via a turbo-generator.

Replacement of the hydraulic PTO (and of the turbo-generator) with either lozenge or cylindrical DEGs (see Section 3.3) could enable local conversion of wave energy into electricity without requiring any mechanical or hydraulic transmission. Beside simplifying the system and reducing part count, this replacement could improve system efficiency, simplify installation and reduce the noise pollution emitted at the coast by the turbo-generator. An artistic drawing of an oscillating flap equipped with a lozenge DEG (hereafter called PolySurge) is reported in Figure 38.

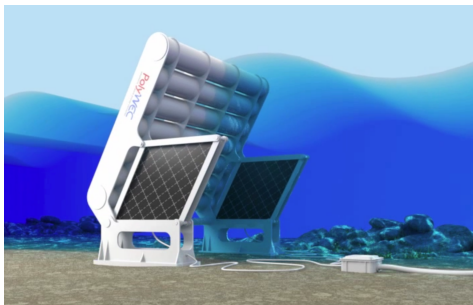


Figure 38 – Oscillating Flap with a lozenge DEG

Since they need to be attached to the seabed, PolySurge systems are suited to be placed near shore at a nominal depth of nearly 10 m, possibly at locations where shoaling effects occur. At this depth, wave energy resource is still very significant, and usually characterized by limited maximum wave heights (due to wave breaking) and limited directional spread between longer and medium period waves.

As for the operating principle, PolySurge systems can be considered as point absorbers that are excited by horizontal fluid accelerations mainly. Due to physical constraints in the oscillatory motion of the flap, PolySurge systems are likely to be not resonant in the working frequency range, and should be designed to maximize wave excitation force and to move at speeds that are adequate to limit vortex losses at the edges.

3.2.2 Oscillating Buoy

A second WEC architecture that could be suited for wave energy harvesting via DEGs is the oscillating buoy. An oscillating buoy WEC consists of a floating body, either submerged or semi-submerged, that moves under the action sea waves with respect to an appropriate number of submerged and nearly fixed reaction points. Depending on the water depth of installation, the reaction points can be located either on the seabed or on a floating body (namely a reaction body) that is submerged enough to be not excited by the wave field. Depending on the means of connection to the reaction points, the wave-induced oscillatory motion of the buoy can be in heave, surge or pitch (or a combination thereof). During these oscillations, the distances between points of the buoy and those of reaction vary. These reciprocating changes in length can be used by PTOs with linear motions to extract energy from waves. Cylindrical DEGs can be used for this purpose. Depending on the size of the device, the linear PTOs can be placed either inside the buoy, close to the reaction points (in particular on the seabed or inside the reaction body) or along the line connecting the reaction points and the buoy.

An artistic drawing of an oscillating buoy connected to a reaction body via a cylindrical DEG (hereafter called PolyBuoy) is reported in Figure 39.

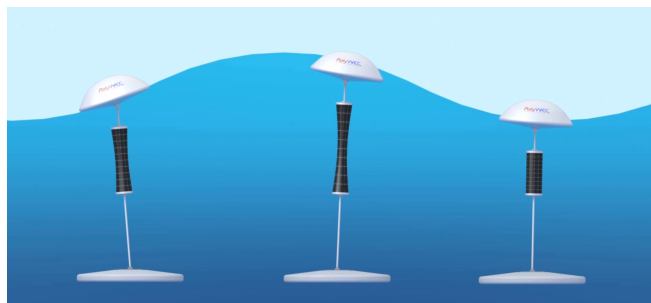


Figure 39 – Oscillating Buoy with a cylindrical DEG

In terms of hydrodynamic properties, PolyBuoys are point absorbers that can be installed both on-shore and off-shore. For standard buoy shapes and aspect ratios, PolyBuoys are likely to be designed so as to be resonant in the working frequency range and their energy capture ability should feature limited dependency on wave propagation direction.

3.2.3 Multi-body Systems

A third architecture that could be suited for wave energy harvesting via DEGs is the multi-body WEC. This kind of device consists in at least two floating bodies (either submerged or semi-submerged) that oscillate nearly in anti-phase under the action of sea-waves. Connection of the oscillating bodies via some mechanical means and PTO makes it possible to extract energy from the wave-induced relative motion of the bodies. Depending on the shape of the bodies and on the means of connection, wave-induced body oscillations can be in surge, pitch and heave.

The resulting relative body motions can be either translational or rotational. Multi-body WECs featuring relative translational motion are suited to be equipped via cylindrical DEG PTOs. Multi-body WECs featuring relative rotational motion are suited to be equipped via either lozenge or cylindrical DEG PTOs. A sketch of a multi-body WEC with cylindrical DEG PTO that exploits the heaving and surging motion of two floating bodies is depicted in Figure 40.a. A sketch of a multi-body WEC with cylindrical DEG PTO that exploits the pitching motion of two floating bodies is depicted in Figure 40.b.

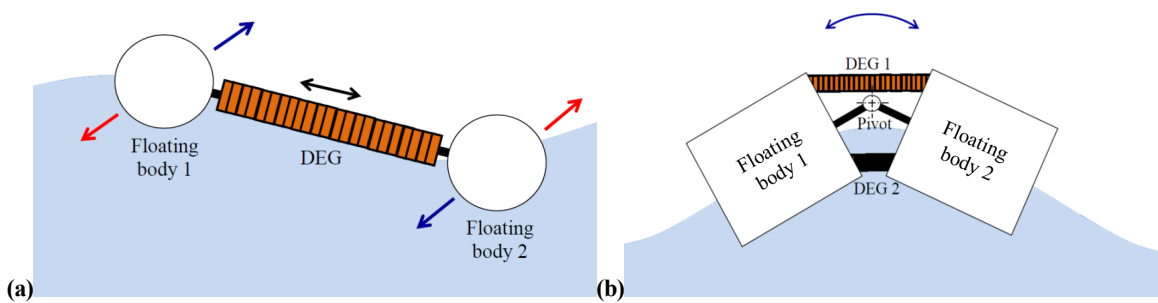


Figure 40 – Multi-body WEC with cylindrical DEG: a) heaving and surging motion; b) pitching motion

Due to the need of having two or more bodies oscillating nearly in anti-phase, the span of multi-body WECs in the direction of the propagating wave should be in the order of the length of the wave. Depending on the size in the direction orthogonal to that of the propagating wave, multi-body WECs can behave either as terminators (in case the orthogonal dimension of the oscillating bodies is comparable to the length of the wave) or as attenuators (in case the orthogonal dimension of the oscillating bodies is negligible with respect to the length of the wave). For example, the system depicted in Figure 40.a could behave as a terminator in case the floating bodies 1 and 2 are very long cylinders with axes perpendicular to the wave direction. In such an instance, multiple DEG could be placed in parallel between the floating bodies so as to enable the possibility of harvesting energy also from secondary relative movements (such as swaying and yawing) that are likely to occur in realistic sea states. Besides, the system depicted in Figure 40.b could behave as an attenuator in case the floating bodies 1 and 2 are very long cylinders with axes parallel to the wave direction.

3.3DEG Architectures

In the present section, some concepts of DEG are described in terms of:

- General layout and material arrangement;
- Technical limitations and criticalities.

Basing on the simple operating principle described in a previous section, different geometries and configurations can be adopted for DEGs, each featuring a different type of motion and, thus, being adaptable to different types of WEC provided with rotary or linear motion.

It can be underlined that the solutions adopted for generation are usually the dual, in terms of operating principle and layout, of a corresponding DE actuator. In terms of design and specifications, of course, different features and specifications may be required.

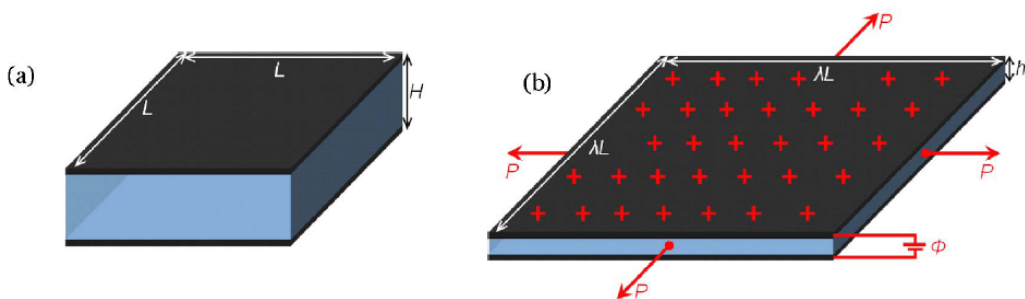


Figure 41 - Equi-biaxial DEG operating principle [24]

3.3.1 Equi-biaxial DEG

The operating principle of a DEG undergoing an equi-biaxial state of deformation has already been described in Section 2.2, where the ideal ECC for such a type of generator has been introduced and discussed. In its basic and simplest implementation (see Figure 41), an equi-biaxial DEG can be realized using a square-shaped membrane

coated with two compliant electrodes [24]. During the operation, the four sides of the membrane are subjected to the same force P that is distributed uniformly along the side length itself. The resulting deformation is characterized by a single value of the stretch that is the same in all planar directions and for all points of the membrane. As a result, among different DEG architectures, equi-biaxial DEGs exhibit the maximal capacitance variation and, thus, are capable to convert the maximum amount of energy per unit of material volume in a cycle.

For a commercial acrylic membrane subjected to an equi-biaxial state of deformation, Koh et al. [24] have assessed a convertible energy per cycle up to 1.7 J/g.

Beyond theoretical optimality, the achievement of a perfect equi-biaxial state of deformation is very difficult to obtain. From the technical standpoint, a similar state of deformation can be achieved via the machine depicted in Figure 42, whose complete mechanical design has been performed within the PolyWEC project.

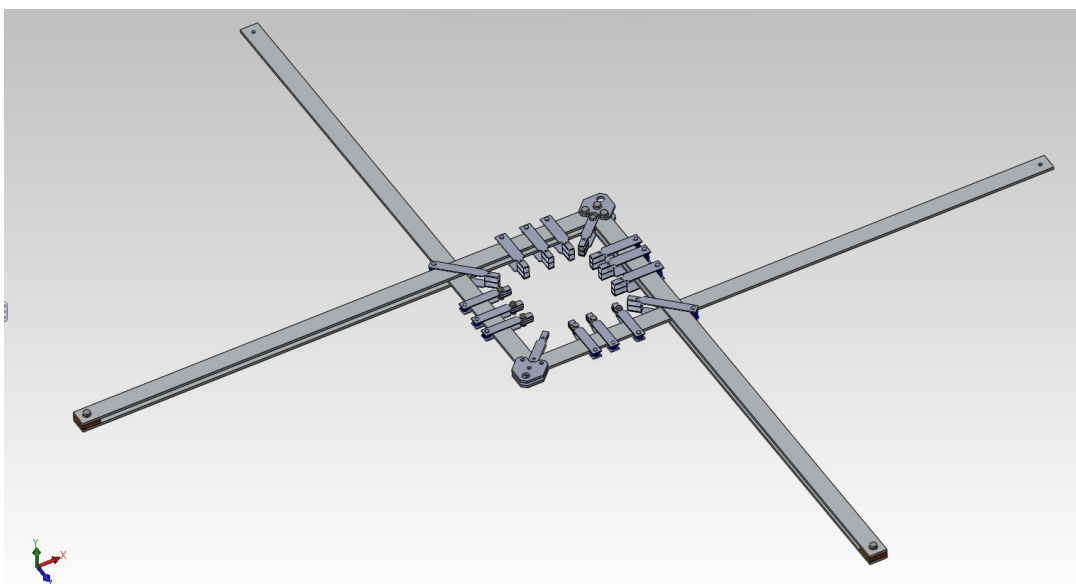


Figure 42 - Equi-biaxial deformation machine

The machine possesses one degree of freedom. It comprises two L-shaped rigid rails on top of which 16 sliding grippers are mounted. The 16 grippers are used to clamp the square DE membrane (3 gripper per side plus one gripper for each corner) that has to undergo equi-biaxial deformations. The rigid rails are commanded to translate one with respect to the other. During this motion: corner grippers displace so as to vary the length of the membrane edges by the same amount; side grippers move freely along the rails so as to limit the lateral shrinkage of the membrane. As compared to the theoretical case, the presence of a finite number of connection points with the membrane intrinsically produces a non-homogeneity in the stress distribution about the grippers and, thus, a non-ideal resulting deformation field, with stress concentrations in the proximity of the gripping points and an extinction region in the neighborhood of the membrane sides, where the deformation field is far from the equi-biaxial condition.

Beside the difficulty of achieving a perfect equi-biaxial deformations, an additional technical criticality is the spatial encumbrance of the system. Equi-biaxial DEGs have a significant planar extension which makes them difficult to fit inside most WEC architectures (in particular within those featuring bodies with regular aspect ratios). Specific applications can however be envisaged like, for instance, within the flap of surging WEC or within the reaction body of a buoy-based WEC.

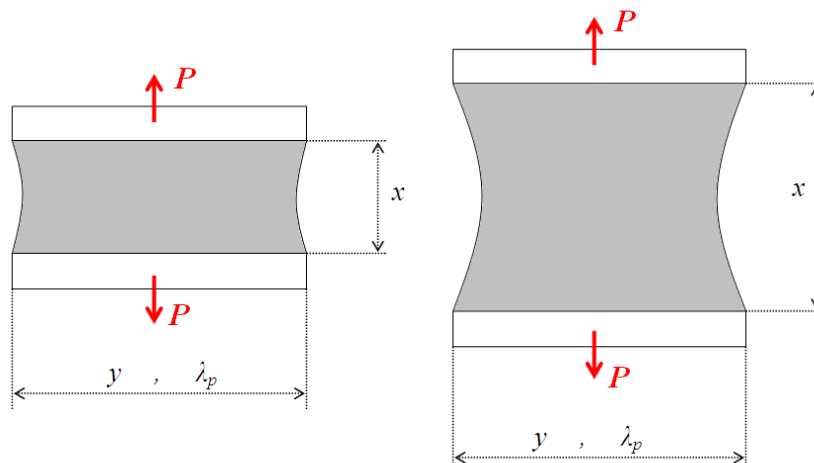


Figure 43 - DE membrane subjected to planar uniaxial deformations

3.3.2 Planar Uniaxial DEG

A simple concept of DEG can be realized exploiting the pure shear deformation of a planar DE membrane (see Figure 43e 43). The considered planar uniaxial DEG includes two rigid elements that hold the membrane along the two sides lying in y direction, with the membrane being pre-stretched by λ_p in the same direction. The DEG works undergoing cyclical deformations along the x direction. Electrodes are placed on the faces of the membrane that are parallel to the x - y plane. This configuration has the advantage of being simple (in terms of design and manufacturing) and easy to be coupled with WECs featuring linear motion. The crucial technical limitation and criticality of this solution is the necking phenomenon that occurs on the free sides of the membrane (see Figure 43). This phenomenon is particularly accentuated when the longitudinal size x of the sample has a length comparable with (or larger than) that along the y direction. From a practical standpoint, necking can be considered negligible when the length x is small with respect to y (namely $x < y/10$). Thus, in order to guarantee a correct operation, planar uniaxial DEGs must have a significant aspect ratio and should operate in a small range of values for the variable x . This makes planar uniaxial DEGs rather encumbering systems which makes them difficult to fit inside most WEC architectures (in particular within those featuring bodies with regular aspect ratios). Specific applications can however be envisaged like, for instance, within the flap of surging WEC or within the reaction body of a buoy-based WEC

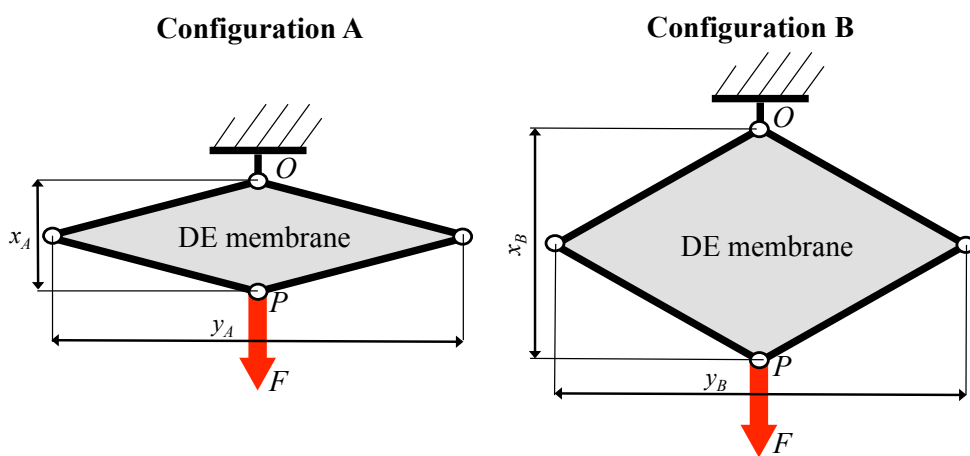


Figure 44 - Scheme of the Lozenge-Shaped DE Generator

3.3.3 Lozenge-Shaped DEG

The lozenge-shaped DEG (LS-DEG) consists in a planar DE membrane that is pre-stretched and clamped to a rigid frame made by a four-bar mechanism with equal-length links (see Figure 44). The LS-DEG position can be uniquely defined by the variable x (hereafter also called ‘transducer length’ or ‘longitudinal length’) that indicates the distance between the centers O and P of the two opposite joints of the four-bar mechanism. The distance between the other two opposite centers of the revolute pairs is indicated with the variable y and is called ‘transversal length’. With the variation of x , the DE membrane deforms uniformly and the deformation is uniquely identified by the first and second principal stretches, λ_1 (along the x direction) and λ_2 (along the y direction). The DE membrane has compliant electrodes on the faces that are parallel to the x - y plane. The membrane is mounted on the frame with a certain level of pre-stretch, indicated with $\lambda_{1,p}$ and $\lambda_{2,p}$ respectively in x and y direction.

During its cyclic operation, the LS-DEG has its longitudinal length that varies in the interval $x \in [x_A; x_B]$, oscillating between configuration A and configuration B (see Figure 44).

With respect to the uniaxial solution described in paragraph 0, the LS-DEG has the advantage that the DE membrane is not affected by necking phenomena. LS-DEGs are of interest for their simplicity and their easy adaptation in existing energy conversion devices featuring one degree of freedom and reciprocating motion. In a first analysis, this type of generator appears particularly suitable to be coupled with WECs featuring rotary motion (like surging flaps, as depicted in Figure 38).

The analysis and characterization of LS-DEGs have been addressed within the PolyWEC project [42]. As results, an energy convertibility of up to 0.3 J/g per cycle can be reached with an acrylic elastomer. This value is about six times smaller as compared to the maximum amount that can be generated by equi-biaxial DEGs based on the same material. The reason behind this lower performance is related to the evolution of the stretch during the cyclic operation of the device. In fact, in LS-DEGs, as the transversal length of the generator increases, the longitudinal length decreases. As a consequence, an increase of the stretch in one direction is combined with a relaxation of the material in the perpendicular direction. This makes the ECC of LS-DEGs be strongly affected by the loss of tension condition of the material (please refer to section 2.2).

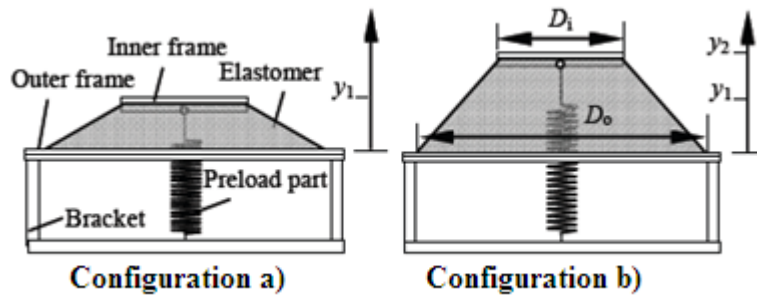


Figure 45 - Conically-shaped DEG

3.3.4 Conical DEG

Conical DE transducers have been largely investigated for actuation purposes [19], but can be exploited as generators as well. Conical DEGs consist in a rigid frame that is made by two separate parts: an outer circular ring (fixed base) and an inner circular disk (moving platform) that is the translating element of the generator. In the undeformed configuration, the polymeric membrane has the shape of a circular ring, with the internal and external bounding circumferences being clamped to the fixed base and moving platform respectively.

During operation, base and platform move one with respect to the other in the longitudinal direction (parallel to the axis of symmetry of the device) and the membrane assumes a conical shape. A pre-loading element (i.e. a spring) can be introduced to pre-stretch the membrane.

With reference to Figure 45, the configuration of the conical DEG is uniquely identified by the variable y (longitudinal length of the transducer along its axis of symmetry), that varies in the interval $y \in [y_1; y_2]$. When

$y=y_1$, the lateral surface of the cone is minimum (thus, the resulting capacitance of the DEG is minimum); when $y=y_2$ the capacitance is maximum.

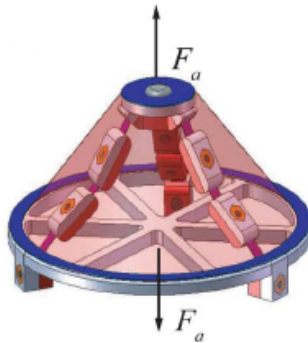


Figure 46- Conical DEG with parallel tripod architecture [44]

As proposed in [43] and as shown in Figure 46, a parallel mechanism with flexural pivots can be used in order to prevent displacements of the moving platform along the radial direction.

Due to their working principle, conical DEGs are suitable for applications in combination with mechanical bodies featuring linear reciprocating motion. The principal limitation affecting conical DEGs is the shrinking phenomenon of the DE membrane. In fact, for a realistic membrane with circular boundaries connected to rigid ring frames, the lateral surface of the membrane assumes a shape that is not perfectly conical, but presents a certain degree of concavity (as shown schematically in Figure 47). In other words, at the points of the membrane lying far from the frames, the material experiments a relaxation and this provokes a non-uniform exploitation of the polymeric material. This phenomenon is particularly accentuated when the membrane is in the un-activated configuration, and, as for the uniaxial generator, it can be prevented by posing a limitation to the longitudinal length of the generator.

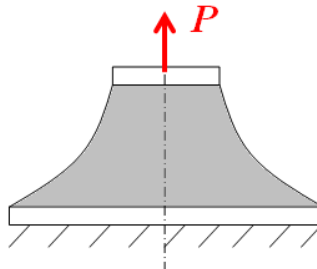


Figure 47 - Shrinking in a DE membrane of a conical DEG

3.3.5 Cylindrical DEG

Cylindrical DEGs are mainly of two types: stack-type and roll-type.

Stack-type cylindrical DEGs are constituted by a pile of circular DE membranes, each coated between compliant electrodes positioned on the circular surfaces. The single layers are superimposed and electrically connected (usually in parallel), as shown in Figure 48. Stack-type cylindrical DEGs are usually conceived to work in compression, with the compressive forces being applied to the two bases of the DEG cylinder (hereafter also referred to connection surfaces). This prevents mechanical separation of the different layers of the DE membranes. When the height of the cylinder is maximum, the cross section (and thus the electrical capacitance) of the generator is minimum (see configuration (a) in Figure 48). When the height of the generator reaches the minimum value, the cross section (and thus the electrical capacitance) of the generator is maximum (see configuration (b) in Figure 48).

Possible criticalities for this type of generator are elastic instability (due to buckling under compression) and the inhomogeneity in the stress field (caused by the rigidity of the connection surfaces) which impose conflicting limits on the length-to-cross-section-ratio of the device.

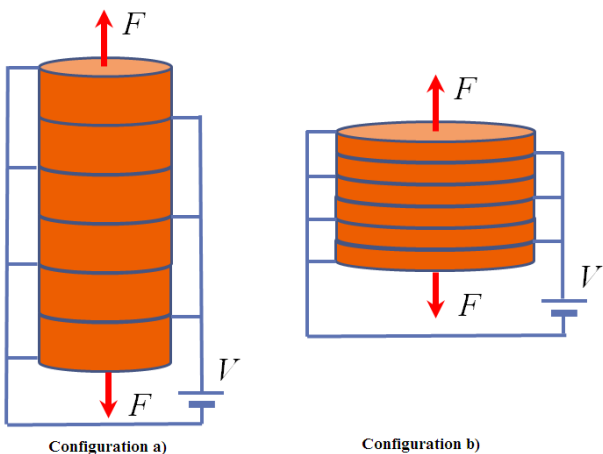


Figure 48 - Operation of a multilayer cylindrical DEG

Roll-type cylindrical DEGs [18] are made by a series of DE membranes rolled into tubes that constitute a bundle of elastomers acting in-parallel (see Figure 49). In most cases, the DE membranes are rolled up around a compressed core spring that maintains longitudinal and circumferential pre-stretch, and allows for longitudinal displacements. Differently from the previous case, here the electrodes are deposited on the longitudinal lateral surface of each rolled sheet. The generator is designed to vary its longitudinal length: when the cylinder height is maximum, the lateral surface of the cylinder is maximum, which also maximizes electrical capacitance; when the cylinder height is minimum, the lateral surface of the cylinder is minimum, which also minimizes electrical capacitance. The main criticality for this type of DEGs concerns the difficulties in the manufacturing and assembly of the rolls.

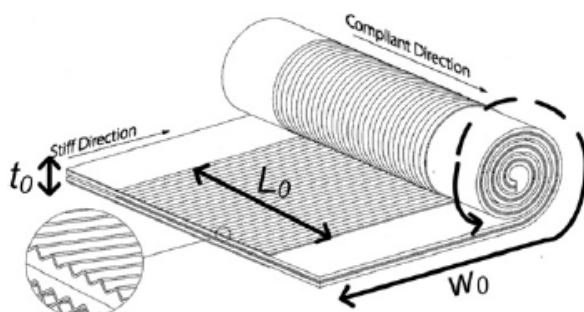


Figure 49 – Roll-type cylindrical DEG

Irrespective of the type, cylindrical DEGs are suited to be coupled with WECs featuring linear translational motion. In particular, they can be used to replace traditional PTOs based on hydraulic rams and linear electromagnetic generators.

3.4 Preliminary hydrodynamic models

The study of the energy harvesting performances of a first generation PolyWEC requires the implementation of a complex model, capable of taking into account the following aspects:

- Hydrodynamics of the oscillating WEC: the devices considered here comprise totally or partially submerged bodies that oscillate at the same frequency of the incident waves (in the assumption of monochromatic sea-

states). A study of the hydrodynamics of the different conversion systems is thus required in order to determine the dynamic parameters of the problem (forces/torques, oscillation amplitude etc.).

- Electro-elasticity of the DEG: first generation PolyWECS consist in a traditional WEC provided with a DEG PTO possessing one of architectures described in Section 3.3. The considered DEG PTO features non-linear behavior, since the forces/torques that they exert on the environment are not proportional to the stroke undergone. A proper electromechanical model of the employed DEG has to be realized, with the aim of assessing the amount of energy that can be converted in a cycle as well as determining the dynamic response of the generator.

As a general rule, the hydrodynamic modeling of WECs is carried out exploiting simplified models that are based on potential theory. The use of more sophisticated methods (such as CFD) could guarantee a better accuracy of the results (by taking into account phenomena like vortices, turbulence etc.), but would be too time-consuming and, thus, non suitable for the aforementioned studies that require reiterated calculations on a large number of configurations and of different sea state conditions.

In the following, a synthetic presentation of the hydrodynamic model usually exploited in the study of WECs is described, with reference to a single degree-of-freedom oscillating converter. Further details and generalization can be found in [46].

The first assumption used in the study of WECs is that incident waves are monochromatic (that means, characterized by a precise value of frequency rather than by a superimposition of harmonics). Basing on this presupposition, the simplest approach is the so-called “linear theory”. Linear theory is based on the assumption that the overall system (WEC+PTO) is linear; the wave induced loads are sinusoidal functions and, consequently, thanks to linearity, the motion of the converter follows a sinusoidal law; thus, the study can be carried out entirely in frequency domain.

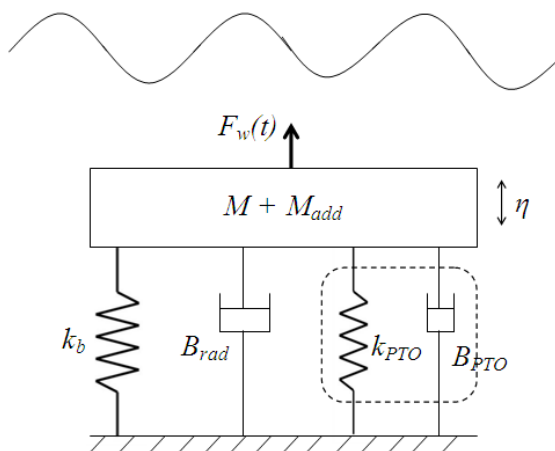


Figure 50 - Schematic of WEC according to linear theory

With reference to a generic oscillating body, the displacement from the equilibrium position can be expressed as $\eta(t) = \text{Re}\{\hat{\eta}(\omega)e^{i\omega t}\}$, where η can identify either a linear or an angular displacement.

The hydrodynamic loads acting on the WEC are:

- Wave induced force/torque: it is a sinusoidal function, $F_w(t) = \text{Re}\{\hat{F}_w e^{i(\omega t+\phi)}\}$ that, in the frequency domain, is generically indicated with \hat{F}_w .
- Buoyancy loads: generally, the combined effect of weight and buoyancy force is non linear, but it can be linearized and expressed in the frequency domain as $\hat{F}_b = -k_b \hat{\eta}$.
- Radiation load: a floating body oscillating in sea waves is a source of waves. As a consequence, a radiation load acts on the body, with a mathematical expression (in the frequency domain) given by

$\hat{F}_r = -i\omega B_{rad}\hat{\eta} + \omega^2 M_{add}\hat{\eta}$. That is, under the hypothesis of linearity, the radiation produces an effect of damping (B_{rad}) plus an effect of added inertia (M_{add}).

- PTO induced force/torque: Linear theory requires that the general expression of the force produced by the generator on the moving body has the form $\hat{F}_{PTO} = -i\omega B_{PTO}\hat{\eta} - k_{PTO}\hat{\eta}$. That is, the generator provides a damping effect (B_{PTO}) and a stiffness component (k_{PTO}).

According to the previous considerations, the schematic model of a WEC is shown in Figure 50. The expression of the wave-induced loads and of the radiation parameters B_{rad} and M_{add} are usually calculated using a boundary-element code (i.e. WAMIT [47]). Of course, this method makes the results reliable only in a small interval of displacements that lie around the position with respect to which the hydrodynamic parameters are evaluated.

In the case of PolyWECS, the intrinsic non-linearity of the polymeric PTO makes necessary the employment of a non-linear approach in the time domain that considers: a sinusoidal incident wave (as in the linear case), a buoyancy load that can be either linear or non-linear, and a non-linear model for the PTO system. For what concerns radiated waves, in the time domain this effect can be expressed by equation (33)

$$F_r(t) = M_{add}\ddot{\eta}(t) - \int_0^t K(t-\tau)\dot{\eta}(\tau)d\tau \quad (33)$$

that is due to an added mass effect plus a time convolution [49], where $K(t)$ is the radiation impulse response function representing the fluid memory effect and is therefore also called ‘memory function’.

Pragmatically, the convolution integral can be approximated by a state-space model. The result is presented in equation (34):

$$y = \int_0^t K(t-\tau)\dot{\eta}(\tau)d\tau = \begin{cases} x = A\dot{x} + B\dot{\eta} \\ y = Cx \end{cases} \quad (34)$$

Of course, the parameters M_{add} , A , B and C are function of the frequency ω of the incident monochromatic wave.

3.4.1 Preliminary Wave to Wire Model of a First Generation PolyWEC

In this paragraph, the study of a first generation PolyWEC is presented. The considered converter is the PolySurge device introduced in Figure 38. The DEG used as PTO is the LS-DEG described in Figure 44. As schematized in Figure 51, the LS-DEG is mounted in a way that, when the flap is in vertical position, the surface of the DE is maximum and has square shape.

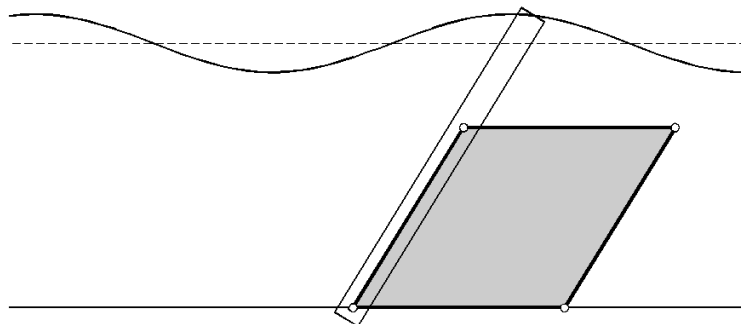


Figure 51– Schematic of a PolySurge WEC

The four-bar mechanism of the LS-DEG has one link attached to the flap and another one attached to the seabed. The adequate amount of DE material required for the energy conversion can be put in place using a side dimension

of the lozenge that is comparable with the flap height and using multiple films, each provided with a couple of compliant electrodes and arranged in a stack along the flap width. The usage of a set of distinct DE membranes instead of a monolithic volume is a necessity in order to guarantee homogeneous exploitation of the material and facility during maintenance operations. Since the generator is submerged, its electrodes must be insulated from the marine water. This can be achieved by adding additional insulating membranes between electrodes and water. For the arrangement considered in Figure 51, in order to prevent the mechanical rupture of the DE membranes, the pitch angular displacement of the flap must be kept below a security value. In presence of storms, featured by unusually intense waves, the PolySurge needs to be provided with some protection mechanism that is capable to decouple the DEG and the flap so as to bring the latter to a security position.

The pre-stretches of the DE membrane in the two principal directions (parallel to the diagonals of the lozenge) are equal, so that the behavior of the device is symmetric with respect to the vertical axis (with the vertical position being the static equilibrium point for the flap). When the generator passes through the vertical position, it is electrically activated so that, as the flap deflects, the surface of the activated membrane reduces (and the capacitance of the generator decreases), thereby producing electrical energy. When the flap reaches the point of maximum angular displacement from the vertical configuration, the membrane gets deactivated so that no electrical work is spent/produced as the flap returns. The key positions of the PolySurge system are shown in Figure 52. During a wave period, two active strokes (and two inactive strokes) are present; that is, the PolySurge system performs two ECCs per single wave period.

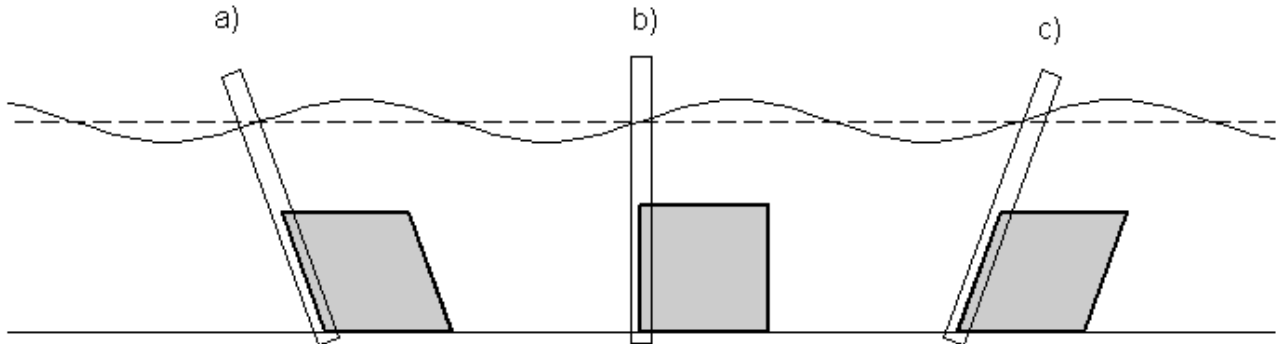


Figure 52–PolySurge: (a) and (c) minimum area configurations; (b) maximum area configuration

3.4.1.1 LS-DEG mathematical model

A model for LS-DEGs has been developed and published within PolyWEC project [37].

With reference to Figure 53, the variable x identifies the longitudinal length of the transducer and y is transversal length. The stretches of the material in x and y direction are indicated with λ_1 and λ_2 respectively, and are expressed by equations (35) and (36).

$$\lambda_1 = \lambda_{1p} \frac{x}{x_p} \quad (35)$$

$$\lambda_2 = \lambda_{2p} \frac{y}{y_p} = \sqrt{\frac{4\ell^2 - x^2}{4\ell^2 - x_p^2}} \quad (36)$$

where ℓ is the side length of the lozenge frame and λ_{1p} and λ_{2p} are the pre-stretches referred to the configuration $(x_p; y_p)$. From the hypothesis of incompressible material, the third stretch λ_3 in thickness direction (z) is easily expressed as

$$\lambda_3 = (\lambda_1 \lambda_2)^{-1} \quad (37)$$

The elastic behavior of a rubber-like material is expressed by mean of a hyperelastic free-energy function Ψ_{hy} [27]. Indicating with t_0 the value of the initial thickness of the membrane (in the undeformed configuration), the principal stresses are expressed by

$$\sigma_1 = \lambda_1 \frac{\partial \Psi_{hy}}{\partial \lambda_1} - p \quad (38)$$

$$\sigma_2 = \lambda_2 \frac{\partial \Psi_{hy}}{\partial \lambda_2} - p \quad (39)$$

$$\sigma_3 = -p = -\varepsilon \frac{V^2}{\lambda_3^2 t_0^2} \quad (40)$$

With reference to Figure 53, the force F acting on the lozenge joints can be calculated for both the active and inactive configuration [16].

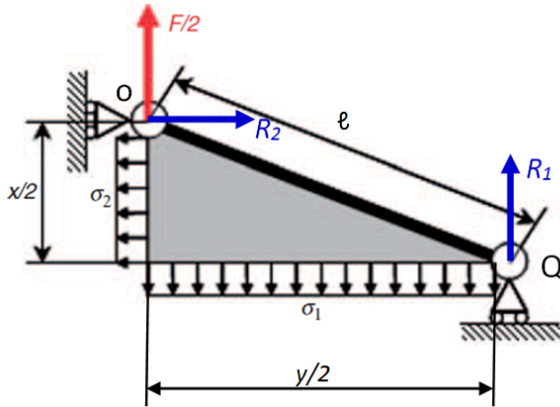


Figure 53 - Force balance for a portion of LS-DEG

In the inactive configuration ($V=0$), when no charge is present on the membrane, the force acting on the joints in the longitudinal direction is

$$F_{off}(x) = \frac{t_0}{2} \left(\frac{\sqrt{4\ell^2 - x_p^2}}{\lambda_{2p}} \frac{\partial \Psi_{hy}}{\partial \lambda_1} - \frac{xx_p}{\lambda_{1p}\sqrt{4\ell^2 - x^2}} \frac{\partial \Psi_{hy}}{\partial \lambda_2} \right) \quad (41)$$

In the active configuration, the equilibrium force is given by the sum

$$F_{on}(x) = F_{off}(x) + F_{em}(x) \quad (42)$$

where the addendum F_{em} that is relative to electrical activation is

$$F_{em}(x) = -\frac{\varepsilon V^2 \lambda_{1p} \lambda_{2p} x (2\ell^2 - x^2)}{t_0 x_p \sqrt{4\ell^2 - x_p^2}} \quad (43)$$

Equations (41-43) allow to assess the force response of the LS-DEG and are employed in the coupled model WEC+DEG to estimate the effect of the polymeric generator on the dynamic response of the WEC.

In order to forecast the maximal energy convertibility per cycle, the ECC formalism (described at paragraph 2.2) is employed.

As already mentioned, the maximum energy density that can be produced by a DEG is limited by different failure mechanisms of the employed DE membrane [24]: 1) electrical breakdown, 2) loss of tension, and 3) mechanical rupture. These failure conditions can be represented as limit curves on the Q - V plane, where Q and V are the charge and the electric potential difference that are applied between the electrodes of the considered DEG. First of all, it is possible to notice that the stretches λ_1 and λ_2 can be related to the longitudinal length x (see equations (35) and (36)). Then, expressing the capacitance of the lozenge generator as a function of x , equations (35) and (36) can be rewritten as

$$\lambda_1 = \frac{\lambda_{1p}}{x_p} \sqrt{2\ell^2 - 2\sqrt{\ell^4 - \frac{BQ}{\varepsilon V}}} \quad (44)$$

$$\lambda_2 = \frac{\lambda_{2p}}{y_p} \sqrt{2\ell^2 - 2\sqrt{\ell^4 - \frac{BQ}{\varepsilon V}}} \quad (45)$$

where ε is the dielectric constant of the considered DE material and $B = xyt/2$ is the volume of the considered DE membrane. Based on the preceding equations, the failure conditions of LS-DEG are next described as limit curves in the Q - V plane.

Geometric constraint: in equations (44) and (45), the argument of the square root has to be positive, which yields the limit curve

$$V = \frac{BQ}{\varepsilon \ell^4} \quad (46)$$

This physically means that the maximum allowable value for the LS-DEG capacitance occurs for $x = \sqrt{2}\ell$. Configurations given by $x \geq \sqrt{2}\ell$ are not considered, since they bring to a reduction of the capacitance. For the purposes of this analysis it is sufficient to restrict the investigation to values of x lower than $\sqrt{2}\ell$.

Electric breakdown: the electric field E acting across the LS-DEG cannot exceed the dielectric strength E_{BD} of the considered DE material, namely $E \leq E_{BD}$. Since

$$E = \frac{V}{t} \quad (47)$$

by the definition of capacitance, the electric breakdown condition yields the following limit curve

$$VQ = \varepsilon B E_{BD}^2 \quad (48)$$

Which describes a hyperbola in the Q - V plane.

Mechanical rupture: the mechanical rupture of DE materials is usually expressed as a limitation on the values of the stretches. For LS-DEGs, there are two rupture conditions: $\lambda_1 \leq \lambda_u$ and $\lambda_2 \leq \lambda_u$, where λ_u is the ultimate

stretch before mechanical failure. Using equations (44) and (45), the rupture conditions yield the following limit curves

$$V = \frac{B}{\varepsilon} Q \left(\ell^4 - \left(\ell^2 - \frac{x_p^2 \lambda_u^2}{2 \lambda_{1p}^2} \right)^2 \right)^{-1} \quad (49)$$

$$V = \frac{B}{\varepsilon} Q \left(\ell^4 - \left(\ell^2 - \frac{y_p^2 \lambda_u^2}{2 \lambda_{2p}^2} \right)^2 \right)^{-1} \quad (50)$$

On the Q - V plane, these equations represent straight lines passing through the origin of the axes.

Loss of tension: to function properly, the DEG membrane should not wrinkle. This requires the stresses σ_1 and σ_2 to be positive. Manipulating the expression for the electrically induced stress, namely

$$p = \frac{QV}{B} \quad (51)$$

the loss-of-tension condition for x and y directions yields the following limit curves

$$\lambda_1 \frac{\partial \Psi_{hy}}{\partial \lambda_1} = \frac{QV}{B}; \quad \lambda_2 \frac{\partial \Psi_{hy}}{\partial \lambda_2} = \frac{QV}{B} \quad (52)$$

Among all the failure conditions, loss of tension is the only one that depends on the constitutive equations of the material. Thus, the prediction of loss of tension is generally related to the specific form of the hyperelastic free-energy function that is chosen to describe the elastic behavior of the LS-DEG. Notice that hysteresis is neglected for the purposes of the present discussion.

The set of limit curves defined by equations (46), (48), (49), (50) and (52) determines the operation domain of the LS-DEG in the Q - V plane. In order to generalize the discussion, making it fit to any possible choice of LS-DEG geometry, equations are next reduced in dimensionless form.

We introduce the following dimensionless parameters:

$$x^* = \frac{x}{\ell}, \quad y^* = \frac{y}{\ell} = \sqrt{4 - x^{*2}} \quad (53)$$

$$Q^* = \frac{Q}{\varepsilon E_{BD} \ell^2} \quad (54)$$

$$V^* = \frac{V}{E_{BD} B / \ell^2} \quad (55)$$

Referring to the new variables, the limit curves assume the expressions below:

Dimensionless geometric constraint:

$$Q^* = V^* \quad (56)$$

Dimensionless electric breakdown condition:

$$Q^*V^* = 1 \quad (57)$$

Dimensionless mechanical rupture condition:

$$V^* = Q^* \left(1 - \left(1 - \frac{x_p^{*2} \lambda_u^2}{2 \lambda_{1p}^2} \right)^2 \right)^{-1} \quad (58)$$

$$V^* = Q^* \left(1 - \left(1 - \frac{y_p^{*2} \lambda_u^2}{2 \lambda_{2p}^2} \right)^2 \right)^{-1} \quad (59)$$

Dimensionless loss of tension condition:

$$\lambda_1 \frac{\partial \psi}{\partial \lambda_1} = \varepsilon E_{BD}^2 Q^* V^* \quad (60)$$

$$\lambda_2 \frac{\partial \psi}{\partial \lambda_2} = \varepsilon E_{BD}^2 Q^* V^* \quad (61)$$

These equations make it possible to compare LS-DEGs having different geometric dimensions and that employ the same DE material.

In the Q^* - V^* plane, any possible ECC describes a closed surface, whose area represents the generated energy in dimensionless form; namely

$$En^* = \frac{En}{\varepsilon E_{BD}^2 B} \quad (62)$$

As a practical example of application of the presented method, we refer to the acrylic elastomer VHB-4905 by 3M. The material has been preliminarily characterized [17], and the following parameters can be assumed:

- Rupture stretch, $\lambda_u=5.5$;
- Hyperelastic model: with reference to a second order Ogden model, the strain-energy function Ψ_{hy} can be expressed in the form

$$\Psi_{hy} = \sum_{i=1}^2 \frac{\mu_i}{\alpha_i} \left(\lambda_1^{\alpha_i} + \lambda_2^{\alpha_i} + \lambda_3^{\alpha_i} - 3 \right) \quad (63)$$

with $[\mu_1 \mu_2] = [-1.01 \ 8e3]$ Pa and $[\alpha_1 \alpha_2] = [-2.0 \ 2.48]$.

- Break-down electric field, $E_{BD}=50$ MV/m.
- Pre-stretches, referred to the square configuration $x_p^* = y_p^* = \sqrt{2}$, $\lambda_{1p} = 6$, $\lambda_{2p} = 2$.

The resulting ECC and the enclosed area (representing the dimensionless converted energy) is shown in Figure 54.

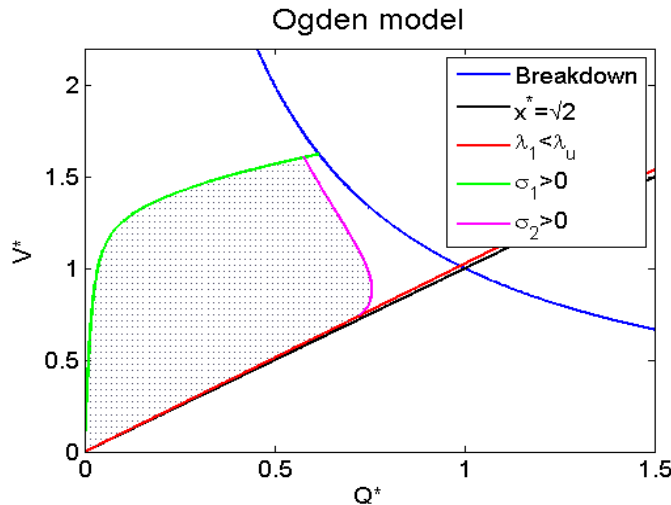


Figure 54 - Example of ECC for a LS-DEG

More generically, it is possible to set up an optimization of the converted energy per unit of material volume by tuning the pre-stretches λ_{1p} and λ_{2p} . In [37], a complete analysis and optimization of LS-DEG based on a VHB acrylic is carried out. Calculations are performed with different hypotheses on the constitutive hyperelastic model and on the break-down field. A maximum energy convertibility per cycle up to 0.3 J/g has been assessed.

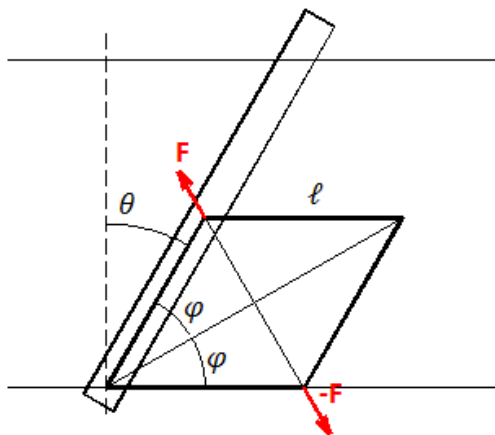


Figure 55 – Scheme for the calculation of the PTO-induced torque

3.4.1.2 PolySurge model

With reference to the coupled PolySurge system described in Figure 38, indicating with F the equivalent force acting on the joint of the lozenge frame connected to the flap (equations (41) and (42)), the PTO torque acting on the flap is

$$T_{PTO} = F\ell \cos \varphi \quad (64)$$

where φ is simply given by $\varphi = (\pi/2 - \theta)/2$.

In order to clarify the modeling procedure for the coupled system, the Simulink scheme of Figure 56 can be considered.

The blocks constituting the scheme represent the key elements behind the simulation of a coupled model WEC+DEG in the time domain.

The main blocks needed to study the problem can be resumed in:

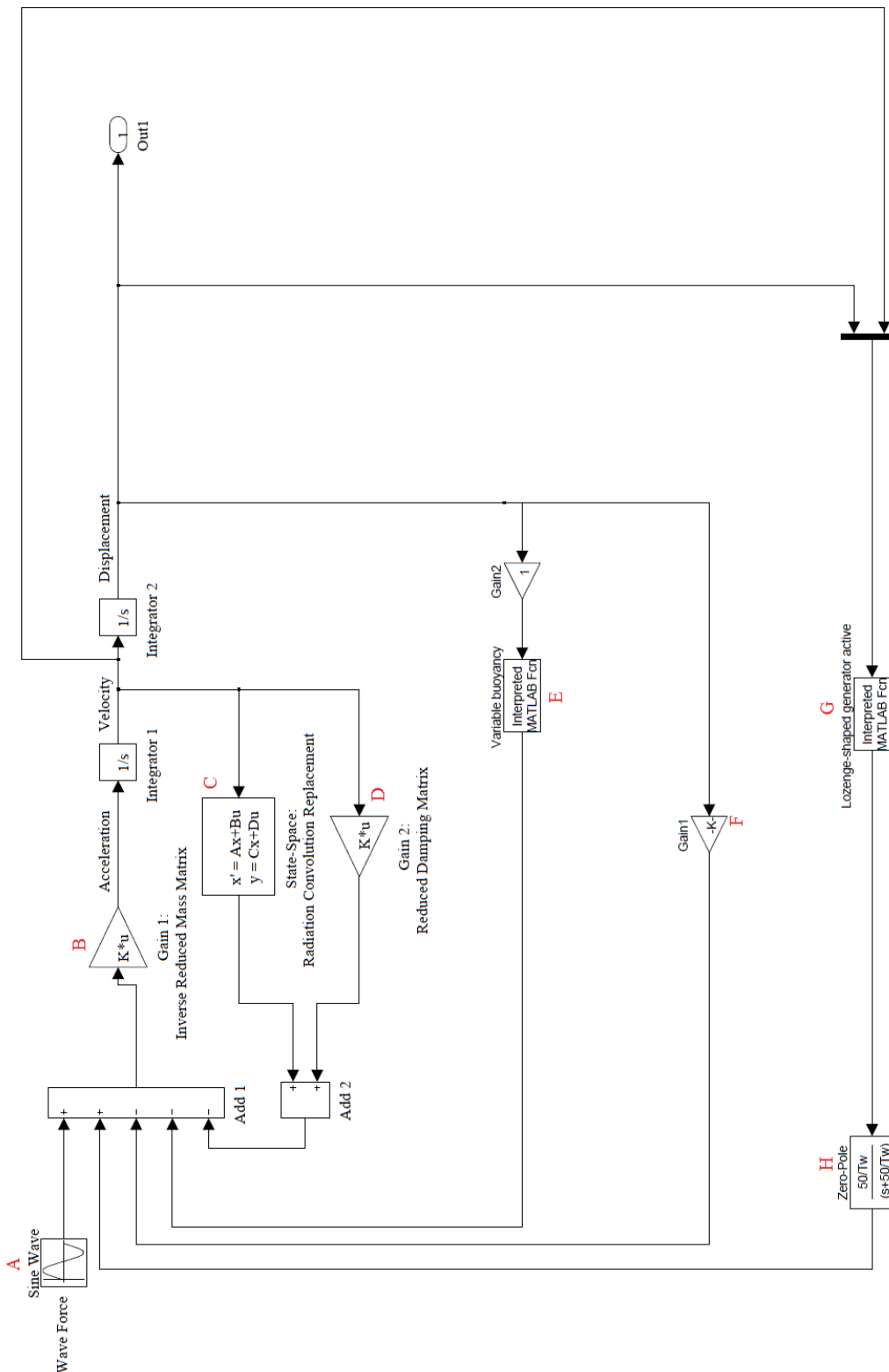


Figure 56 - Simulink model for the PolySurge

- A. Wave induced torque: it is modeled as a sinusoidal signal, with characteristic parameters calculated by mean of a boundary-elements code (like WAMIT [47]). Thanks to the properties of linearity within the linear wave theory, the module of the wave induced torque acting on the flap varies linearly with the wave amplitude. Therefore, it is sufficient to employ the WAMIT code to calculate the wave induced torque for a waves with unitary amplitude and different frequencies. With these results, for a generic incident wave, the effective value of the torque acting on the flap can be calculated interpolating on the frequency and multiplying by the value of the wave amplitude. It is important to notice that the output of the WAMIT code is obtained with reference to a specific angular position of the flap, that is the vertical equilibrium position. A more accurate analysis could consider the variability of the wave induced torque with the angular position.
- B. Inverse reduced mass matrix: this block is a gain, whose value is equal to the reciprocal of the flap moment of inertia around the pivot axis. Multiplying the torque by this value, the angular acceleration of the flap is obtained. Subsequently, with a double integration, the value of the angular position of the flap is found.
- C. Radiation block: As previously mentioned, in the time domain, the effect of radiation has to be modeled calculating the convolution integral between the velocity and the impulse response function. Anyway, the convolution term can be replaced by a state-space model, the parameters of which are calculated on the basis of WAMIT output results.
- D. External damping: an external damping source can be present. This block simulates the presence of a traditional electric (or hydraulic) PTO system. The external damping torque is expressed in the form $T_{damp} = B\dot{\theta}$. Even if this work is focused on the study of polymeric PTOs, the external damping block is present for the aim of making comparisons. When the system works with a polymeric PTO, the value of external damping is set to zero.
- E. Non-linear buoyancy: The combined effect of buoyancy force and weight force produces a non-linear torque on the flap. The buoyancy torque can be expressed as a function of θ as

$$T_b = - (F_A r_{buoy} - F_W r_{weight}) \quad (65)$$

where F_A and F_W are the Archimede's and the weight forces respectively, and r_{buoy} and r_{weight} are the corresponding lever arms. Referring to Figure 57, two sub-cases can be identified. Let indicate with $\theta_{IMM} = \arccos(h/L)$ the limit angle: h is the water depth (above the pivot) and L is the flap height (above the pivot). For $\theta < \theta_{IMM}$ the flap partially emerges from the water (using as a reference, for simplicity the SWL), while for $\theta \geq \theta_{IMM}$ the flap is fully submerged. In both of the cases, the force F_W is equal to the whole weight of the flap and is applied to its center of mass. The Archimede's force F_A is equal to the weight of an amount of water corresponding to the volume of the submerged portion of the flap, and is applied to the center of mass of the submerged section of the flap itself.

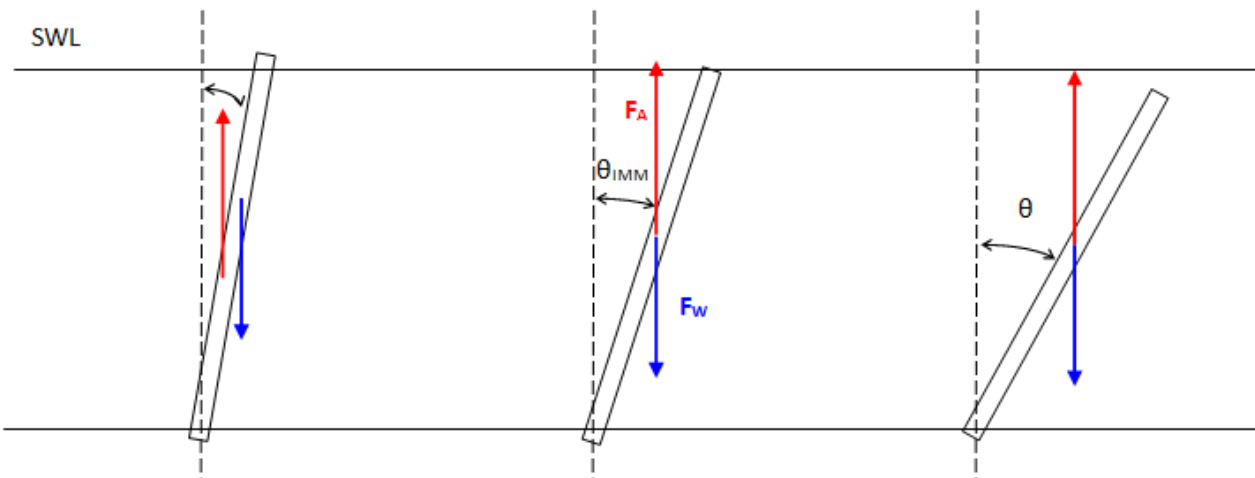


Figure 57 - Buoyancy torque calculation

- F. **Stiffness of the system:** When the buoyancy torque is linearized, its effect is represented by a simple gain block rather than by the complex function described at point E. This block is also used to take into account the presence of eventual external mechanical spring-like components (used, for instance, to bring the system to the resonance condition).
- G. **PTO block:** This block calculates the instantaneous torque provided by the LS-DEG as a function of the input pitch position of the flap (equations (41), (42) and (64)). The design parameters of the generator are given. In particular, the pre-stretches of the membrane in the principal directions are equal, $\lambda_{1p} = \lambda_{2p}$. Due to the mechanical rupture condition, a maximum allowed inclination angle θ_u for the flap exists. For a given generic incident wave, the flap oscillation range is $\theta \in [0; \theta_{\max}]$, where $\theta_{\max} < \theta_u$ is the oscillation amplitude of the flap, that depends on the general dynamics of the system. The implemented control scheme for the DEG is schematically shown in Figure 58. The solid blue line represents the break-down condition. The control of the ECC can be performed by acting on the value of the electric field (iso-electric-field transformation), using a value lower than E_{BD} (dashed line in Figure 58). This operation, at a first sight, appears to reduce the area enclosed by the cycle (in the $Q-V$ plane), since the iso-electric-field line moves towards the origin of the axes. Nevertheless, if the new value of the electric field allows larger values of θ_{\max} , the slope of the corresponding line (in magenta in Figure 58) increases, and this may compensate the reduction in the electric field. Controlling the value of the electric field allows, in a certain sense, to control the stiffness of the generator. In conclusion, the value of the controlled electric-field can be modified in order to maximize the power output of the WEC.

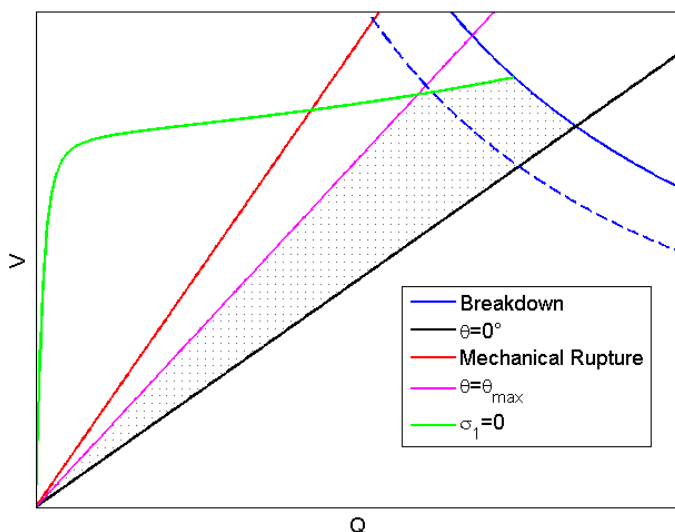


Figure 58 - Control scheme for the ECCs of the LS-DEG

- H. **Generator dynamics:** the LS-DEG is alternately activated and deactivated. The injection of charge on membrane electrodes is theoretically instantaneous. Nevertheless, since the activation provokes a significant change in the torque applied by the PTO to the flap, in order to guarantee the numerical stability of the solution, such PTO torque needs to be filtered out with a system with first order dynamics. Rigorously, the real dynamics should be determined on the basis of appropriate measurements performed on electrode resistivity.

In the described analysis some aspects are neglected:

- the inertia contributions of the DE material and of its frame are not considered: the only inertia is that of the flap (own inertia plus added inertia);
- DE material visco-elasticity is neglected;
- The fluid-dynamics effects caused by the presence of the LS-DEG are not examined.

From the results produced by the model, the oscillation angle of the flap is known, thus, the operative range of the LS-DEG also is known (since the oscillation amplitude defines a value of the maximum/minimum

length assumed by the lozenge diagonals during the operation). Using this information, since the control strategy of the generator is known, the energy per unit volume converted by the generator in one stroke can be calculated and used to forecast the mean power output of the system in correspondence of a given sea state condition.

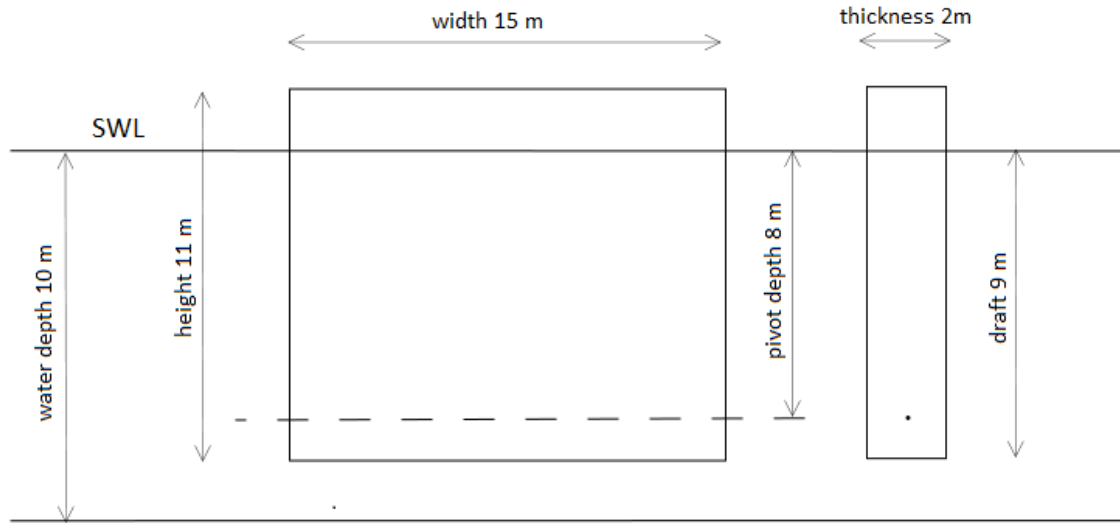


Figure 59 - Reference dimensions for the WEC

Application Example

The described procedure and the coupled model for the PolySurge is here applied to a practical example. Let us consider a specific layout for the oscillating flap. The geometry of the device is shown in Figure 59. The device is installed at a nominal water depth of 10 m. The flap is a rectangular cuboid with a height of 11 m, a width of 15 m and a thickness of 2 m. The draft of the flap is 9 m, so that, in the equilibrium condition, the flap extends by 2 m above the water surface. The pivot depth of the flap is 8 m, so that there is 1 m of the flap below the pivot. The buoyancy torque acting on the flap is non-linear, and no further external stiff components (like torsional springs) are present. Let us consider a monochromatic wave with period $T=10.5$ s and height $H=1.5$ m.

For illustrative purposes, we consider here a volume of polymeric material equalling 90 m^3 . Assuming pre-stretches $\lambda_{1p} = \lambda_{2p} = 4.21$, a maximum allowed value of 45° for θ_u is obtained.

The reference material is the acrylic elastomer VHB-4905 by 3M. With reference to the control strategy shown in Figure 58, simulations of the dynamics of the system are carried out with different values of the controlled electric-field E , with $E < E_{BD}$ ($E_{BD}=70 \text{ MV/m}$).

In Table 4, for the different choices of E , the resulting values of the oscillation amplitude for the flap and the mean power output of the DEG are reported.

| $E \text{ [MV/m]}$ | $\theta \text{ [deg]}$ | $P \text{ [kW]}$ |
|--------------------|------------------------|------------------|
| 40 | 0.75 | 339 |
| 50 | 0.71 | 477 |
| 60 | 0.63 | 516 |
| 70 | 0.50 | 442 |

Table 4 – PolySurge performances for different values of the controlled electric field

From Table 4 and Figure 60, it can be seen that the optimal value for the control electric field E is lower than the break-down value, since large values of E bring to a reduction of the oscillation amplitude, which penalizes the dynamic of the overall system.

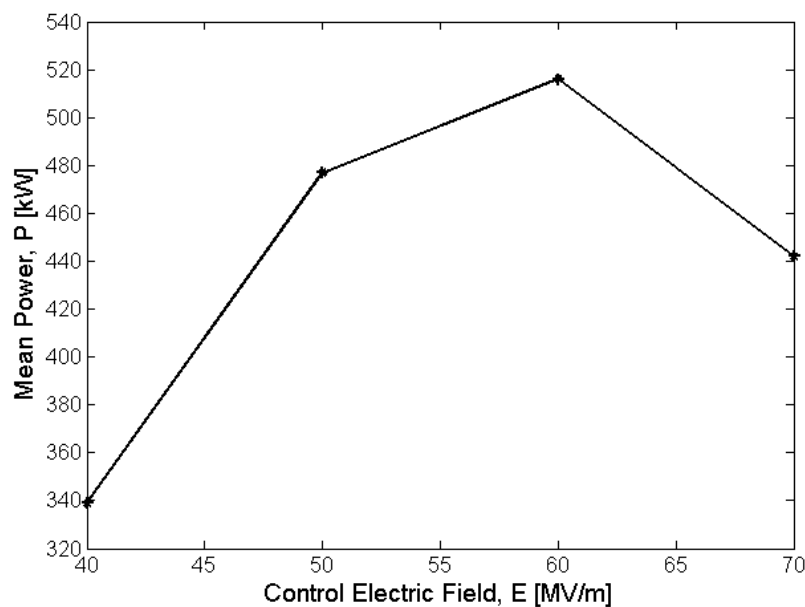


Figure 60 - Power output vs. Control Electric Field

3.5 Conclusions

In this section, first generation PolyWECS architectures are described. Three concepts are presented:

- Oscillating Wave Surge provided with lozenge-shaped DEG, which exploits pitch angular motion to induce deformations of the elastomeric capacitor.
- Heaving buoy connected with linear DEG (i.e., cylindrical or conical DEG).
- Articulated multi-body WECs, which exploit relative motion of multiple oscillating bodies connected by DE transducers.

A review of the principal DEGs architectures is outlined. A number of different layouts exists, this provides many possibilities in terms of DEG-WEC coupling.

A general hydro-electro-elastic model for first generation PolyWECS is proposed and a numerical case study on a DE-based surging converter (Poly-Surge) is presented.

The general model is based on simplified hydrodynamics, based on potential flow theory. Hydrodynamics can be either linear or non linear (i.e., non-linear buoyancy can be implemented). An analytic electro-mechanical model is adopted for the DEG. Although the method is based on some simplifications (e.g., the presence of the DEG in the WEC surroundings does not affect the fluid-dynamic fields), it allows to quickly assess the devices performance and to carry out optimizations.

4. ARCHITECTURE OF SECOND-GENERATION POLYWECS

4.1 Introduction

First-generation PolyWECS are characterized by indirect interaction between dielectric elastomer generator unit (DEGU) and fluid. That is, the deformations of DE membranes are not directly generated by fluid pressures but by a mechanical interface.

On the contrary, second-generation PolyWECS are characterized by direct interaction between DEGU and fluid, which occurs over wide contact surfaces. That is, fluid-DEGU interaction is not mediated by any mechanical means, and DE membrane deformation is directly generated by wave-induced fluid pressures. As a result, second-generation PolyWECS are highly-integrated wave-energy converters that feature the minimal number of mechanical and electrical components beside the DEG. Moreover, thanks to their intrinsic and tuneable compliance, second-generation PolyWECS make it possible to achieve maximal wave-energy extraction efficiency. This second type of WECs is however characterized by number of technical issues both on theoretical modelling and manufacturing.

In this section, different layout and architectures are defined for second-generation PolyWECS. A basic distinction among the possible architectures is done distinguishing different the working principle and different type of fluid dynamic interaction.

A first kind of systems is based on oscillating water column principle and took the name of Poly-OWC device. This type of device is characterised by having a closed chamber in which a mass of water assumes an oscillatory motion. Such a column of water mediates the dynamic interaction between wave and DEGU. A second type of devices employs DEGU which are freely interacting with the waves. In this case, membranes are directly deformed by wave motion and the fluid dynamic interaction is direct. These devices took the name of Poly-SubMe (Polymeric Submerged Membranes).

4.2 Architecture of Poly-OWC

Oscillating Water Column (OWC) wave energy converters are based on movement of a water column enclosed in chamber (tube or duct) that has at least one submerged opening. The water inside the closed chamber is moved by wave-induced oscillating pressures on the opening. In traditional OWC concepts, the movement of the oscillating water column induces a pressure variation inside a closed air chamber. Such a pressure variation is used to drive a Turbo Generator (TG), which converts such a pneumatic power into usable electricity. Due to reciprocating air-flow, energy harvesting from traditional OWC devices requires either a self-rectifying turbine [53] or a complex system of non-return valves which makes it possible to rectify the flow passing through a conventional turbine [54].

The basic architecture of a Polymeric Oscillating Water Column (Poly-OWC) converter is based on a traditional OWC, where the turbo generator is replaced by a DE transducer. A Poly-OWC device exploits the oscillating pressure, which is produced by the reciprocating motion of the free surface of water inside the closed air-chamber, to induce a cyclical deformation of a DE membrane. This deformation causes a variation of the DE membrane capacitance, which can then be used to generate electricity via the variable-capacitance electrostatic generator principle.

The use of DE transducers in OWC converters has several potential advantages with respect to traditional electromechanical solutions in terms of:

- low costs: the relative inexpensiveness of DE materials together with the intrinsic simplified architecture, with reduced additional electrical components (inverters, transformers, etc.), make it possible to develop WECs with lower capital and operation costs;
- easy installation and maintenance: DE generators are soft and light-weight, thus they do not require high grade tolerances for mechanical installation and do not require powerful handling machines to be moved or installed;
- high energetic efficiency: Poly-OWC could be more efficient than TG-OWC due to: limited friction losses, larger bandwidth and limited electrical losses. However, a technological demonstrator still needs to be realized which proofs such a higher energy conversion efficiencies.

- reduced noise: the operation noise of Poly-OWCs is likely to be lower than that of TG-OWCs, which could enable their installation in close proximity to habited coastal areas (for instance in ports).
- climate adaptability: due to the capacitive nature of Poly-OWCs, their electrical efficiency is rather independent of cycle amplitude and frequency; thus they are easy to scale-up or –down, and can be very attractive not only for locations with consistent and large waves, but also in mild-to-moderate wave climates and where large seasonality effects occur.

Poly-OWC can be classified into two categories: (a) *Dry* where DE membrane is not in contact with water and (b) *Wet* where DE membrane is submerged.

- *Dry*: The working principle is similar to a traditional OWC concept. The DEGs are not in contact with water and the deformation of the DE membrane is induced by air pressure. There are several options for the implementation of a Poly-OWC. We can distinguish different layouts according to the way the force produced by the oscillating pressure is transmitted to the DE membrane:

- (1) Direct-pressure: The DE membrane directly covers one or more openings of the OWC air-chamber and is directly deformed by the air pressure without the presence of any additional moving rigid element. Figure 61-a shows a possible scheme of such an implementation. As examples, the DE membrane can have the shape of a spherical cap or the shape of a horizontal cylindrical cap.
- (2) Object-mediated: The interaction between DE membrane and chamber-pressure is completely mediated by an additional object, such as a moving piston (see Figure 61-b). This configuration may allow the adoption of different known architectures of DE transducers; for instance conically-shaped or lozenge-shaped DE transducers.
- (3) Hybrid: The DE membrane is connected to some additional moving rigid elements. The air-chamber pressure directly acts on both DE membrane and on the rigid elements at the same time (see Figure 61-c). This solution could lead to an improved exploitation of the DE transducer thanks to a more uniform strain and/or a strain-amplification effect.

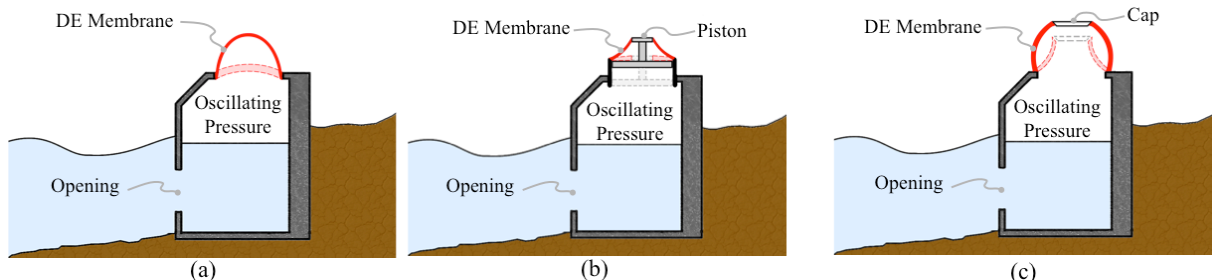


Figure 61: Schematics of possible implementations of Dry Poly-OWC: (a) Direct-pressure, (b) Object-mediated, and (c) Hybrid.

- *Wet*: The DE membrane of the Poly-OWC is submerged and directly deformed by pressure field exerted by the water included into chamber (see Figure 62). Two types of architectures can be identified. The first one (Figure 62-a) is partially submerged that is one of the faces of the membrane is not exposed to liquids. The second (Figure 62-b) is characterized by fully submerged DE membrane. Wet-Poly-OWCs are functionally similar to Dry-Poly-OWCs but, from the point of view of the modelling, the direct contact between water and membrane entail the use of more complex/coupled dynamic model. The problem of fluid-membrane interaction have to be solved, however it is foreseen to find simplified solutions for the fluid dynamic problem thanks to the dominating dynamic behaviour of the mass of oscillating water column over the local distribution of pressures on the membrane.

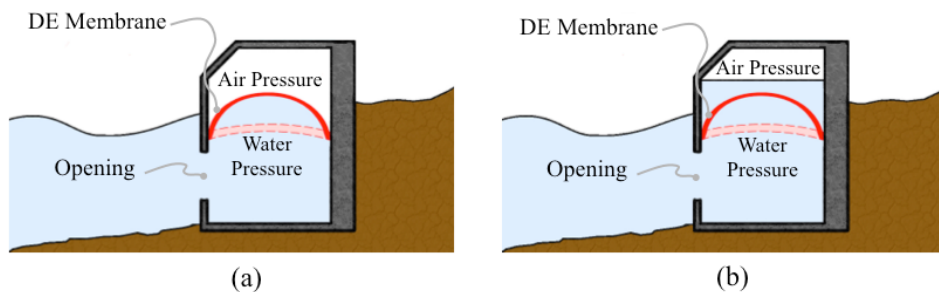


Figure 62: Schematics of possible implementations of Wet Poly-OWC: (a) Partially submerged membrane membrane
(b) fully submerged membrane.

4.3 Architecture of Poly-SubMe

Polymeric Submerged Membranes (Poly-SubMe) WECs are characterized by having a submerged DE membrane that has at least one of the faces exposed to the open sea. The membrane could have initial flat or curved shape and can be arranged according different architectures.

In Poly-SuMe, the deformation of the membrane is produced by pressure distribution induced by a direct interaction between the membrane and the water particles. The dynamic of the system is governed by complex hydrodynamic interactions between water and membrane. The modelling of this kind of devices have to go through fully coupled hyper-elastic-fluido-dynamic models that take into account all the relevant physical phenomena.

Different topological solutions can be conceived to guarantee the required initial pre-stretch. In particular, the membrane can be framed (or partially framed), inflated or arranged in a hybrid combinations.

The following variants of architectures can be conceived:

- Submerged air chamber:

A rigid structure forms an opened submerged air chamber that is inflated and its opening is covered by a DE membrane (see Figure 63). The system is quite similar to a Wet Poly-OWC system (see 4.2) in which the membrane is brought in correspondence to the opening of the air chamber. However, differently from OWC systems, the dynamic behaviour of the system is not governed by a water column since the membrane exposed to the action of the open sea. The deformation of the membrane is caused by the pressure generated by water particles on one side and air pressure on the opposite side. The modelling of this type of PolyWEC has to go through a fully coupled physical model. However the device could be potentially interesting because:

- Differently from fixed OWCs, which mainly allow only on-shore installation, submerged membrane devices could be installed in shoreline or deep water.
- even though the device is submerged, a dry air chamber could be employed for hosting components and materials that are less tolerant to direct contact with water.
- if the volume of the air-chamber is properly dimensioned the non-linear response pressure/volume could be useful for protecting the membrane from overstretch;
- like in OWC, a membrane with flat shape when undeformed can be efficiently employed.

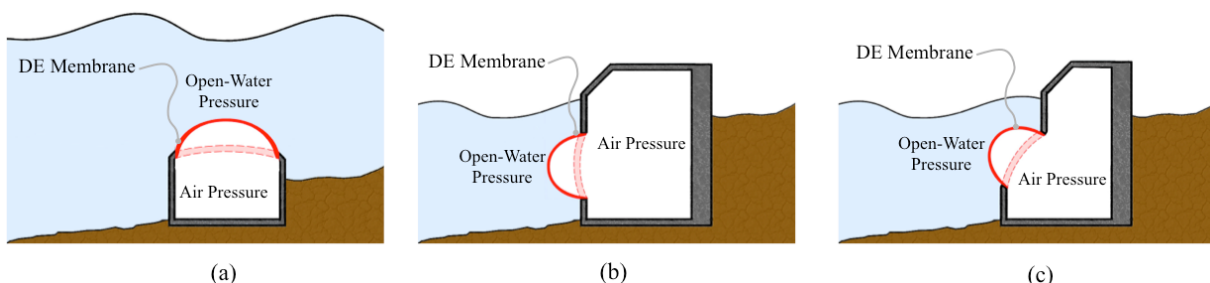


Figure 63: Schematics of possible implementations of Poly-SubMe: (a) Vertical (b) Horizontal (c) slanted.

- Balloon/Tube

Poly-SubMe can assume shapes like a submerged inflated balloon or a tube (Figure 64-a). The pressure differential generated by waves on the surface of the membrane generates expansion and contraction of the balloon volume, inducing variation of the DEGU surface/capacitance and enabling the production of electrical energy.

Balloon/Tube shaped PoyWECs is a very simple and effective type of device since:

- it is free of any mechanical parts;
- does not required complex assembly procedures;
- the stretching kinematics of a pressurized balloon allow deformations that are close to equi-biaxial state; enabling optimal conversion capabilities of the DE.

However, the finite compressibility of the air mass included in the balloon/tube could represent a limit to the efficiency and to the capability of converting energy especially when a small-scale device is sought after.

Moreover, manufacturing process of a balloon/tube shaped DEGU could be more complex since the undeformed shape of the membrane might not be flat but curved. Another aspect that could be critical is the mooring of a highly deformable structure that has to be studied in order to guarantee the reliability/survivability of the system.

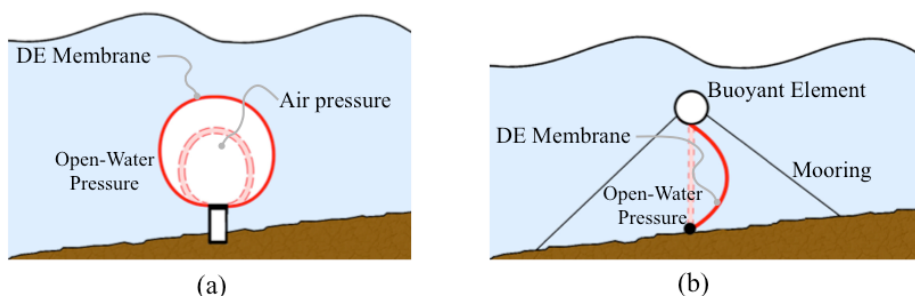


Figure 624: Scheme of the (a) Balloon/tube and (b) open membrane implementations

- Open Membrane

Open Membrane Poly-SubMes are characterized by a DEGU membrane which is exposed to the open sea on both its sides. The DE membrane is held by a frame which could be rigid or flexible. The frame could be also obtained as represented in Figure 64-b through a proper combination of buoyant elements and moorings. The deformation of the membrane surface is directly induced by water pressure. Both kinetic and potential energy contribution of waves can contribute to the deformation of the DE membrane.

Such a system can show the following advantages:

- Employs few mechanical parts that are mainly static;
- The frame could be designed in a way to guarantee overload protection of the membrane (for example in Figure 64-b the buoyancy could be dimensioned in order to saturate at maximum force value);

- Hybrid: Buoy membrane/tube

Hybrid concepts can be prospected which integrates in the same device different kind architecture topologies. Hybrid Poly-SubMe can show aspects of different type of second-generation device but also integrates elements of first-generation systems in order to provide optimal efficiency and power conversion. In Figure 65 examples of such hybrid systems are presented. Figure 65-a present a system that integrated a submerged membrane and a buoy system. In this case, the cyclical deformation of the DE is generated by both direct interaction of water pressure on the membrane and indirect forces transmitted through the floating element. The buoyant element could be dimensioned in a way to guarantee the needed preload for

initial pre-stretching of the elastomer. Figure 65-b shows a schemes that combines air-pressure differential submerged DE membrane with a buoy converter.

Architectures of this kind are the most complex to be modelled since the dynamics is governed by the coupled effect of fluid interaction with deformable bodies and rigid floating elements.

However, such a combined effects could also be a key solution for an optimal efficiency leading to high radiation and capture width ratios.

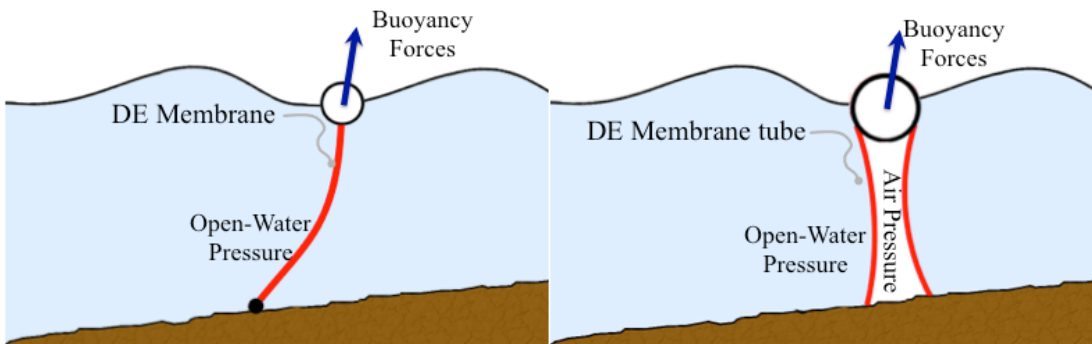


Figure 65: Scheme of hybrid architectures (a) Surging-Flap Buoy (b) Buoy with Tube shaped DEGU

4.4 Preliminary wave to wire models of second-generation PolyWECS

In this first phase of the project, two architectures have been preliminary analysed through analytical models. They are two different examples of Poly-OWC. The first one is characterized by having a DEG with rectangular membrane while the second assumes a circular shape. In the following subsections the details of the developed models are reported and preliminary simulation results are analysed. The detailed description of the two models can be found in [55] and [56].

4.3.1 Rectangular Diaphragm Oscillating Water Column

Analysis, design and control of Poly-OWCs require adequate multi-physic models capable of representing the complex mutual interactions occurring among water waves, OWC structure, compressing/expanding air and DE generator. Continuum multi-physic models for the study of Poly-OWC can be very cumbersome and computationally demanding, especially for three-dimensional geometries and complex shapes. Despite fundamental for the accurate study and optimization of real devices, these models are hardly suited for the basic understanding of general functioning principles as well as for the preliminary assessment of Poly-OWC systems.

With this in mind, this preliminary work considers the ideal two-dimensional problem depicted in Figure 66. The system comprises a fixed rectangular OWC structure opened to a wave basin of constant depth and employing a Cylindrically-Curved DE Membrane (CCDEM) as polymeric power take-off mechanism.

Introducing the spatial horizontal and vertical coordinates x and z (that are positive when pointing rightward and up-ward, respectively), the wave basin extends from $-\infty \leq x \leq 0$ and has constant depth H_B . The OWC structure has constant span c and is opened to the wave basin on its front-wall (at $x = 0$), with the submerged aperture being described by the constant distances a and b measured from the Mean Water Level (MWL). The OWC air-chamber comprises a rectangular part which extends by the constant length d from the MWL, plus (or minus, as depicted in Figure 66) the horizontal cylindrical segment that is subtended by the CCDEM with constant chord $2e$ and variable tip height h (h is positive when pointing up-ward). As indicated in Figure 66, P_{atm} is the constant atmospheric pressure acting on the air-water interface of the physical space outside the OWC, P_{OWC} is the air-chamber pressure acting on the air-water interface within the OWC, and P_E is the excitation pressure acting on the underwater part of the water column that is exposed to the wave field.

A lumped-parameter multi-physic model for the considered system is constructed in the following subsections.

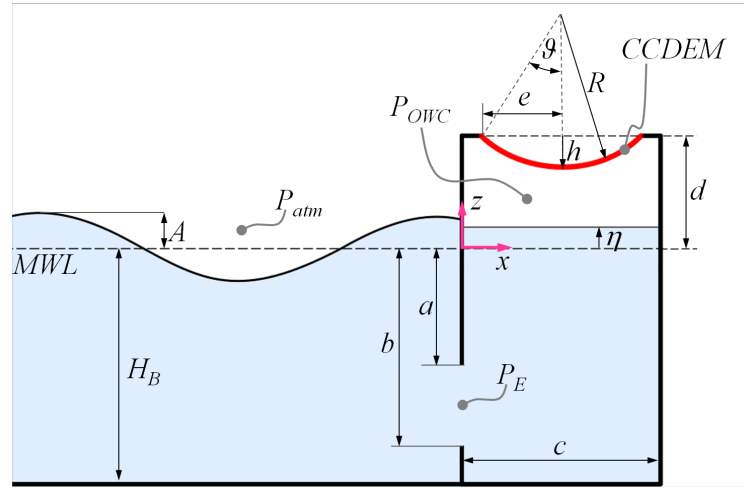


Figure 66: Scheme of the Poly-OWC model showing the relevant geometrical parameters.

4.3.1.1 Hydrodynamic model of OWC devices

Study of the Poly-OWC depicted in Figure 66 requires a hydrodynamic model that is capable of representing the oscillatory response of the water column to the pressures P_E and P_{OWC} . Several approaches are available in the literature which can be categorized in: 1) continuum linear models which enable the accurate study of problems with simple geometry in the frequency domain [57]-[63]; 2) continuum models which enable the accurate study of problems with simple geometry in the time domain [64]; 3) discrete models (for instance via the boundary element method and the finite volume method) which enable the accurate study of problems with complex geometries [65]-[68]; 4) lumped-parameter models which are suited for the preliminary study of problems with simple geometry in the time domain [69]-[70]. As a preliminary investigation, a lumped-parameter model is constructed here which relies on the following coarse assumptions:

- ideal fluid and linear water-wave theory;
- harmonic monochromatic waves on water of constant depth;
- perfect wave reflection from the OWC front-wall;
- no disturbance (for instance radiation) is caused by the OWC to the outer wave field;
- the free-water surface inside the OWC is replaced by a weightless rigid piston, whose motion with respect to the MWL can be described by the single displacement variable η .

With these simplifications, the hydrodynamic behavior of the water particles moving in the basin (as well as in close vicinity to the OWC front-wall) is characterized by the following velocity potential

$$\phi(x, z, t) = -\frac{2gA}{\omega} \frac{\cosh[K(z + H_B)]}{\cosh(KH_B)} \cos(Kx) \sin(\omega t), \text{ with } \omega = \frac{2\pi}{T}, \text{ for } -\infty \leq x \leq 0 \quad (65)$$

where t is the time variable, g is the gravitational constant, A and T are the amplitude and period of the incident wave, and K is angular repetency of the propagating wave (also called wave number) given by the dispersion relation

$$K \tanh(KH_B) = \frac{\omega^2}{g}. \quad (66)$$

Note that the potential given by equations (65) and (66) represents the total potential of both incident and diffracted wave. Accordingly, the dynamic pressure field permeating the wave basin (and acting on the OWC front-wall) results as³¹

$$p_E(x, z, t) = -\rho \left[\frac{\partial \phi}{\partial t} + \frac{1}{2} \left(\frac{\partial \phi}{\partial x} \right)^2 + \frac{1}{2} \left(\frac{\partial \phi}{\partial z} \right)^2 \right] \approx -\rho_w \frac{\partial \phi}{\partial t} = 2\rho_w g A \frac{\cosh[K(z + H_B)]}{\cosh(KH_B)} \cos(Kx) \cos(\omega t), \quad (67)$$

with ρ_w being the constant water density. Based on this hydraulic excitation, the equation of motion of the water column oscillating within the hollow structure depicted in Figure 66 can be written as

$$\ddot{\eta} = \frac{P_{atm} + P_E(t) - P_{OWC}(t) - \rho_w g \eta - D_1 \dot{\eta}}{\rho_w(a + \eta)}, \quad (68)$$

where D_1 is a linear damping coefficient accounting the hydraulic losses occurring within the OWC, and P_E results from Eq. (67) as the spatial average (along the z coordinate) of the dynamic pressure field acting on the OWC front-wall aperture (at $x=0$), namely

$$P_E(t) = \frac{1}{b-a} \int_{-b}^a p_E(0, z, t) dz \approx \frac{2\rho g A}{(b-a)} \frac{\sinh[K(H_B - a)] - \sinh[K(H_B - b)]}{K \cosh(KH_B)} \cos(\omega t). \quad (69)$$

The expression for P_{OWC} is detailed in the following sections.

4.3.1.2 Electro-elastic model of pressurized Dielectric Elastomer Membrane

The second element which requires to be modeled is the DE power take-off mechanism. The CCDEM is an electroactive element which undergoes out-of-plane deformations under the action of both the pressure P_{OWC} and the electric field E generated by the electric potential V that is applied between the CCDEM electrodes.

A number of approaches are available in the literature which can be employed for the study of the out-of-plane electro-elastic deformation of DE membranes. These approaches can be categorized in: 1) continuum thin-shell models which enable the accurate study of simple geometries via the numerical solution of systems of non-linear partial differential equations[71]-[72] 2) finite element models which enable the accurate study of complex geometries [73]-[75]; 3) simplified uniform-deformation models which enable the approximate study of simple geometries either via closed form expressions or via the numerical solution of algebraic equations.

For this preliminary investigation, a simple uniform-deformation model is considered which relies on the following coarse assumptions:

- The CCDEM is a Horizontal Circular Cylindrical Shell Segment (HCCSS) with small uniform thickness in any of its deformed configurations;
- The CCDEM does not undergo any axial deformation (a similar assumption provided good modeling results for similar DE membrane configurations);
- The CCDEM capacitance is assumed to be equal to that of a planar parallel plate capacitor with area and thickness equaling those of the CCDEM. That is, the electric field is considered uniform throughout the whole CCDEM.

With the abovementioned assumptions, for the considered HCCSS define: the radius R , the central semi-angle ϑ , the center of mass location \bar{h} (measured along the z coordinate), and the circumferential and axial principal stretches λ_1 and λ_2

$$R(h) = \frac{(e^2 + h^2)}{2h}, \quad (70)$$

$$\vartheta(h) = \cos^{-1} \left(1 - \frac{h}{R(h)} \right), \quad (71)$$

$$\bar{h}(h) = \left(\frac{e}{\vartheta(h)} - R(h) \right). \quad (72)$$

$$\lambda_1(h) = \lambda_{1,p} \frac{R(h)}{e} \vartheta(h), \quad (73)$$

$$\lambda_2 = \lambda_{2,p}. \quad (74)$$

which are functions of the fixed HCCSS chord e and the variable HCCSS height h . In Eqs. (73) and (74), $\lambda_{1,p}$ and $\lambda_{2,p}$ represent the constant CCDEM principal pre-stretches measured in the flat membrane configuration ($h = 0$).

In addition, assuming DEs as incompressible solids which exhibit non-linear elastic finite deformations and linear strain-independent dielectric properties [76], introduce the circular and axial stretches σ_1 and σ_2 (defined in the deformed configuration)

$$\sigma_1(h) = \mu_1 (\lambda_1^{\alpha_1}(h) - \lambda_3^{\alpha_1}(h)) + \mu_2 (\lambda_1^{\alpha_2}(h) - \lambda_3^{\alpha_2}(h)) - \varepsilon E^2, \quad (75)$$

$$\sigma_2(h) = \mu_1 (\lambda_2^{\alpha_1}(h) - \lambda_3^{\alpha_1}(h)) + \mu_2 (\lambda_2^{\alpha_2}(h) - \lambda_3^{\alpha_2}(h)) - \varepsilon E^2, \quad (76)$$

where μ_1 and μ_2 are the constant material shear moduli, α_1 and α_2 are constant dimensionless parameters (a two-term Ogden model has been considered for the hyperelastic response of the CCDEM), ε is the constant electrical permittivity of the CCDEM, and with λ_3 being the principal stretch in radial direction of the CCDEM

$$\lambda_3(h) = \frac{1}{\lambda_2} \frac{1}{\lambda_1(h)}. \quad (77)$$

Then, the equation of motion for the CCDEM follows as

$$\ddot{h} = \left[\frac{\lambda_{1,p} \lambda_{2,p}}{\rho_{DE} t_0} \left(P_{OWC}(t) - P_{atm} - t_0 \frac{\lambda_3(h)}{R(h)} \sigma_1(h) \right) - \frac{\partial^2 \bar{h}(h)}{\partial h^2} \dot{h}^2 \right] \sqrt{\frac{\partial \bar{h}}{\partial h}} - D_2 \dot{h}, \quad (78)$$

where ρ_{DE} and t_0 are the constant DE density and undeformed membrane thickness, and D_2 is a linear damping coefficient accounting for the visco-elastic losses occurring within the CCDEM.

4.3.1.3 Coupled electro-elastic-hydraulic model of Poly-OWC

Equations (68) and (78) represent the dynamic models of the two fundamental parts of a PolyOWC. Coupling of the two equations requires a relation for the expansion/compression of the air entrapped between the water column and the CCDEM.

Assuming an adiabatic process, the coupling relation is

$$P_{OWC}(t) = P_{OWC}(\eta, h) = \frac{C_0}{(V_{OWC}(\eta, h))^\gamma}, \quad (79)$$

where C_0 is a constant, V_{OWC} is the chamber volume (per unit width in the direction orthogonal to the plane of Figure 66) depending on both water column position η and CCDEM position h , namely

$$V_{OWC}(\eta, h) = c(e - \eta) + \text{sign}(h) \vartheta(h) R(h)^2 - e(R(h) - h). \quad (80)$$

In Eq. (79), the constant C_0 sets the steady condition of the air-chamber (pressurized, depressurized, or at atmospheric pressure) in the absence of the wave field.

4.3.1.4 Control model for Poly-OWC

Equations (68), (78) and (79) model the deformation response of the CCDEM under the action of the water waves that break on the OWC front-wall. As a result of the wave-induce deformations, the CCDEM capacitance C (expressed per unit width in the direction orthogonal to the plane of Figure 66) varies according to the relation

$$C(h) = \varepsilon \frac{2e}{t_0} \frac{\lambda_{2,p}}{\lambda_{1,p}} \lambda_l^2(h). \quad (81)$$

This variation of capacitance can be used for electrostatic energy generation in different modes, namely: constant charge, constant potential and constant electric field. The latter mode is considered here which involve (refer to Figure 67): 1) a first phase at zero electric field ($E = 0$), in which the CCDEM is made expand in area from $\lambda_{1,\text{low}}$ to $\lambda_{1,\text{high}}$; 2) a second phase at constant deformation ($\lambda = \lambda_{1,\text{high}}$), in which the CCDEM is charged from zero up to the maximum electric field E_{\max} ; 3) a third phase at constant electric field ($E = E_{\max}$), in which the CCDEM is made contract in area from $\lambda_{1,\text{high}}$ to $\lambda_{1,\text{low}}$; and 4) a fourth phase at constant deformation ($\lambda = \lambda_{1,\text{low}}$), in which the CCDEM is discharged from E_{\max} down to zero electric field ($E = 0$).

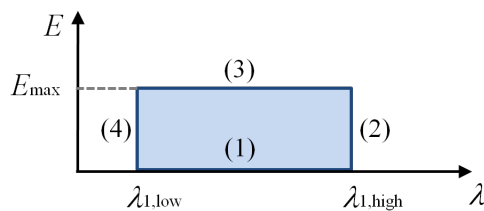


Figure 67: Representation of the generation cycle in the stretch/electric-field plane

In this mode of operation, during generation at constant electric field ($E = E_{\max}$), the electrical energy stored in the CCDEM remains constant, and the electric potential V and charge Q existing on the CCDEM electrodes result as

$$V(h) = E_{\max} \frac{t_0}{\lambda_{2,p}} \frac{1}{\lambda_l(h)}, \quad (82)$$

$$Q(h) = \varepsilon E_{\max} \frac{2e}{\lambda_{l,p}} \lambda_l(h). \quad (83)$$

Correspondingly, the net electrical power, W , and energy per cycle, U_{cycle} , (both defined per unit width in the direction orthogonal to the plane of Figure 66) that are generated by the CCDEM read as

$$W(t) = \varepsilon E_{\max}^2 \frac{2et_0}{\lambda_{l,p}\lambda_{2,p}} \frac{\partial(\ln[\lambda_l(h)])}{\partial t}, \quad (84)$$

$$U_{cycle} = \varepsilon E_{\max}^2 \frac{2et_0}{\lambda_{l,p}\lambda_{2,p}} \ln\left(\frac{\lambda_{l,low}}{\lambda_{l,high}}\right). \quad (85)$$

In Eqs. (84) and (85), negative values indicate power and energy exiting from the CCDEM.

For a given material, Eq. (21) shows that the specific energy output of a CCDEM is larger the larger is E_{\max} and the lower is the ratio between $\lambda_{l,low}$ and $\lambda_{l,high}$. In practice, $\lambda_{l,high}$ and E_{\max} are constrained by the relations

$$E_{\max} \leq E_{BD}, \quad (86)$$

$$\lambda_{l,high} \leq \lambda_{BD}, \quad (87)$$

with λ_{BD} and E_{BD} being the maximal stretch and electric field the DE material can withstand; whereas $\lambda_{l,low}$ is constrained by the relations

$$\sigma_1 = \mu_1 \left(\lambda_{l,low}^{\alpha_1} - \lambda_{l,low}^{-\alpha_1} \lambda_{2,p}^{-\alpha_1} \right) + \mu_2 \left(\lambda_{l,low}^{\alpha_2} - \lambda_{l,low}^{-\alpha_2} \lambda_{2,p}^{-\alpha_2} \right) - \varepsilon E_{\max}^2 \geq 0, \quad (88)$$

$$\sigma_2 = \mu_1 \left(\lambda_{2,p}^{\alpha_1} - \lambda_{l,low}^{-\alpha_1} \lambda_{2,p}^{-\alpha_1} \right) + \mu_2 \left(\lambda_{2,p}^{\alpha_2} - \lambda_{l,low}^{-\alpha_2} \lambda_{2,p}^{-\alpha_2} \right) - \varepsilon E_{\max}^2 \geq 0, \quad (89)$$

which prevent the loss of tension of the CCDEM.

For Poly-OWC devices, the quantities $\lambda_{l,low}$, $\lambda_{l,high}$ and E_{\max} cannot be chosen a priori only on the bases of Eqs. (85)-(89). Indeed, for a given DE (with specific material constants $\mu_1, \mu_2, \alpha_1, \alpha_2$ and ε) and OWC structure (with dimension H_B, a, b, c, d), and for any set $[e, t_0, \lambda_{l,p}, \lambda_{2,p}, E_{\max}]$ of CCDEM parameters, $\lambda_{l,low}$ and $\lambda_{l,high}$ result by the coupled dynamic response of the system described by Eqs. (68), (78) and (79), which also requires the definition of C_0 .

In practice, finding the optimal choice of the CCDEM parameters $[e, t_0, \lambda_{l,p}, \lambda_{2,p}, E_{\max}]$ and of air-chamber constant C_0 which maximizes U_{cycle} requires multivariable optimization procedures based on the numerical solution of Eqs. (68), (78) and (79) and on the constraints (86)-(89).

4.3.1.5 Simulation results

Simulation results are presented in this section which provide insights on the potential performances of Poly-OWCs, as well as on the influences of the CCDEM parameters on the amount of energy that can be harvested by this kind of polymeric WECs.

The reported results have been obtained via the numerical solution of Eqs. (68), (78) and (79) in Matlab/Simulink, and for an OWC having the following dimensions: $H_B = 8$ m, $a = 6$ m, $b = 8$ m, $c = 12$ m and $d = 7.29$ m (these dimensions resemble those of the full-scale Pico plant). The considered DE material is an acrylic elastomer (VHB-4910, by 3M) with the following constitutive properties: $\mu_1 = 12.6$ Pa, $\mu_2 = 26$ kPa, $\alpha_1 = 6.06$, $\alpha_2 = 1.7$, $\varepsilon = 4.7 \cdot 8.8 \cdot 10^{-12}$ F/m, $\lambda_{BD} = 5.5$, $E_{\max} = E_{BD} = 85$ MV/m.

Figures 68 report the response of a Poly-OWC with the abovementioned characteristics and with the CCDEM parameters [$e = 5$ m, $t_0 = 0.01$ m, $\lambda_{1,p} = 2.85$, $\lambda_{2,p} = 5.5$, $C_0 = 1.37e^9$ Pa·m²], to the action of an incident monochromatic wave field with amplitude $A = 1/\sqrt{2}$ m and period $T = 10$ s.

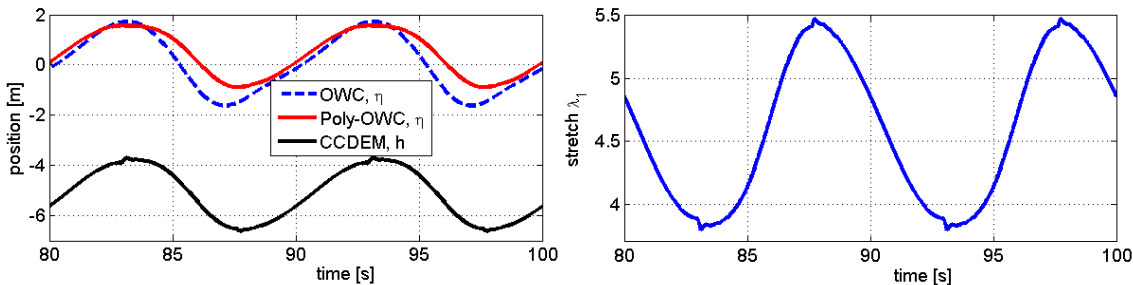


Figure 68: Left picture-Vertical displacement of the tip of CCDEM (solid-black), OWC surface η when DE membrane is working (solid-red) and OWC surface η when no membrane is present (dashed blue). Right picture – stretch of the CCDEM.

In particular, the left plot of Figure 68 reports the tip displacement h of the CCDEM (black solid line) and the motion of the free surface η of the water column (red solid line) for two wave periods. For comparison, the motion of the free-water surface η in the absence of the CCDEM is also reported (blue dashed line), which highlights the mutual dynamic interaction between OWC and CCDEM (in particular the energy-absorbing action by the CCDEM on the OWC). The right plot of the same figure reports the stretch variation of the CCDEM which enables to estimate (via Eqs. (84) and (85)) the net harvested maximal electrical power, $W_{\max} \approx 30$ kW/m, and energy per cycle, $U_{\text{cycle}} \approx 98$ kJ/m. The considered power and energies are quite significant and comparable to OWCs of similar dimensions but equipped with traditional power take-off mechanisms. However, the utilization efficacy of the considered DE material is quite low since the CCDEM exhibits a harvested energy-per-cycle density of about 107 J/kg (which is far below the theoretical limit of 1700 J/kg³). Better utilization of the DE material requires optimal tuning of the dynamic response of both OWC and CCDEM which can be accomplished by acting on the parameters $a, b, c, d, e, C_0, t_0, \lambda_{1,p}, \lambda_{2,p}$ and E_{\max} .

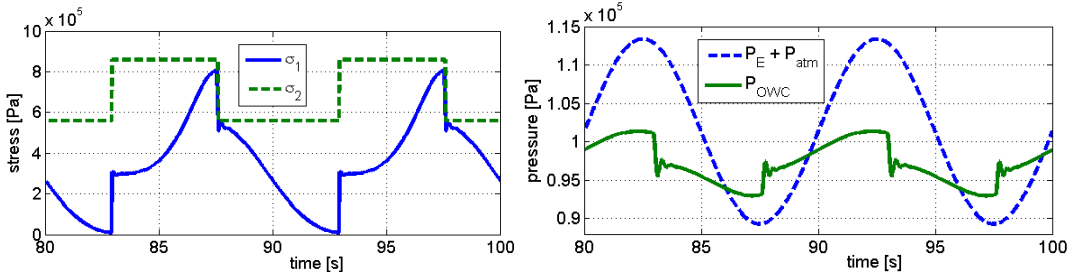


Figure 69 Left picture – Time plot of principal stresses due to mechanical and electrical loads. Right picture – time plot of exciting pressure on the front-wall aperture (dashed-blue) and pressure inside the air chamber (solid-green).

The left plot of Figure 69 reports the principal stresses, σ_1 and σ_2 , of the CCDEM. The sharp up-ward and down-ward variations respectively indicate deactivation and activation of the CCDEM which, according to the constant electric field generation mode (see Figure 67), occur at the inversion of the minimal and maximal values of λ_1 . The right plot of Figure 69 reports the exciting pressure due to the water-wave field, as well as the pressure within the OWC air-chamber. The sharp variations of the air-chamber pressure, P_{OWC} , are directly related to those of the CCDEM stresses, with the damped high-frequency oscillations being due to the CCDEM dynamics. For the considered case, P_{OWC} oscillates about a mean value which is lower than the atmospheric pressure. This occurs since, to reduce the dead-volume of compression/expansion, the air-chamber has been slightly depressurized in the steady state condition.

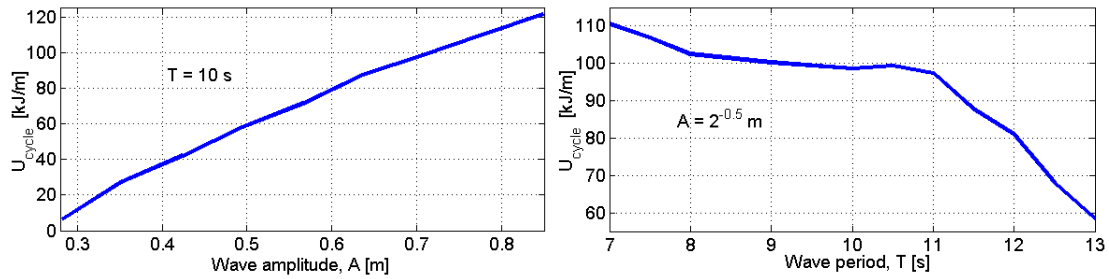


Figure 70: Left picture – Harvested energy per unit width for each cycle versus wave amplitude. Right picture - Harvested energy per unit width for each cycle versus the wave period.

To highlight the varying behavior of Poly-OWC in different sea conditions, Figure 70 shows the energy per cycle, U_{cycle} , generated by CCDEM for different amplitudes, A , and periods, T , of the wave breaking on the OWC structure. The plot on the left is obtained at constant period $T = 10\text{ s}$, whereas the plot on the right is obtained at constant amplitude $A = 2^{-0.5} \text{ m}$. Overall, the harvested energy per cycle is slightly non-linear with respect to wave amplitude variations and significantly non-linear with respect to wave period variations. Different real sea conditions are characterized by specific pairs of amplitude and period values (and not by independent variations as considered in Figure 70). For instance, the wave climate of the Pico plant can be characterized by nine sea states, the first five being: 1) $A = 0.2828 \text{ m}$ and $T = 9 \text{ s}$; 2) $A = 0.4243 \text{ m}$ and $T = 9.5 \text{ s}$; 3) $A = 0.5657 \text{ m}$ and $T = 10 \text{ s}$; 4) $A = 0.7071 \text{ m}$ and $T = 10.5 \text{ s}$; 5) $A = 0.8485 \text{ m}$ and $T = 11 \text{ s}$. The response of the considered Poly-WEC to different but realistic sea climates is thus reported in Figure 71, which plots the energy harvested in 100s, $U_{100\text{s}}$, by the CCDEM for the five sea states described above. As shown, the average power harvested by the considered Poly-OWC varies rather linearly with the strength of the five sea states.

Finally, to highlight the influence of the CCDEM geometry on Poly-OWC response, Figure 72 reports how the harvested energy and the utilization efficacy of employed DE material varies with the CCDEM thickness. As shown, larger CCDEM thicknesses lead to higher values of harvested energy, but also to a worst utilization of the DE material which is likely to make the use of CCDEM less cost-effective. In obtaining the results shown in Figure 71, a maximum electric field equal to $E_{\text{max}} = 65 \text{ MV/m}$ has been employed, which significantly decreases the Poly-OWC performances as compared to case $E_{\text{max}} = E_{\text{BD}}$ (for $E_{\text{max}} = 85 \text{ MV/m}$ indeed, $U_{\text{cycle}} \approx 98 \text{ kJ/m}$ for a CCDEM thickness (at $h=0$) equaling 10cm).

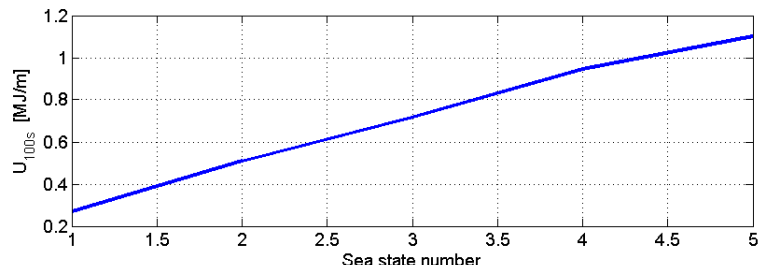


Figure 71: Harvested energy per unit width for each cycle versus the following sea states: 1) $A = 0.2828 \text{ m}$ and $T = 9 \text{ s}$; 2) $A = 0.4243 \text{ m}$ and $T = 9.5 \text{ s}$; 3) $A = 0.5657 \text{ m}$ and $T = 10 \text{ s}$; 4) $A = 0.7071 \text{ m}$ and $T = 10.5 \text{ s}$; 5) $A = 0.8485 \text{ m}$ and $T = 11 \text{ s}$.

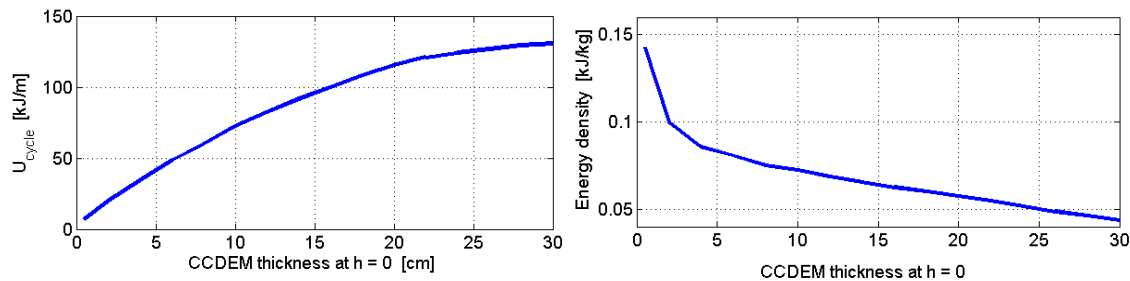


Figure 72: Left picture - Harvested energy per unit width for each cycle versus thickness of the DE membrane. Right picture - Energy per unit weight of DE versus thickness of the DE membrane.

4.3.2 Circular Diaphragm Oscillating Water Column

A Poly-OWC is a partially submerged hollow structure featuring an immersed part opened to the sea action, and an upper part closed by a DEG membrane and forming an air chamber. The structure partially encloses a column of water which is exposed to the incident wave field at the bottom and to the chamber air pressure at the top. As the waves break on the Poly-OWC structure, wave-induced pressure oscillations at the underwater interface cause the reciprocating motion of the water column, with a concomitant compression-expansion of the air entrapped in the upper chamber, and the resulting inflation-deflation of the DEG membrane. To generate electricity, electric charges are put on the DEG electrodes when the membrane is expanded in area. As the membrane contracts, DEG capacitance decreases which makes the charges increase their electric potential, thereby converting the work done by the air-chamber pressure on the DEG membrane into usable direct current electricity.

In this subsection, an Inflated Circular Diaphragm DEG (ICD-DEG) PTO is investigated by also including DE material visco-elasticity. First, a reduced, but yet accurate, dynamic model of visco-hyperelastic ICD-DEGs is presented. Second, a lumped-parameter model of OWC hydrodynamics is introduced and coupled to the reduced model of the ICD-DEG PTO. Third, the resulting fluido-electro-elastic model is used in a simulation case-study to evaluate the potential performances of a realistic OWC equipped with an ICD-DEG PTO.

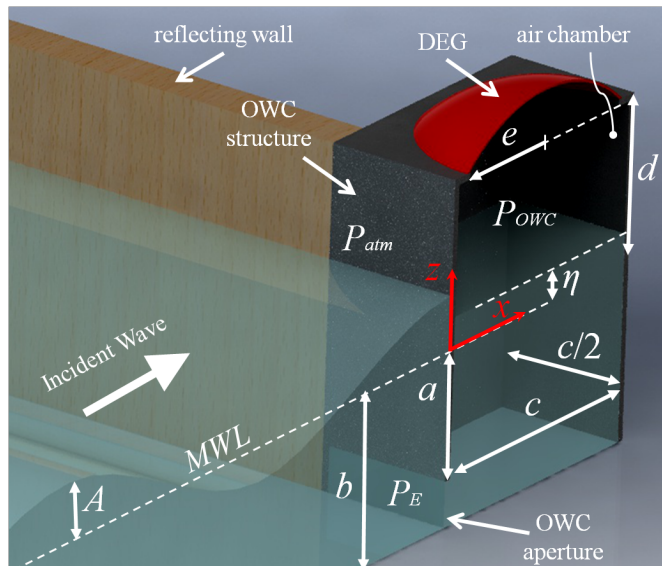


Figure 73 Polymeric Oscillating Water Column (Poly-OWC) wave energy converter.

4.3.2.1 Modelling of inflated circular diaphragm dielectric elastomer generators

An ICD-DEG is depicted in Figure 74. It consists of a pre-stretched planar circular DE Membrane (DEM) that is clamped along its perimeter at radius e and with thickness t (whereas e_0 and t_0 indicate the

radius and thickness of the DEM in its planar undeformed state). When the opposing sides of the ICD-DEG are subjected to a differential pressure and to an electric potential difference (voltage), the ICD-DEG undergoes an out of plane axial-symmetric (bubble-like) deformation (area expansion). In Figure 74(c), h identifies the resultant displacement of the ICD-DEG tip.

This section presents: 1) the general continuum model of ICD-DEGs which involves solution of partial differential equations and which is not suited for real-time applications; 2) a reduced one-degree-of-freedom model of ICD-DEGs which can be used for fast design optimization, hardware-in-the-loop simulation and control; 3) the validation of the reduced model via the Finite Element Method.

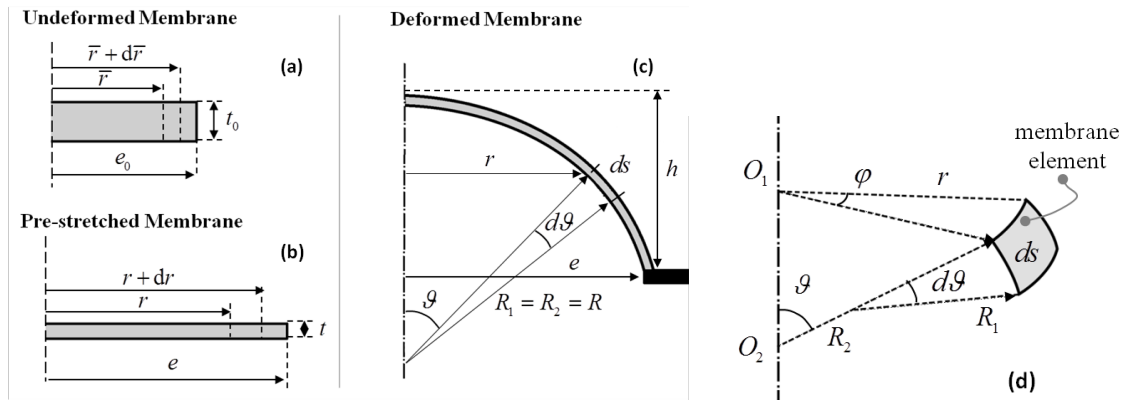


Figure 74 Inflated Circular Diaphragm Dielectric Elastomer Generator (ICD-DEG): a) ICD-DEG undeformed state, b) ICD-DEG pre-stretched state with no differential pressure and electric potential, c) ICD-DEG deformed state with differential pressure and/or electric potential, d) infinitesimal ICD-DEG element.

4.3.2.2 Continuum Model

Continuum models for the bubble-like electro-elastic deformations of axial-symmetric DEMs have been proposed in [77]-[79]. They rely on the finite deformation formulation for incompressible hyper-elastic shells proposed by Adkins and Rivlin [80], and employ a free-energy function which includes the electrostatic energy stored in the DE material in addition to the standard strain energy function term. With reference to Figure 74 (a), let \bar{r} indicate the radial position of the infinitesimal longitudinal element $d\bar{r}$ of the undeformed DEM. Upon bubble-like deformation (area expansion, see Figure 74(b-d)), this infinitesimal element varies its length to ds and moves to a new configuration which is characterized by the radial distance r from the axis of symmetry, and by the principal radii of curvature R_1 and R_2 (R_1 being in the meridian plane). For kinematic compatibility, Codazzi's equations impose

$$\frac{r}{R_1 R_2} \left(\frac{ds}{dr} \right)^3 = \frac{d^2 s}{dr^2}, \quad \frac{d}{dr} \left(\frac{r}{R_1} \right) = \frac{1}{R_1}. \quad (90)$$

In this setting, DEM deformations are described by the following principal stretches

$$\lambda_1 = \frac{ds}{dr}, \quad \lambda_2 = \frac{r}{\bar{r}}, \quad \lambda_3 = \lambda_1^{-1} \lambda_2^{-1}, \quad (91)$$

with λ_1 and λ_2 being in the longitudinal and latitudinal directions respectively. The third of equations (91) imposes the material incompressibility condition. In addition, balance of momentum yields:

$$\frac{dN_1}{dr} = \frac{N_2 - N_1}{r} - T \frac{ds}{dr}, \quad \frac{N_1}{R_1} + \frac{N_2}{R_2} = P, \quad (92)$$

where P and T are the externally applied forces (per unit area of the membrane element) respectively acting in the directions normal and tangential to the longitudinal infinitesimal element ds , whereas N_1 and N_2 are the membrane forces (per unit length of latitudinal and longitudinal length). Forces N_1 and N_2 are functions of the membrane principal stresses σ_1 and σ_2 , namely

$$N_1 = t_0 \lambda_3 \sigma_1, \quad N_2 = t_0 \lambda_3 \sigma_2, \quad (93)$$

$$\sigma_1 = \lambda_1 \frac{\partial \Psi}{\partial \lambda_1}, \quad \sigma_2 = \lambda_2 \frac{\partial \Psi}{\partial \lambda_2}, \quad \Psi = \Psi(\lambda_1, \lambda_2), \quad (94)$$

where Ψ is the free-energy density that accounts for the specific constitutive behavior of the considered material.

DEs are elastic solids that feature linear strain-independent dielectric properties, so that Ψ can be decomposed as

$$\Psi = \Psi_{st}(\lambda_1, \lambda_2) + \Psi_{es}, \quad \Psi_{es} = -\frac{1}{2} \varepsilon \lambda_1^2 \lambda_2^2 \left(\frac{V}{t_0} \right)^2, \quad (95)$$

where Ψ_{st} is a suitable strain energy function, and Ψ_{es} is the electrostatic energy density, with ε and V respectively being the dielectric constant of the considered DE material and the electric potential difference acting between the DEM electrodes. Thus, for DEs,

$$\sigma_1 = \lambda_1 \frac{\partial \Psi_{st}}{\partial \lambda_1} - \varepsilon \lambda_1^2 \lambda_2^2 \left(\frac{V}{t_0} \right)^2, \quad \sigma_2 = \lambda_2 \frac{\partial \Psi_{st}}{\partial \lambda_2} - \varepsilon \lambda_1^2 \lambda_2^2 \left(\frac{V}{t_0} \right)^2. \quad (96)$$

Equations (89)-(93) and (96) govern the static and dynamic response of an ICD-DEG.

For the static case, P and T account for the inflating pressure and the gravitational forces, and Ψ_{st} can be chosen as one of the known hyperelastic strain-energy functions. Choosing Ψ_{st} in the Gent's form, namely

$$\Psi_{st}(\lambda_1, \lambda_2) = -\mu \log \left(\frac{I_m - \lambda_1^2 - \lambda_2^2 - \lambda_1^{-2} \lambda_2^{-2}}{I_m - 3} \right), \quad (97)$$

where μ and I_m are specific constitutive parameters of the considered DE material, for the static case equations (96) become

$$\sigma_1 = \sigma_{e,1} - \varepsilon \lambda_1^2 \lambda_2^2 \left(\frac{V}{t_0} \right)^2, \quad \sigma_{e,1} = 2\mu \frac{\lambda_1^2 - \lambda_1^{-2} \lambda_2^{-2}}{I_m - \lambda_1^2 - \lambda_2^2 - \lambda_1^{-2} \lambda_2^{-2}} \quad (98.1)$$

$$\sigma_2 = \sigma_{e,2} - \varepsilon \lambda_1^2 \lambda_2^2 \left(\frac{V}{t_0} \right)^2, \quad \sigma_{e,2} = 2\mu \frac{\lambda_2^2 - \lambda_1^{-2} \lambda_2^{-2}}{I_m - \lambda_1^2 - \lambda_2^2 - \lambda_1^{-2} \lambda_2^{-2}}. \quad (98.2)$$

For the dynamic case, P and T are augmented with DEM inertia forces, and material visco-elasticity is accounted by adding in each of equations (98) a non-equilibrium stress which depends on the time evolution of the principal stretches $\lambda_1(\tau)$ and $\lambda_2(\tau)$ (with τ being the time variable). Specifically, assuming a Quasi-Linear Viscoelastic (QLV) formulation,

$$\sigma_1(\tau) = \sigma_{e,1}(\tau) - \varepsilon \lambda_1^2(\tau) \lambda_2^2(\tau) \left(\frac{V(\tau)}{t_0} \right)^2 + \int_0^\tau \sigma_{e,1}(\tau - \xi) \frac{dG(\xi)}{d\xi} d\xi, \quad (99.1)$$

$$\sigma_2(\tau) = \sigma_{e,2}(\tau) - \varepsilon \lambda_1^2(\tau) \lambda_2^2(\tau) \left(\frac{V(\tau)}{t_0} \right)^2 + \int_0^\tau \sigma_{e,2}(\tau - \xi) \frac{dG(\xi)}{d\xi} d\xi, \quad (99.2)$$

where $G(\xi)$ is the reduced relaxation function

$$G(\xi) = \kappa_0 + \sum_{i=1}^n \kappa_i e^{-\nu_i \xi}, \text{ with } \kappa_0 + \sum_{i=1}^n \kappa_i = 1, \quad (100)$$

depending on the DE constitutive parameters κ_0 , κ_i and ν_i .

For both static and dynamic problems, fast solution of the abovementioned partial differential equations can be difficult to achieve, which calls for the need of reduced, but yet accurate, real-time models of ICD-DEGs.

4.3.2.3 Reduced Model

In this subsection, the continuum electro-elastic model of the ICD-DEG that has been described above is reduced to a one-degree of freedom model. This reduced model provides sufficiently accurate results for pre-stretched ICD-DEGs featuring limited mass density ($\rho \approx 1000 \text{ kg}\cdot\text{m}^{-3}$), and working in the range $|h| < e$ with limited accelerations ($|\ddot{h}| < g$, with $g = 9.8 \text{ m}\cdot\text{s}^{-2}$).

The reduced model is based on the following simplifying assumptions:

- 1) the ICD-DEG deforms as a perfect spherical shell segment with tip height h and radius R ;
- 2) ICD-DEG deformation is prevalently equi-biaxial, with the amount of deformation depending on h and varying with the radial distance r (or equivalently with \bar{r});
- 3) ICD-DEG capacitance is assumed to be equivalent to that of a planar circular capacitor with variable thickness.

According to the first assumption, equations (89) are identically satisfied. Moreover, according to Figure 74(c), the following holds

$$R_1 = R_2 = R, \text{ where } R = \frac{h^2 + e^2}{2h}, \quad (101)$$

$$ds = R d\vartheta, \quad r = R \sin \vartheta, \quad dr = R \cos \vartheta d\vartheta, \quad (102)$$

$$\lambda_1 = R \frac{d\vartheta}{dr}, \quad \lambda_2 = R \frac{\sin \vartheta}{r}, \quad (103)$$

where ϑ is the zenith angle indicating the location of the deformed DEM element ds along the longitudinal direction.

According to the second assumption, to the first order of approximation, equations (103) reduce to

$$\lambda = R \frac{d\vartheta}{dr} = R \frac{\sin \vartheta}{r}, \quad (104)$$

which, upon solution of the last equality, yields

$$\vartheta(h, \bar{r}) = 2\arctan\left(\frac{h\bar{r}}{ee_0}\right), \quad (105)$$

$$\lambda(h, \bar{r}) = ee_0(h^2 + e^2)/(e^2 e_0^2 + h^2 \bar{r}^2), \quad (106)$$

thereby providing the expression of the prevalent equi-biaxial stretch, λ , as function of the ICD-DEG height h and undeformed radial distance \bar{r} .

Based on the kinematic constraints given by relations (101)-(106), the reduced equation of motion for the ICD-DEG could be obtained by a global energy balance. For the dynamic case, this would require the definition of a suitable energy term to account for the visco-elasticity of the DE material. Besides, to a first order of approximation, the reduced equation of motion can be estimated by only considering the second of equations (92) evaluated at the ICD-DEG tip, namely

$$N = PR/2, \quad (107)$$

with

$$N = t_0 \bar{\lambda}^{-2} \sigma, \quad \bar{\lambda}(h, \bar{r} = 0) = (h^2 + e^2)/(ee_0) \quad (108)$$

$$\sigma = \sigma_e(\tau) - \varepsilon \bar{\lambda}^4(\tau) \left(\frac{V(\tau)}{t_0} \right)^2 + \int_0^\tau \sigma_e(\tau - \xi) \frac{dG(\xi)}{d\xi} d\xi, \quad (109)$$

$$\sigma_e = 2\mu \frac{\bar{\lambda}^2 - \bar{\lambda}^{-4}}{I_m - 2\bar{\lambda}^2 - \bar{\lambda}^{-4}}, \quad (110)$$

$$P = p(\tau) - \rho t_0 \bar{\lambda}^{-2} (g + \ddot{h}), \quad (111)$$

where p (which depends on time τ) is the differential pressure acting between the opposing sides of the DEM.

Equations (107)-(111) make it possible to study the time evolution of the ICD-DEG tip height h as function of the time-varying pressure p and voltage V . Evaluation of the amount of electrical energy that can be generated by the ICD-DEG (when it is subjected to an exciting pressure $p(\tau)$) requires the additional knowledge of the variable ICD-DEG capacitance, as well as a suitable choice for the control law which regulates $V(\tau)$.

With regard to ICD-DEG capacitance C , based on the third assumption mentioned before,

$$C(h) = \int_0^{\text{asin}(e/R)R} \varepsilon \frac{2\pi r}{t} ds = \frac{\pi \varepsilon ee_0}{3t_0} \bar{\lambda} \left(\bar{\lambda}^2 + \frac{e}{e_0} \bar{\lambda} + \frac{e^2}{e_0^2} \right). \quad (112)$$

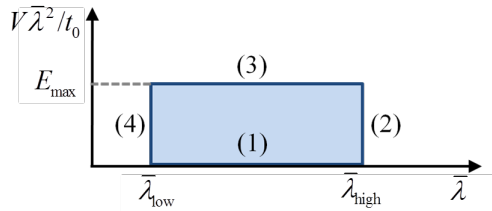


Figure 75: Representation of the considered energy harvesting cycle in the stretch/electric-field plane.

With regard to the control law, a “constant electric-field harvesting mode” is considered (see Figure 75), which features a cyclical series of electromechanical transformations: 1) at zero electric field ($V\bar{\lambda}^2/t_0 = 0$), in which the ICD-DEG is made expand in area from $\bar{\lambda}_{low}$ to $\bar{\lambda}_{high}$ (with $\bar{\lambda}_{low} < \bar{\lambda}_{high} < \lambda_{BD}$, where λ_{BD} is the maximum stretch that can be sustained by the DE material); 2) at constant deformation ($\bar{\lambda} = \bar{\lambda}_{high}$), in which the ICD-DEG is charged from zero up to the maximum electric field E_{max} (where the value of E_{max} is close to the electric breakdown strength of the considered DE material); 3) at constant electric field ($V\bar{\lambda}^2/t_0 = E_{max}$), in which the ICD-DEG is made contract in area from $\bar{\lambda}_{high}$ to $\bar{\lambda}_{low}$; and 4) at constant deformation ($\bar{\lambda} = \bar{\lambda}_{low}$), in which the ICD-DEG is discharged from E_{max} down to zero electric field ($V\bar{\lambda}^2/t_0 = 0$). Note that for $h \neq 0$, the electric field acting across the ICD-DEG is not uniform; for any given V , the considered value of $V\bar{\lambda}^2/t_0$ is the maximum electric field that occurs at the ICD-DEG axis of symmetry.

Based on equation (112) and on the chosen harvesting control law (Figure 76), the electric power, W , and the energy per cycle, U_{cycle} , that can be generated by the ICD-DEG are

$$W = \left[V \frac{dQ}{d\bar{\lambda}} - \frac{d}{d\bar{\lambda}} \left(\frac{1}{2} CV^2 \right) \right] \dot{\bar{\lambda}}, \quad (113.1)$$

$$U_{cycle} = \int_{\bar{\lambda}_{high}}^{\bar{\lambda}_{low}} \left[V \frac{dQ}{d\bar{\lambda}} - \frac{d}{d\bar{\lambda}} \left(\frac{1}{2} CV^2 \right) \right] d\bar{\lambda}, \quad (113.2)$$

with

$$V = E_{max} t_0 \bar{\lambda}^{-2}, \quad Q = CV = \frac{\pi \varepsilon e e_0 E_{max}}{3} \left(\bar{\lambda} + \frac{e}{e_0} + \frac{e^2}{e_0^2} \bar{\lambda}^{-1} \right), \quad (114)$$

which yield

$$W(\tau) = \frac{\pi \varepsilon e e_0 t_0 E_{max}^2}{6} \left(3\bar{\lambda}^{-2} + 2\frac{e}{e_0} \bar{\lambda}^{-3} + \frac{e^2}{e_0^2} \bar{\lambda}^{-4} \right) \dot{\bar{\lambda}}, \quad (115.1)$$

$$U_{cycle} = \frac{\pi \varepsilon e e_0 t_0 E_{max}^2}{6} \left[3\left(\bar{\lambda}_{high}^{-1} - \bar{\lambda}_{low}^{-1}\right) + \frac{e}{e_0} \left(\bar{\lambda}_{high}^{-2} - \bar{\lambda}_{low}^{-2}\right) + \frac{e^2}{3e_0^2} \left(\bar{\lambda}_{high}^{-3} - \bar{\lambda}_{low}^{-3}\right) \right]. \quad (115.2)$$

4.3.2.4 Model Validation

In this section, the reduced model of the ICD-DEG given by equations (107)-(111) and (112)-(115) is validated via the Finite Element Model (FEM) formulation for DEMs.

Validation is performed by considering an ICD-DEG PTO for a realistic OWC (like the Pico plant in the Azores [81]). The considered ICD-DEG is made of a commercial DE material (VHB-4910 by 3M), with $\rho = 960 \text{ kg}\cdot\text{m}^{-3}$, $\mu = 4.09 \text{ MPa}$ and $I_m = 431$, and having the following geometrical dimensions: $e = 5 \text{ m}$, $t = 0.1 \text{ m}$ and $e_0 = 2 \text{ m}$. A quasi-static case is studied where the ICD-DEG is subjected to gravity, to a constant voltage $V = 1 \text{ MV}$ (which has been chosen to provide the ICD-DEG with a maximum electric field of about $40 \text{ MV}\cdot\text{m}^{-1}$ that is compatible with the electric breakdown strength of the considered material), and to a differential pressure p varying between -1 Pa to -4.5 kPa .

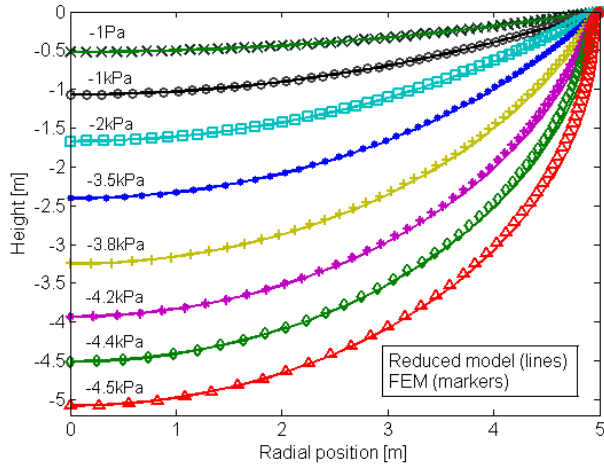


Figure 76: Deformed shape plot of a ICD-DEG: Reduced model (lines) vs Finite Element Model (markers)

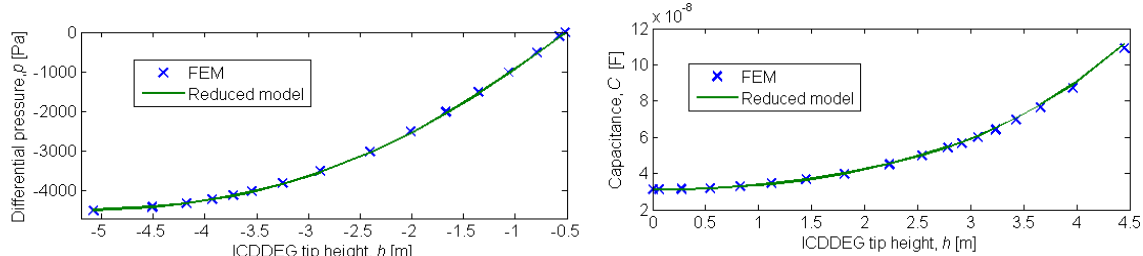


Figure 77: On the left Inflating pressure vs ICD-DEG tip displacement: Reduced model (line) vs Finite Element Model (marker); on the left the ICD-DEG capacitance vs ICD-DEG tip displacement: Reduced model (line) vs Finite Element Model (marker).

Figure 76 reports the comparison between the deformed shape plots (at different inflating pressures and at the same voltage) predicted by the reduced model (solid lines) and by FEM analysis (markers). As shown, within the range $|h| < e$, the deformed shapes of the ICD-DEG are approximated quite well by perfect spherical shell segments with radii R given by equation (101).

Figure 77-left reports the relation between ICD-DEG tip displacement and inflating pressure as predicted via equations (107)-(111) (solid line) and FEM analysis (marker). Figure 77-right reports the relation between ICD-DEG tip displacement and ICD-DEG capacitance as predicted via equation (23) (solid line) and FEM analysis (marker). For both cases, within the range of validity of the considered assumptions, the reduced model of the ICD-DEG matches very well with FEM results.

4.3.2.5 Polymeric oscillating water column model

Investigating the performances of ICD-DEG PTOs into Poly-OWCs (like the one depicted in Figure 74) requires to couple the reduced electro-elastic model described by equations (107)-(111) and (115) with a suitable hydrodynamic model that is capable of representing the oscillatory response of the water column to both the excitation pressure P_E , which is due to the water wave field, and the air-chamber pressure P_{OWC} , which also acts on the ICD-DEG (namely, $p = P_{OWC} - P_{atm}$, where P_{atm} is the atmospheric pressure).

Similarly to a previous study, a lumped-parameter hydrodynamic model of an ideal OWC system is considered here. With reference to Figure 73, the system comprises a fixed cuboid OWC structure opened to a wave basin of semi-infinite extension and constant depth. Introducing the spatial horizontal and vertical coordinates x , y and z (z being positive when pointing up-ward), the wave basin extends from $-\infty \leq x \leq 0$ and $-\infty \leq y \leq \infty$, and has a depth equal to b . The OWC structure has a square cross section, with edge equal to c , and is opened to the wave basin on its front-wall (at $x = 0$), with the submersed aperture being defined by the constant distance a measured from the Mean Water Level (MWL). The OWC air-chamber comprises a cuboid part which extends by the constant length d from the MWL, plus (or minus) the spherical segment with height h that is subtended by the ICD-DEG.

Beside the specific OWC geometry, the considered lumped-parameter hydrodynamic model relies on the following assumptions:

- ideal fluid and linear water-wave theory;
- harmonic monochromatic waves on water of constant depth;
- perfect wave reflection from the OWC front-wall;
- no disturbance (for instance radiation) is caused by the OWC to the outer wave field;
- the free-water surface inside the OWC is replaced by a weightless rigid piston, whose motion with respect to the MWL can be described by the single displacement variable η ;
- adiabatic compression-expansion of the air entrapped between the free-water surface of the column and the ICD-DEG.
- With these simplifications, the equation of motion of the column of water oscillating within the hollow structure follows as

$$\ddot{\eta} = \frac{P_{atm} + P_E(\tau) - P_{OWC}(\tau) - \rho_w g \eta - D_1 \dot{\eta}}{\rho_w(a+\eta)}, \quad (116)$$

where ρ_w is the constant water density, D_1 is a linear damping coefficient that accounts for the hydraulic losses occurring within the OWC duct, and where the pressures P_{OWC} and P_E take the forms

$$P_{OWC}(\tau) = P_{OWC}(\eta, h) = \frac{C_0}{[V_{OWC}(\eta, h)]^\gamma}, \quad (117)$$

with γ being the adiabatic compression-expansion index for air ($\gamma = 1.4$), C_0 being a constant that sets the steady condition of the air-chamber (pressurized, depressurized, or at atmospheric pressure) and V_{OWC} being the air-chamber volume

$$V_{OWC}(\eta, h) = c^2(d - \eta) + \frac{\pi h}{6}(3e^2 + h^2), \quad (118)$$

and

$$P_E(\tau) = \frac{2\rho_w g A}{(b-a)} \frac{\sinh[K(b-a)]}{K \cosh(Kb)} \cos\left(\frac{2\pi}{T}\tau\right), \quad (119)$$

with A and T being the amplitude and period of the incident wave, and K being the angular repetency of the propagating wave (also called wave number) that is obtained by the solution of the dispersion relation

$$K \tanh(Kb) = \frac{1}{g} \left(\frac{2\pi}{T} \right)^2. \quad (120)$$

Equations (116)-(120), together with (107)-(111) and (115), provide a fully coupled fluido-electro-elastic wave-to-wire model for the PolyOWC equipped with an ICD-DEG PTO.

4.3.2.6 Simulation results

The fluido-electro-elastic wave-to-wire model that has been described in the previous sections, is used here to investigate the influence of design parameters on the energy that can be harvested by a PolyOWC equipped with an ICD-DEG PTO.

The reported results have been obtained via the numerical solution of equations (107)-(111) and (115)-(120) in Matlab Simulink; specifically for an OWC with dimensions: $a = 6$ m, $b = 8$ m, $c = 12$ m and $d = 7.29$ m (these dimensions resemble those of the Pico plant installed at the Azores [81]), and with an ICD-DEG PTO featuring $e = 5$ m, $\rho = 960$ kg·m⁻³, $\mu = 4.09$ MPa, $I_m = 431$, $\kappa_1 = 0.57$, $\kappa_2 = 0.189$, $\kappa_3 = 0.086$, $\kappa_4 = 0.0543$, $v_1 = 0.31$ s, $v_2 = 3.35$ s, $v_3 = 35.7$ s, $v_4 = 370$ s, $\varepsilon = 4.5 \cdot 8.8 \cdot 10^{-12}$ F/m, $\lambda_{BD} = 7$.

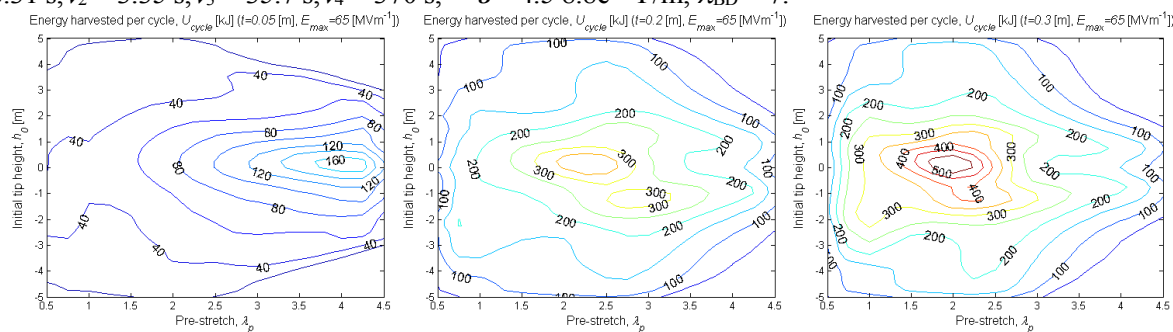


Figure 79: Energy harvested per cycle by the Poly-OWC with ICD-DEG PTO as function of ICD-DEG initial tip height h_0 and pre-stretch λ_p . Different plots are for the same E_{max} and for different ICD-DEG thicknesses t (measured at $h = 0$).

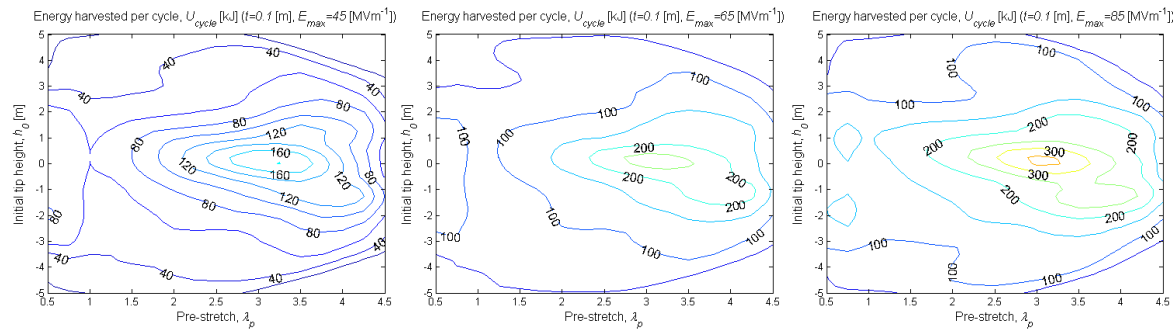


Figure 80 Energy harvested per cycle by the Poly-OWC with ICD-DEG PTO as function of ICD-DEG initial tip height h_0 and pre-stretch λ_p . Different plots are for the same ICD-DEG thickness t (measured at $h = 0$) and for different E_{max} .

Figures 79 and 80 report the energy harvested per cycle, U_{cycle} , as function of the ICD-DEG pre-stretch $\lambda_p = e/e_0$ and of the steady state tip height h_0 (i.e. with no incident wave field, with h_0 being positive or negative depending on whether the air-chamber is pressurized or depressurized). Results are obtained for a monochromatic wave with $A = 2^{-0.5}$ m and $T = 10.5$ s. Figure 79 refers to ICD-DEGs controlled at the same E_{max} ($E_{max} = 65$ MVm⁻¹) and with different thicknesses, namely $t = 0.05$ m, $t = 0.2$ m and $t = 0.3$ m (with t being measured at $h = 0$). Figure 80 refers to ICD-DEG with the same thicknesses, $t = 0.1$ m (with t being measured at $h = 0$), and controlled at different E_{max} , namely $E_{max} = 45$ MVm⁻¹, $E_{max} = 65$ MVm⁻¹ and $E_{max} = 85$ MVm⁻¹. As a general trend, Figures 79 and 80 show that the ICD-DEG tends to work at its best when mounted with zero or small tip deflections ($h_0 \approx 0$) and with moderate pre-stretches (the optimal pre-stretch depending on the considered membrane thickness t). With such mounting conditions, the ICD-DEG operates so that its tip height h alternates from a positive to a negative direction, and energy is generated at

twice the frequency of the exciting water wave. Overall, harvested energy increases as both ICD-DEG thickness, t , and controlled electric field, E_{\max} , increase.

4.3.2.7 Conclusions

Inflated Circular Diaphragm Dielectric Elastomer Generators (ICD-DEGs) offer promising potentials as Power-Take-Off (PTO) mechanisms for Oscillating Water Column (OWC) wave energy devices. In this paper, a reduced, yet accurate, electro-elastic model for ICD-DEGs has been presented. As compared to available continuum models valid for axial-symmetric Dielectric Elastomer membranes, the proposed one does not involve solution of partial differential equations, and thus can be more easily integrated into existing wave-to-wire models of OWC systems. Coupling of the proposed electro-elastic model with a lumped-parameter model of the OWC hydrodynamics has also been described which provides an effective fluido-electro-elastic wave-to-wire model for fast design optimization, real-time control and hardware-in-the-loop simulation of realistic systems. A simulation case study has also been presented which shows how a wave-to-wire model of this kind can be used for the parametric analysis and design of OWCs equipped with an ICD-DEG PTO.

In the near future, the presented ICD-DEG model will be coupled with more complex and accurate hydrodynamic models that take into account aspects that have been ignored in this simplified analysis (for instance, wave radiation). Floating Poly-OWCs will also be considered.

4.4 Conclusions

In this section, we reported the possible architectures of second-generation PolyWECS. The definition of possible layout is very preliminary since a detailed architectural design can be achieved only after an in depth study and modelling of the fluid dynamic interaction with DE membranes. However, preliminary considerations are useful for a classification of feasible devices and analysis of main evident aspects.

In this analysis we propose a classification of the devices based on aspects that are relevant for the prospected effectiveness of the device and for the level of complexity required for their study/analysis.

A first class of device has been identified which took the name of Poly-OWC. The working principle of this device is based on a mass of water contained in a chamber (duct or tube) that is brought to oscillate by wave pressures.

A second type of device is based on DE membranes that are directly opened to wave forces without any mediation. Lastly, hybrid device can be conceived which employs a combination of different principles including components that are typical of first-generation devices.

5. CONCLUSIONS AND FUTURE WORKS

5.1 Conclusions

The main aim of the present Project is to develop new knowledge, proof of concepts and demonstrate with small scale prototypes the feasibility of a completely new technology for wave energy harvesting based on Polymeric Wave Energy Converters (PolyWECS). PolyWECS employ Dielectric Elastomer Generation Units (DEGUs) as basic transduction element to convert mechanical energy into electricity.

The efficient development of PolyWECS requires the understanding of physics principles involved, formulation of new system concepts, and conception of tools and techniques required for their development, implementation and assessment.

In this document we have reported the activities that have been carried out within the work package 1 during the first 12 months. According the PolyWEC general approach, activities have been organized on two successive levels of development: first-generation and second-generation devices. First-generation PolyWECS are characterized by indirect interaction between dielectric elastomer generator unit (DEGU) and fluid. That is, the deformations of DE membranes are not directly generated by fluid pressures but by a mechanical interface. On the contrary, second-generation PolyWECS are characterized by direct interaction between DEGU and fluid, which occurs over wide contact surfaces. That is, fluid-DEGU interaction is not mediated by any mechanical means, and DE membrane deformation is directly generated by wave-induced fluid pressures.

In this framework, the first activities within WP1 of the PolyWEC project focussed on:

1. identification of possible architectures for the DE generator component;
2. the development of mathematical models which describe the response of DE transducers and provide forecast on their efficiency and performances;
3. on the base of the developed mathematical model, the required material properties have been defined which optimize efficiency and mechanical response;
4. the identification of possible architectures and layouts for innovative WECs based on DE transducers for both first-generation and second-generation devices;
5. the development of preliminary hydrodynamic models which includes the response of the novel DE transducers;

The following preliminary conclusions can be outlined:

1. the large number of possible DEGU layouts, combined with the large amount of traditional solutions for wave energy conversion, make PolyWECS a flexible and promising solution for wave energy conversion. That is, several different architectures can be identified for specific installation locations and tailor-made solutions can be set up on the basis of specific operating requirements.
2. the proposed hydro-electro-elastic models for PolyWECS provide a versatile tool to preliminary assess the devices performance in relatively short computation times. With the mentioned approach, predictions of the devices energy performance are not completely reliable in absolute terms, nonetheless, suggestive comparisons with existing technologies are possible.
3. preliminary numerical simulations on selected devices (oscillating wave surge converter and oscillating water column with DE power take-off) show good but improvable energetic performances. According to such models, PolyWECS that employs commercially available DE materials provide already reasonable energy efficiency, with excellent adaptability to a broad range of different sea conditions, and architectural simplicity (with consequent reduced operating costs and design efforts).

5.2 Future works

This section describes the works that are going to be developed in the next future in the framework of work package 1.

First, experimental in tank tests and model validation are going to be carried out for systems belonging to first-generation and second-generation PolyWECS. In particular, simplified wave-flume tests are currently on-going for Poly-Surge (first-generation) and Poly-OWC (second-generation) WECs. Moreover, preliminary tests are planned on a device based on submerged membrane.

The scope of these experimental works is to validate the hydrodynamic models and to provide a proof of the capabilities of the DE generators when coupled with structures interacting with ocean waves.

In order to conduct such tests, reduced models for the implementation of real-time control systems are going to be developed.

For second-generation devices that feature direct interaction between water and DE membranes, fully coupled fluido-electroelastic continuum models are currently being investigated and it is foreseen to get preliminary results in the next period of the project.

To assess economical viability of first and second-generation PolyWECs a tecno-economical module is going to be developed and integrated with the validated physics based wave to wire models.

REFERENCES

- [1] Cruz J., *Ocean Wave Energy: Current Status and Future Perspectives*, Springer, ISBN 978-3-540-74894-6, 2008.
- [2] Gunnar M., Barstow S., Kabuth A., Pontes M.T., *Assessing the global Wave Energy Potential*, Proceedings of OMAE2010 29th International Conference on Ocean, Offshore Mechanics and Arctic Engineering, 2010.
- [3] Trust C., *Future Marine Energy. Results of the Marine energy Challenge. Cost Competitiveness and Growth of Wave and Tidal Stream Energy*, Carbon Trust, 2006.
- [4] European Ocean Energy Association, *Oceans of Energy: European Ocean Energy Roadmap 2010-2050*, 2010.
- [5] McCormick M.E.; *Ocean Wave Energy Conversion*; Dover Publications; 2007.
- [6] Falcão A.F.; *Wave EnergyUtilization: A Review of the Technologies*; Renewable and Sustainable Energy Reviews 14; 2010.
- [7] Hiroisa T.; *Sea trial of a Heaving Buoy Wave Power Absorber*; Proceedings of 2nd International Symposium on Wave Energy Utilization, Trondheim, Norway; 1982.
- [8] Rodrigues L.; *Wave power conversion systems for electrical energy production*; Nova University of Lisbon; 2008.
- [9] Salter S. H.; *Apparatus and Method for Extracting Wave Energy*; US Patent 3928967; 1975.
- [10] Folley M., Whittaker T., van't Hoff J.; *The Design of Small Seabed-Mounted Bottom-Hinged Wave Energy Converters*; Proceedings of the 7th European Wave and Tidal Energy Conference, Porto, Portugal; 2007.
- [11] Folley M., Whittaker T., Osterried M.; *The Oscillating Wave Surge Converter*; Fourteenth International Offshore and Polar Engineering Conference, (ISOPE 2004), Toulon; 2004.
- [12] Whittaker T., Collier D., Folley M., Osterried M., Henry A., Crowley M.; *The Development of Oyster – A Shallow Water Surging Wave Energy Converter*; 7th European Wave and Tidal Energy Conference, Aporto, Portugal; 2007.
- [13] Thorpe T.W.; *A Brief Review of Wave Energy*; UK Department of Trade and Industry. ETSU-R120; 1999.
- [14] Parmeggiani S., Kofoed J.P., Friis-Madsen E.; *Experimental Update of the Overtopping Model Used for the Wave Dragon Wave Energy Converter*; Energies 6 1961-1992; 2013.
- [15] Carpi F., De Rossi D., Kornbluh R., Pelrine R.E., Sommer-Larsen P.; *Dielectric Elastomers as Electromechanical Transducers*; Elsevier Ltd.; 2008.
- [16] Pelrine R.E., Kornbluh R., Jospeh J.; *Electrostriction of Polymer Dielectrics with Compliant Electrodes as a Means of Actuation*; Sensors and Actuators A 64 77-85; 1998.
- [17] Vertechy R., Berselli G., Parenti Castelli V., Vassura G.; *Optimal Design of Lozenge-Shaped Dielectric Elastomer Linear Actuator: Mathematical procedure and Experimental Validation*; Journal of Intelligent Material Structures, vol 21, 503-515; 2010.
- [18] Kofod G., Wirges W., Paajanen M., Bauer S.; *Energy Minimization for Self-Organized Structure Formation and Actuation*; Applied Physics Letters 90, 081916; 2007.
- [19] Sarban R., Jones R.W., Mace B.R., Rustighi E.; *A Tubular Dielectric Elastomer Actuator: Fabrication, Characterization, and Active Vibration Isolation*; Mechanical Systems and Signal Processing 25 2879-2891; 2011.
- [20] Wang H., Zhu Y., Zhao D., Luan Y.; *Performance Investigation of Cone Dielectric Elastomer Actuator Using Taguchi Method*; Chinese Journal of Mechanical Engineering Vol. 24; 2011.
- [21] Choi H.R., Jung K.M., Kwak J.W., Lee S.W., Kim H.M., Jeon J.W., Nam J.D.; *Multiple Degree-of-Freedom Digital Soft Actuator for Robotic Applications*; Proceedings of SPIE, 5051:262; 2003.
- [22] Wang H., Zhu Y., Wang L., Zhao J.; *Experimental Investigation on Energy Conversion for Dielectric Electroactive Polymer Generator*; Journal of Intelligent Material Systems and Structures 23(8) 885-895; 2012.
- [23] Pelrine, R., Kornbluh, R., Eckerle, J., Jeuck, P., Oh, S., Pei, Q., Stanford, S.; *Dielectric Elastomers: Generator Mode Fundamentals and Applications*; In Proc. SPIE (Vol. 4329, pp. 148-156); 2001.

- [24] Koh, S.J.A., Zhao, X., Suo, Z.; *Maximal Energy that can be Converted by a Dielectric Elastomer Generator*; Applied Physics Letters 94, 262902; 2009.
- [25] Koh S., Keplinger C., Li T., Bauer S., Suo Z.; *Dielectric Elastomer Generators: how much Energy can be converted?*; IEEE Transactions on Mechatronics, 16(1): 33-41; 2011.
- [26] Jean-Mistral C., Basrour S., Chaillout J-J.; *Modelling of Dielectric Polymers for Energy Scavenging Applications*; Smart Mater. Struct. 19, 105006; 2010.
- [27] Holzapfel G.; *Nonlinear Solid Mechanics: a Continuum Approach for Engineering*; Willey & Sons, New York; 2001.
- [28] Nam J. D., Choi H. R., Koo J. C., Lee Y. K., & Kim K. J.; *Dielectric Elastomers for Artificial Muscles*; In "Electroactive Polymers for Robotic Applications" (pp. 37-48), Springer London; 2007.
- [29] Steinmann P., Hossain M., Possart G.; *Hyperelastic Models for Rubber-like Materials: Consistent Tangent Operators and Suitability for Treolar's Data*; Archive of Applied Mechanics, Volume 82, Issue 9, pp 1183-1217; 2012.
- [30] Chiba S., Waki M., Masuda K., Ikoma T; *Current status and future prospects of electric generators using electroactive polymer artificial muscle*; OCEANS 2010 IEEE-Sydney (pp. 1-5). IEEE, 2010.
- [31] Kornbluh R.D., Eckerle J., and McCoy B; *A scalable solution to harvest kinetic energy*; Solar & Alternative Energy, SPIE, 2011.
- [32] Chiba S., Waki M., Wadac T., Hirakawa Y., Masuda K., Ikoma T.; *Consistent ocean wave energy harvesting using electroactive polymer (dielectric elastomer) artificial muscle generators*; Applied Energy, Elsevier, 104, 497–502, 2013
- [33] Jean, P., Wattez, A., Ardoise, G., Melis, C., Van Kessel, R., Fourmon, A., Queau, J. P; *Standing wave tube electro active polymer wave energy converter*; SPIE Smart Structures and Materials, pp. 83400C-83400C, 2012.
- [34] Muetze, A. and Vining, J. G.; *Ocean wave energy conversion-a survey*; In Industry Applications Conference, 2006. 41st IAS Annual Meeting. Conference Record of the 2006 IEEE (Vol. 3, pp. 1410-1417); 2006.
- [35] Vertechy R., Berselli G., Parenti Castelli V., Bergamasco M.; *Electro-Elastic Continuum Models for Electrostrictive Elastomers*; Advances in Elastomers I; Springer Berlin Heidelberg; pp. 453-491, 2013.
- [36] Vertechy R., Berselli G., Parenti Castelli V.; *Electro-Elastic Model for Dielectric Elastomers*; Advances in Mechanisms, Robotics and Design Education and Research; Springer International Publishing; pp. 245-250, 2013.
- [37] Vertechy R., Berselli G., Parenti Castelli V., Bergamasco M.; *Continuum thermo-electro-mechanical model for electrostrictive elastomers*; Journal Of Intelligent Material Systems And Structures; 24; pp. 761-778, 2013.
- [38] Ab-Malek K., Stevenson A.; *The effect of 42 year immersion in sea-water on natural rubber*; Journal of materials science, 21(1), 147-154, 1986.
- [39] Mott P. H., Roland C. M.; *Aging of natural rubber in air and seawater*; Rubber chemistry and technology, 74(1), 79-88, 2001.
- [40] Mars W.V., Fatemi, A.; *Factors that affect the fatigue life of rubber: a literature survey*; Rubber Chemistry and Technology, 77(3), 391-412, 2004.
- [41] Yuan W., Brochu P., Zhang H., Jan A. and Pei, Q. ; *Long lifetime dielectric elastomer actuators under continuous high strain actuation*; In SPIE Smart Structures and Materials + Nondestructive Evaluation and Health Monitoring (pp. 72870O-72870O). International Society for Optics and Photonics. 2009
- [42] Moretti G., Fontana M., Vertechy R.; *Modeling and Control of Lozenge-Shaped Dielectric Elastomer Generators*; Proceedings of the SMASIS 2013 Conference, Snowbirdh, Utah, 2013.
- [43] Wang H., Zhu Y., Zhao D., Luan Y.; *Performance Investigation of Cone Dielectric Elastomer Actuator Using Taguchi Method*; Chinese Journal of Mechanical Engineering Vol. 24; 2011.
- [44] Berselli G., Vertechy R., Vassura G., Parenti-Castelli V.; *Optimal Synthesis of Conically Shaped Dielectric Elastomer Linear Actuators: Design Methodology and Experimental Validation*; IEEE/ASME Transactions on Mechatronics, vol. 16 no. 1; 2011

- [45] Sarban R., Jones R.W., Mace B.R., Rustighi E.; *A Tubular Dielectric Elastomer Actuator: Fabrication, Characterization, and Active Vibration Isolation*; Mechanical Systems and Signal Processing 25 2879-2891; 2011.
- [46] Vertechy R., Berselli G., Parenti Castelli V., Vassura G.; *Optimal Design of Lozenge-Shaped Dielectric Elastomer Linear Actuator: Mathematical procedure and Experimental Validation*; Journal of Intelligent Material Structures, vol. 21, 503-515; 2010.
- [47] Price A.A.E.; *New Perspectives on Wave Energy Converter Control*; University of Edinburgh, PhD thesis; 2009.
- [48] de Araujo Alves M.A.; *Numerical Simulation of the dynamics of point absorber Wave Energy Converters Using Frequency and Time Domain Approaches*; Universidade Tecnica de Lisboa, Instituto Superior Técnico, PhD thesis in Mechanical Engineering; 2012.
- [49] Babarit A., Hals J., Muliawan M.J., Kurniawan A., Moan T., Krokstad J.; *Numerical benchmarking study of a selection of wave energy converters*; Renewable Energy 41, 44-63; 2012.
- [50] Yu Z., Falnes J.; *State-Space Modelling of a Vertical Cylinder in Heave*; Applied Ocean Research 17 265-275; 1995.
- [51] Holzapfel G.; *Nonlinear Solid Mechanics: a Continuum Approach for Engineering*; Wiley & Sons, New York; 2001.
- [52] WAMIT User Manual Version 7; WAMIT INC., Chestnut Hill, MA (USA); 2013.
- [53] Raghunathan, S., "The Wells air turbine for wave energy conversion," Progress in Aerospace Sciences 31(4), 335–386 (1995).
- [54] Falcão, A.F.O., and Justino, P.A.P., "OWC wave energy devices with air flow control," Ocean Engineering 26(12), 1275–1295 (1999).
- [55] Vertechy, R., Fontana, M., Papini, G. R., & Bergamasco, M. (2013, April). Oscillating-water-column wave-energy-converter based on dielectric elastomer generator. In *SPIE Smart Structures and Materials+ Nondestructive Evaluation and Health Monitoring* (pp. 86870I-86870I). International Society for Optics and Photonics.
- [56] Papini, G. P. R., Vertechy, R., & Fontana, M. Dynamic Model Of Dielectric Elastomer Diaphragm Generators For Oscillating Water Column Wave Energy Converters. Evans, D. V. "The oscillating water column wave-energy device." *IMA Journal of Applied Mathematics* 22.4 (1978): 423-433.
- [57] Newman, J.N., "Interaction of water waves with two closely spaced vertical obstacles," J. Fluid Mech 66(part 1), 97–106 (1974).
- [58] Evans, D. V., "The oscillating water column wave-energy device," IMA Journal of Applied Mathematics 22(4), 423–433 (1978).
- [59] Evans, D. V., "Wave-power absorption by systems of oscillating surface pressure distributions," Journal of Fluid Mechanics 114(1), 481–499 (1982).
- [60] Reitan, A., "Wave-power absorption by an oscillating water column in a channel," Journal of fluid mechanics 158, 153–175 (1985).
- [61] Sarmento, A., and Falcao, A.F.O., "Wave generation by an oscillating surface-pressure and its application in wave-energy extraction," Journal of Fluid Mechanics 150, 467–485 (1985).
- [62] Sarmento, A., "Wave flume experiments on two-dimensional oscillating water column wave energy devices," Experiments in fluids 12(4), 286–292 (1992).
- [63] Brendmo, A., Falnes, J., and Lillebekken, P.M., "Linear modelling of oscillating water columns including viscous loss," Applied ocean research 18(2), 65–75 (1996).
- [64] Falcão, A.F.O., and Justino, P.A.P., "OWC wave energy devices with air flow control," Ocean Engineering 26(12), 1275–1295 (1999).
- [65] Josset, C., and Clement, A.H., "A time-domain numerical simulator for oscillating water column wave power plants," Renewable energy 32(8), 1379–1402 (2007).
- [66] Evans, D. V, and Porter, R., "Hydrodynamic characteristics of an oscillating water column device," Applied Ocean Research 17(3), 155–164 (1995).
- [67] Delauré, Y.M.C., and Lewis, A., "3D hydrodynamic modelling of fixed oscillating water column wave power plant by a boundary element methods," Ocean engineering 30(3), 309–330 (2003).
- [68] Paixão Conde, J.M., and Gato, L.M.C., "Numerical study of the air-flow in an oscillating water column wave energy converter," Renewable energy 33(12), 2637–2644 (2008).

- [69] Aalbers, A.B., "The water motions in a moonpool," Ocean engineering 11(6), 557–579 (1984).
- [70] Morrison, I.G., and Greated, C.A., "Oscillating water column modelling," in Proceedings of the International Conference on Coastal Engineering 1(23) (1992).
- [71] Goulbourne, N.C., Mockensturm, E.M., and Frecker, M.I., "Electro-elastomers: large deformation analysis of silicone membranes," International journal of solids and structures 44(9), 2609–2626 (2007).
- [72] He, T., Zhao, X., and Suo, Z., "Dielectric elastomer membranes undergoing inhomogeneous deformation," Journal of Applied Physics 106(8), (2009).
- [73] Zhao, X., and Suo, Z., "Method to analyze programmable deformation of dielectric elastomer layers," Applied Physics Letters 93(25), (2008).
- [74] O'Brien, B., McKay, T., Calius, E., Xie, S., and Anderson, I., "Finite element modelling of dielectric elastomer minimum energy structures," Applied Physics A: Materials Science and Processing 94(3), 507–514 (2009).
- [75] Vertechy, R., Frisoli, A., Bergamasco, M., Carpi, F., Frediani, G., and De Rossi, D., "Modeling and experimental validation of buckling dielectric elastomer actuators," Smart Materials and Structures 21(9), (2012).
- [76] Vertechy, R., Berselli, G., Castelli, V.P., and Bergamasco, M., "Continuum thermo-electro-mechanical model for electrostrictive elastomers," Journal of Intelligent Material Systems and Structures, DOI: 10.1177/1045389X12455855 (2012).
- [77] Li, T., Qu, S., Yang, W., 2012. "Energy harvesting of dielectric elastomer generators concerning inhomogeneous fields and viscoelastic deformation", J. Appl. Phys., 112, pp. 034119.
- [78] Goulbourne, N.C., Mockensturm, E., Frecker, M., 2007. "Electro-elastomers: Large deformation analysis of silicone membranes", International Journal of Solids and Structures, 44(9), pp. 2609-2626.
- [79] He, T., Zhao, X., Suo, Z., 2009. "Equilibrium and stability of dielectric elastomer membranes undergoing inhomogeneous deformation," Journal of Applied Physics, 106, pp. 083522.
- [80] Adkins, J.E., Rivlin, R.S., 1952. "Large Elastic Deformations of Isotropic Materials: IX The Deformation of Thin Shells", Philosophical Transactions of the Royal Society of London. Series A, Mathematical and Physical Sciences, 244(888), pp. 505-531.
- [81] Falcão, A.F.O., 2000. "The shoreline OWC wave power plant at the Azores," in Proceedings of the Fourth European Wave Energy Conference, Aalborg, Denmark, 42–48.
- [82] Moretti, G., Forehand, D., Vertechy, R., Fontana, M. and Ingram, D., 2014, June. Modeling of an oscillating wave surge converter with dielectric elastomer power take-off. In ASME 2014 33rd International Conference on Ocean, Offshore and Arctic Engineering (pp. V09AT09A034-V09AT09A034). American Society of Mechanical Engineers.